§

Doctoral Dissertation

Study on Effect of Migratory-Behavior Driven Epigenetic Memory Formation on Cardiomyogenic Fate Commitment of Human Mesenchymal Stem Cells in Dendrimer-Immobilized Surface

Fitria Dwi Ayuningtyas

January 2023

Graduate School of Engineering

Osaka University

Table of Contents

Abstract

Human mesenchymal stem cells (hMSCs) have become a promising cell source for regenerative therapies and tissue engineering due to their self-renewal ability and potential to differentiate into several specific cell lineages. In the development of stem cells study, regulation of stem cell differentiation mainly focused on culture strategies using chemical and biological factors to provide exogenous stimulation. However, recent studies have emerged alternate research efforts to examine the effect of cellular microenvironment on the regulation of stem cell behavior, which induced differentiation potential through endogenous stimulation.

Culture surfaces with immobilized polyamidoamine dendrimers have been developed to regulate cellular behavior and, as a result, provide the ability to induce cellular functions such as differentiation potential in hMSCs. The fifth generation of dendrimer-immobilized surface (G5) has provided a suitable environment for cardiomyogenic-lineage commitment. Although the influence of mechanical factors from the dendrimer-immobilized surface seems to affect the differentiation process directly, the changes in stem cell behavior and mechanotransduction processes related to epigenetic functions within cells remain unclear. Thus, this study aims to understand the mechanism underlying cardiomyogenic lineage differentiation commitment of hMSCs related to cellular mechanotransduction and epigenetic modification through migratory behavior driven by dendrimer-immobilized. Moreover, through understanding the epigenetic regulation caused by cellular migratory behavior, this study also examined the suitable culture process to enhance the differentiation efficiency of hMSCs towards cardiomyogenic lineage on the dendrimer-immobilized surface.

In the first chapter of this study, the migratory behavior of hMSCs on various generations of the dendrimer-immobilized surface was investigated in a time-dependent manner. With an increase in dendrimer generation number, cells exhibited highly dynamic migratory behavior

due to cell-substrate interaction. Regulation of extracellular matrix components and focal adhesion complex as a cell response to mechanical forces derived by immobilized dendrimer in the substrate leads to alteration of the cytoskeleton and nuclear skeleton structures. The mechanical forces from cell-substrate to intracellular properties were transduced through the cytoskeleton and nuclear skeleton structure, promoting intracellular signaling pathways within cells. The increase of nuclear deformation in hMSCs culture through mechanotransduction derived by cell migratory behavior was evaluated. The decreased nuclear lamin expression regulated global histone modification by suppressing H3K9me3 and up-regulation of H3K27me3 and H3K9ac. Thus phenomena of reorganizations of the cytoskeleton and nuclear skeleton related to migratory changes on dendrimer-immobilized surface are responsible for the integrated regulation of epigenetic formations through histone modification, which leads to switching differentiation commitment of hMSCs to smooth, skeletal and cardiac muscle lineages.

In the second chapter of this study, the further investigation of epigenetic formations driven by migratory-behavior changing during culture on the dendrimer-immobilized surface was developed with focusing on fifth-generation dendrimer as a potential provider for cardiomyogenic differentiation commitment. The G5 surface promotes cell aggregate formation through dynamic migration. The migration-driven aggregate behavior exhibited an essential role in enhancing cardiomyogenic differentiation commitment during passage on a dendrimer-immobilized surface through the regulation of epigenetic memory. Passage culture of cell aggregates showed consecutive deformation of the cytoskeleton and nuclear skeleton structure; meanwhile, passage culture of dissociated cell aggregate exhibited recovery of the cytoskeleton and nuclear skeleton structure. The epigenetic regulation remarked by global histone modification markers of repressive (H3K9me and H3K27me3) and activating modifications (H3K9ac) shows that on cell aggregate passage culture, the epigenetic memory regulation was

obtained; on the other hand, in the single cells passage culture, epigenetic regulation shows recovery as at the beginning of culture. The constitutive alteration of the cytoskeleton and nuclear skeleton structure and memory of epigenetic regulation on cell aggregate passage culture increase the cardiomyogenic differentiation potential of hMSCs. This phenomenon shows that epigenetic memory regulation through migration-driven aggregate behaviors is essential in enhancing the cardiomyogenic differentiation of hMSCs on the dendrimer-immobilized surface. The maintenance of epigenetic memory through the serial passage of the cell aggregates was achieved and promotes the enhancement of differentiation commitment into the cardiomyogenic lineage.

This study provides an understanding of the role of epigenetic modification through migratory-cell behavior related to cellular mechanotransduction provided by a suitable designated surface, using dendrimer-immobilized, to induce differentiation of hMSCs towards cardiomyogenic lineage. Moreover, integrating improved culture processes and appropriate microenvironmental cues could enhance the efficiency of hMSCs differentiation commitment toward specific cell lineages.

General Introduction

Cardiomyogenic differentiation potential of human mesenchymal stem cells

Cardiovascular disease (CVDs) is one of the leading causes of death worldwide. It has been reported by World Health Organization (WHO) that an estimated 17.9 million people died from CVDs in 2019, representing 32% of all global deaths. Of these deaths, 85% were due to heart attack and stroke. Regenerative therapy to overcome CVDs being increasingly investigated in recent studies. The potential capacity of stem cells to develop into cardiomyocytes, vascular endothelial cells, and smooth muscle cells is under investigation. As well as the ability of stem cells to secrete cytokines and growth factors to support endogenous repairment in cardiac systems.

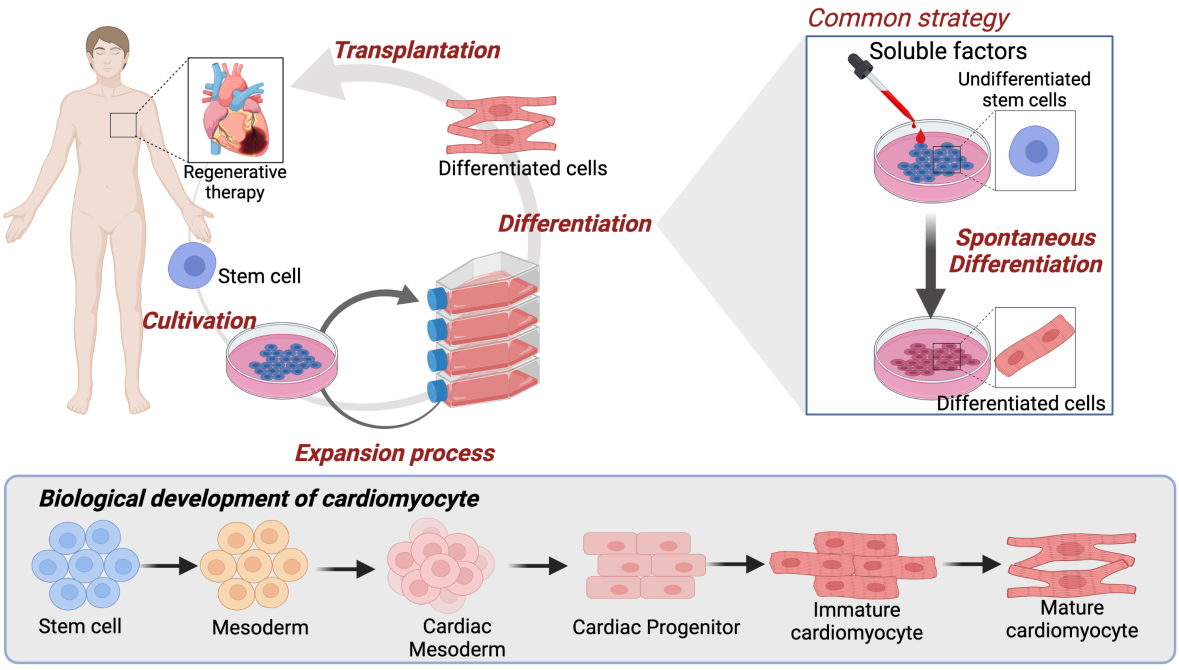

Figure 1. Regenerative therapy potential to overcome cardiovascular disease and common strategy applied in stem cell engineering to achieve differentiation towards cardiomyogenic lineage.

Human mesenchymal stem cells (hMSCs) are adult multipotent stem cells that can undergo self-renewal and differentiate into several specific cell lineages, such as osteoblasts, chondrocytes, adipocytes, and other lineages. This ability has emerged as a promising cell source for regenerative therapies and tissue engineering applications (Baksh et al., 2004; Caplan & Correa, 2011). The heterogeneity of hMSCs to perform multi-directional differentiation limits its self-renewal capacity and gives rise to specific cell types with terminally differentiated phenotypes. The commitment and differentiation of hMSCs to specific mature cell types is a tightly and temporally controlled process involving the activities of various transcription factors, cytokines, growth factors, and extracellular matrix (ECM) molecules (Baksh et al., 2004; Cruz Walma & Yamada, 2020).

The expansion process to obtain a high yield of differentiated stem cells as a source for regenerative therapy requires considerable expenses to be conducted in parallel with the differentiation process induced by exogenous stimulation. On the other hand, cell heterogeneity is usually obtained after induction with soluble factors, resulting in a different state of commitment in the cell population (Hwang et al., 2008; Costa et al., 2020). Thus inefficiency of the stem cell differentiation process by induction through exogenous stimulation should be overcome with an alternative strategy.

The role of biophysical induction in stem cell differentiation has been well-studied recently. The studies in stem cell differentiation showed that through proper induction, applying chemical and physical stimulation in hMSCs could promote differentiation toward cardiomyogenic lineage (Toma et al., 2001; Mohanty et al., 2013; Burridge et al., 2012). In recent studies, Tijore et al. (2015) discovered that regulation of cytoskeletal tension through culture on the micropatterned surface induced hMSCs towards cardiomyogenic differentiation, showing that biophysical regulation is essential in the stem cell differentiation process.

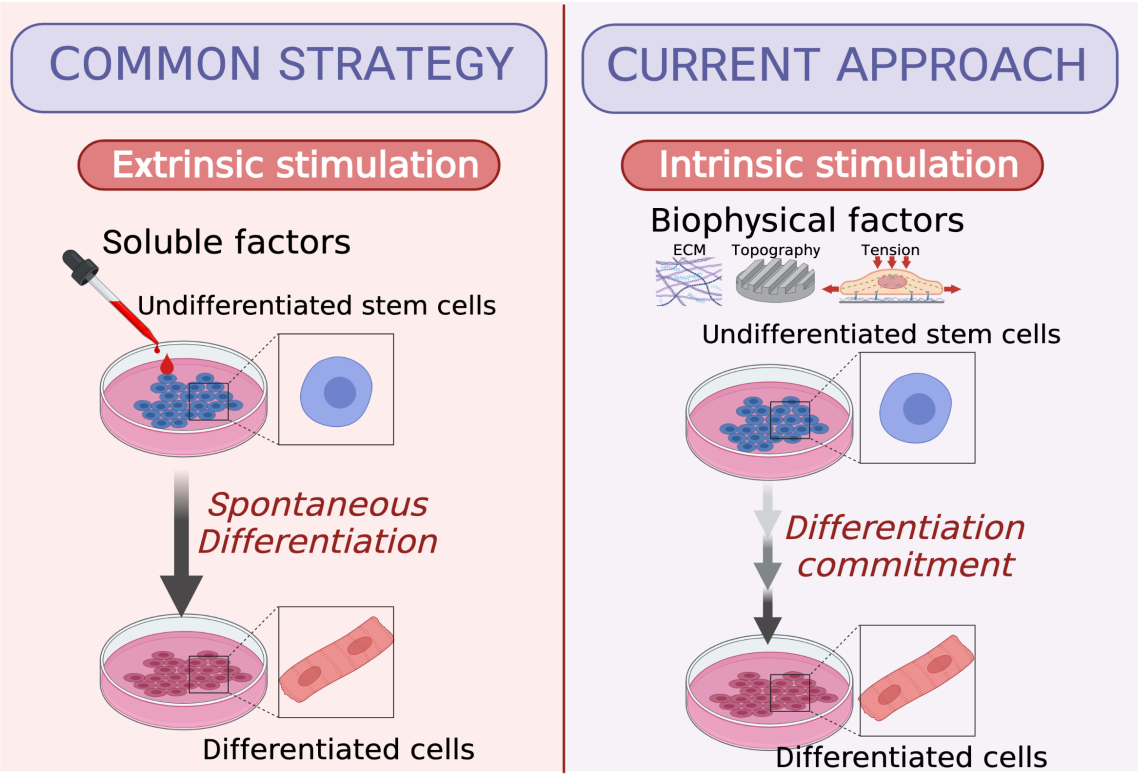

Figure 2. Common strategy applying extrinsic stimulation and the approach in the current study by applying intrinsic stimulation through biophysical factors to directed stem cell fate.

Mechanotransduction in hMSCs differentiation

In a natural condition *in vivo,* cells are exposed to various mechanical forces depending on their niches, including hMSCs (Engler et al., 2006). Stem cells can sense and respond to physical forces and exert forces on the surrounding microenvironments (Engler et al., 2006; Al-Rekabi et al., 2013).

Stem cell fate, however, could be regulated by a wide repertoire of signals from biochemical factors and biophysical events that can transduce biochemical signals within cells (Conway et al., 2012; Gattazzo et al., 2014). Recent studies have emerged alternate research efforts to examine the effect of biophysical events in the cellular microenvironment on the regulation of stem cell behavior, which induced differentiation potential through endogenous stimulation (Keung et al. 2010; Sun et al., 2012).

Biophysical signals can be governed by force-induced changes in the extracellular biophysical cues to activate the specific intracellular biochemical signaling pathways to regulate cell fate (Kumar et al., 2017). Mechanical forces outside and inside the cell can be transduced into molecular signaling activities to direct cellular function and fate, a process known as mechanotransduction (McCain & Parker, 2011; Teo et al., 2013).

The mechanical forces at the plasma membrane can be altered either via changes in cell-substrate adhesion due to modifications in ECM density, rigidity, and orientation or through the formation or dissociation of cell-cell junctions. The altered forces at the plasma membrane can biochemically or mechano-physically affect membrane-bound mechanosensitive proteins, such as integrin-ECM adhesion, cadherin junction proteins between cells, and linker proteins bound to them. This, in turn, may induce the reorganization of cytoskeletal proteins, such as actin filaments, which are anchored at the cell-ECM and cell-cell adhesion junctions.

The cytoskeleton provides a pathway for mechanical forces to be transferred from the plasma membrane to internal cellular structures, including the nucleus (Janmey & Miller, 2011; Changede & Sheetz, 2016; Bachir et al., 2017; Kechagia et al., 2019; Bouzid et al., 2019). The nuclear-cytoplasmic connections facilitated by the nuclear envelope (NE) proteins, such as the linker of nucleoskeleton and cytoskeleton (LINC) complex, provide spatial and structural integrity for the nucleus, as well as allow for the transfer of mechanical force into the nucleus resulting in mechanotransduction (Bouzid et al., 2019; Hieda, 2019).

Recent developments have established a collective role of integrins, focal adhesions (FAs), and the actin cytoskeleton as integral in various mechanotransduction pathways (Lee et al., 2007; Geiger et al., 2009; Wang *et al.,* 2013). The formation of integrin-ECM binding motifs enables cells to sense the surrounding microenvironment and activate several mechanotransduction pathways to initiate a series of cell responses, including FAs formation,

cytoskeleton reorganization, nuclear lamins reorganization, and alteration of genes expression (Sun et al., 2016; Martino et al., 2018).

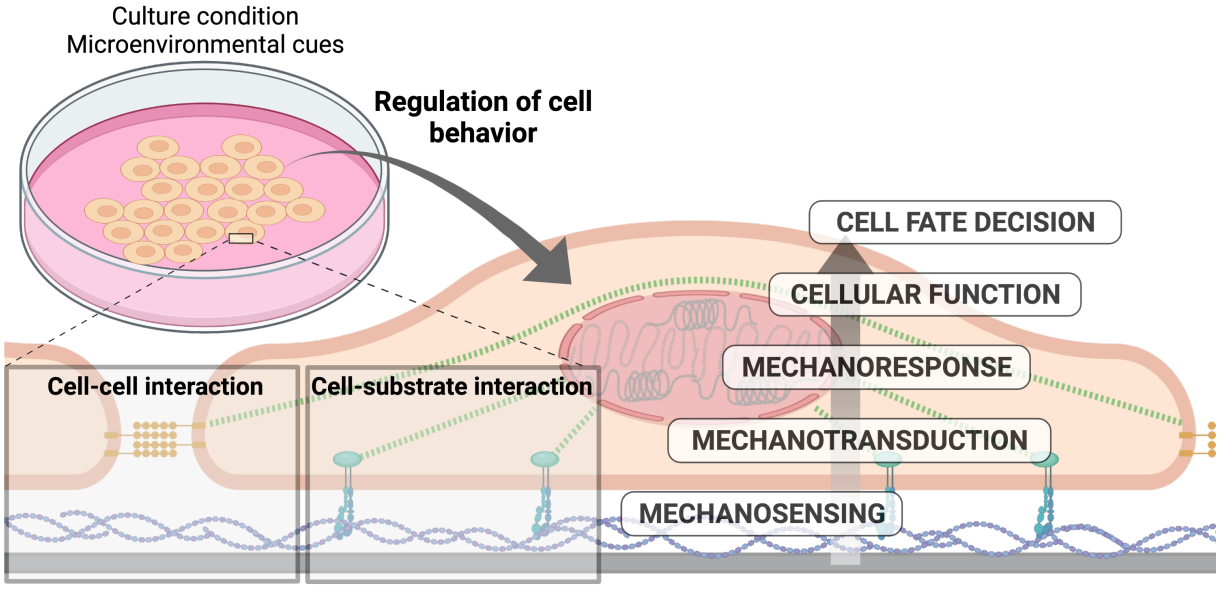

Figure 3. Mechanotransduction phenomena during cell culture

Cellular mechanical forces and their interaction with the ECM have begun to emerge as critical determinants of cell behavior. Topography-induced cell behavior is caused by a change in FA arrangement, leading to a change in the actin cytoskeleton and mechanotransduction of the cells, resulting in differential gene expression and cell function (Teo et al., 2013; Ray et al., 2017; Yang et al., 2020). In the absence of soluble differentiation factors, biophysical-induced stem cell differentiation observed in hMSCs is a translation of cellular responses through mechanotransduction pathways.

Lamina-associated domains (LADs), which are chromatin domains that interact with lamins, are involved in the reorganization of the nucleoskeleton resulting in alternations in the chromatin structure and regulation of histone modifications (Steensel & Belmont, 2017; Lochs et al., 2019). In the mechanism of epigenetic changes, histone modification plays an essential role in epigenetic memory regulation. Post-translational modifications of histones, including acetylation and methylation of conserved lysine residues, are also dynamically regulated by

chromatin structure, putting the histone modifications as one of the mechanisms in epigenetic memory formation (Handy et al., 2011; Miller & Grant, 2013).

In hMSCs' epigenetic regulation, two repressive markers of histone modification, H3K9me3, and H3K27me3, play an essential role in its differentiation commitment (Gopinathan et al., 2013; Zhang et al., 2015). On the other hand, the acetylation process of H3K9 plays an essential role in the regulation of epigenetic memory and activation of gene transcription in stem cells (Ninova et al., 2019; Trisciuoglio et al., 2018). These histone modifications have been found to regulate chromatin modifications and gene transcription during developmental stages and cellular differentiation (Ninova et al., 2019; Bannister et al., 2011).

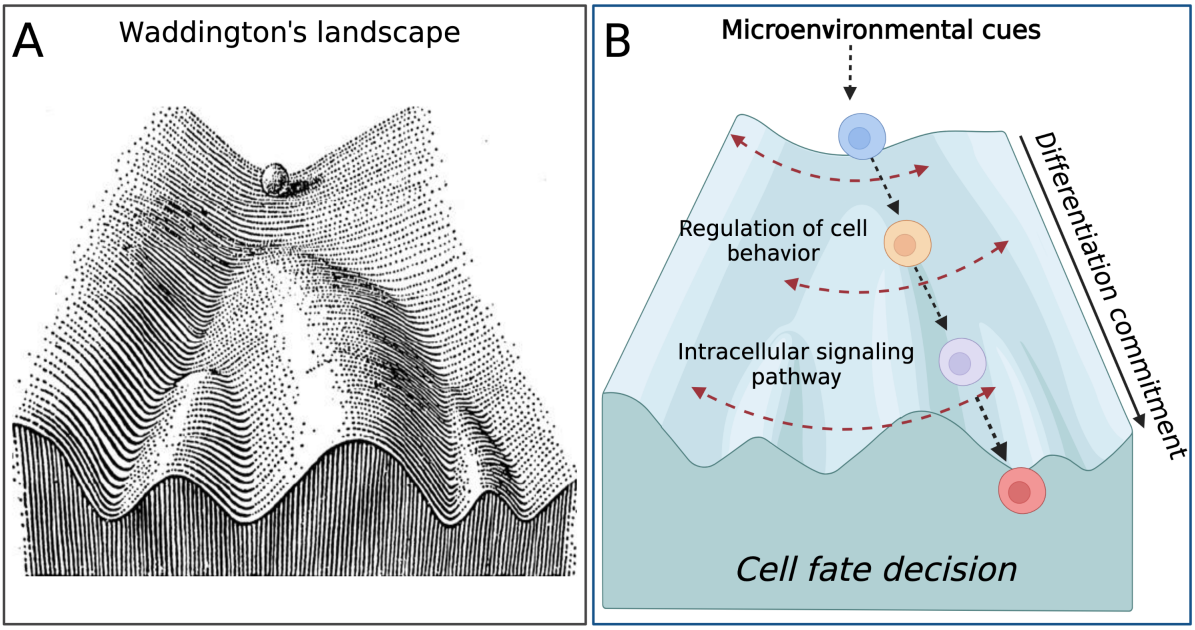

Figure 4. Epigenetic landscape in stem cell differentiation. (A) The epigenetic landscape of Waddington, a path of the ball in this landscape illustrates a cell developmental fate. (B) The direction of differentiation commitment of stem cells as a response to microenvironmental cues according to the epigenetic landscape.

Changes in heterochromatin markers during migration induction were observed in recent studies, indicating that mechanical forces were transduced and affected epigenetic regulation

(Gerlitz et al., 2010; Segal et al., 2018). The intrinsic and extrinsic signals generated within the cell or its microenvironment are likely to trigger a cascade of events regulating the epigenetic changes (Tee & Reinberg, 2014; Nivet, 2016; Wahane et al., 2019). Accumulative signals of epigenetic memory factors from microenvironmental cues during the culture process of stem cells were assumed to maintain the epigenetic changes and enhance the cellular transcription and differentiation commitment of stem cells (Han & Yoon, 2012; Shrinageshwar et al., 2016).

Dendrimer-immobilized surface in hMSCs differentiation

For the past decades, modification of culture surface with immobilized poly-amidoamine dendrimers was developed to regulate cell morphologies and behaviors (Kim et al., 2009; Kim et al., 2010; Kim et al., 2014; Ogawa et al., 2016). The changes in cell morphology were observed on the immobilized dendrimer with D-glucose molecules as peripheral ligands and mainly dependent on the generation number of dendrimer (Kim et al., 2009). It was also demonstrated that the morphological changes accompanied the dynamic cytoskeletal formation in the cells under culture on a dendrimer-immobilized surface (Kim et al., 2010; Kim et al., 2014).

In the previous study about hMSCs culture on dendrimer surface, the morphological changes derived from cytoskeletal reorganization were found to be related to differentiation capacities into myogenic lineages (Kim et al., 2010), while in the higher generation of dendrimer-immobilized surface, shows the differentiation commitment towards cardiomyogenic lineage (Kim et al., 2014). In the culture of hMSCs on the dendrimer surface, dynamic changes of morphologies were investigated with different capacities for fibronectin adsorption related to changes in dendrimer generation number. It shows that amount and structure of fibronectin affected dynamic hMSCs behaviors through the formation of the cytoskeleton and focal adhesions (Ogawa et al., 2016). Various generation of dendrimer-

immobilized surfaces, i.e., first-generation (G1), third-generation (G3), and fifth-generation (G5) surfaces, through the dynamic morphological changes and their interaction with ECM, promotes hMSCs to commit into specific lineages of differentiation commitment.

Although the influence of mechanical factors from dendrimer-immobilized surface appears directly affected to differentiation process, the related changes in stem cell behavior and mechanotransduction process remain unclear. The correlation between mechanotransduction through cytoskeleton and nuclear skeleton reorganization to the downstream effect in genome regulation still needs to be discovered. Recent studies in the stem cell engineering field have revealed a direct link between nuclear architecture and cellular differentiation, suggesting that chromatin organization might be important in the lineage commitment of stem cells (Heo *et al.,* 2016).

Previous studies in stem cell engineering using a designated surface with immobilized dendrimer also showed that the differentiation potency of hMSCs towards cardiomyogenic lineage was induced (Kim et al., 2010). The changes in cell morphology and behavior are driven by dynamic migration in the designated surface, activating intracellular signaling pathways and transcription of cardiomyocyte genes. The positive cells of the cardiomyocyte protein marker, cTnT, were exhibited from hMSCs cultured in the G5 surface (Kim et al., 2010; Ogawa et al., 2016). Based on those previous studies, further assessment of cardiomyogenic differentiation of hMSCs needs to be elucidated to gain a deeper understanding of intracellular mechanisms induced by the regulation of microenvironmental cues.

This doctoral study aims to understand the mechanism underlying the cardiomyogenic lineage differentiation commitment of hMSCs related to cellular mechanotransduction and epigenetic modification through migratory behavior driven by dendrimer-immobilized. Moreover, through understanding the epigenetic regulation and maintenance of epigenetic memory driven by cellular migratory behavior, this study also examined the suitable culture

process to enhance the differentiation efficiency of hMSCs towards cardiomyogenic lineage on the dendrimer-immobilized surface.

In the first chapter, the migratory behavior of hMSCs in various generations of the dendrimer-immobilized surface was investigated time-dependent to understand the dynamic migratory behavior due to cell-substrate interaction. Regulation of extracellular matrix component and focal adhesion complex as a cell response to mechanical forces derived by immobilized dendrimer in the substrate leads to alteration of cytoskeleton and nucleoskeleton structures. Nucleoskeleton deformation in hMSCs culture related to the regulation of global histone modification in H3K9me3, H3K27me3, and H3K9ac. Thus phenomena of reorganizations of the cytoskeleton and nuclear skeleton related to migratory changes on dendrimer-immobilized surface are responsible for the integrated regulation of epigenetic formations through histone modification, which leads to switching differentiation commitment of hMSCs to smooth, skeletal and cardiac muscle lineages.

In the second chapter, the further investigation of epigenetic formations driven by migratory-behavior changing during culture on the dendrimer-immobilized surface was developed with focusing on higher-generation dendrimer as a potential provider for cardiomyogenic differentiation commitment. The G5 surface promotes cell aggregate formation through dynamic migration. The migration-driven aggregate behavior exhibited an essential role in enhancing cardiomyogenic differentiation commitment during passage on a dendrimer-immobilized surface through the regulation of epigenetic memory. The constitutive alteration of the cytoskeleton and nucleoskeleton structure regulates the global histone modification markers of repressive (H3K9me and H3K27me3) and activating modifications (H3K9ac) shows that on aggregate-based passage culture, the memory of epigenetic regulation was obtained. In contrast, in the single cell-based passage culture, epigenetic regulation shows recovery at the beginning of the culture. This phenomenon indicates that epigenetic memory regulation through

migration-driven aggregate behaviors is essential in enhancing the cardiomyogenic differentiation of hMSCs on the dendrimer-immobilized surface. The maintenance of epigenetic memory through the serial passage of the cell aggregates was achieved and promotes the enhancement of differentiation commitment into the cardiomyogenic lineage.

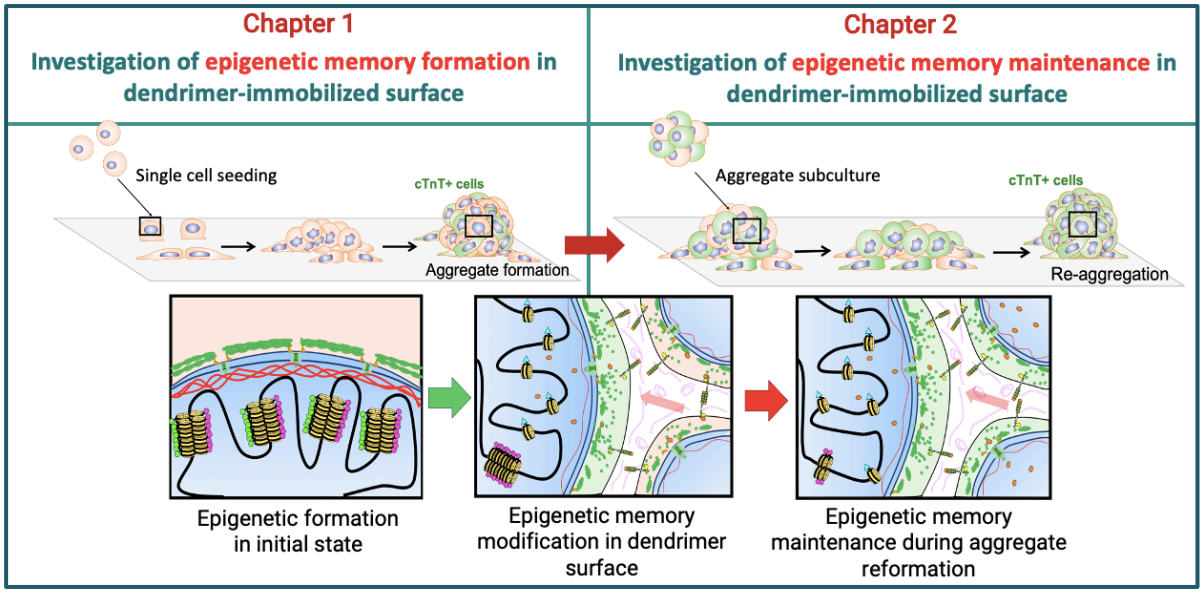

Figure 5. Schematic diagram showing the outline of the study

This study provides an understanding of the role of epigenetic modification through migratory-cell behavior related to cellular mechanotransduction provided by a suitable designed surface using dendrimer-immobilized to induce differentiation commitment of hMSCs towards cardiomyogenic lineage. Moreover, integrating improved culture processes and appropriate microenvironmental cues could enhance the efficiency of hMSCs differentiation commitment toward specific cell lineages.

Chapter 1

Migratory behavior-driven epigenetic modification of hMSCs on dendrimer-immobilized surface promotes myogenic commitment

1.1. Introduction

Microenvironmental cues play a significant role in regulating stem cell fate commitment and its responses to various microenvironmental factors, such as biochemical or biophysical stimuli (Keung et al., 2010; Zhang et al., 2019). In recent studies, growing evidence suggests that mechanical stimuli significantly impact the regulation of specific lineage commitment of stem cells through the regulation of gene transcription and signaling pathways (Li et al., 2011; Park et al., 2012).

Mechanical forces of the cellular microenvironment initially came from outside cells and were transduced into the intracellular site through the cytoskeleton (Mammoto et al., 2012). The cell responds to external forces through focal adhesions and adherence junctions, which play a role in the linkage between ECM or neighboring cells with the cytoskeleton. The forces transmitted through integrin- and cadherin-mediated adhesions are derived from contractile actin-myosin networks and outside the cell (Mammoto et al., 2012; Mui et al., 2016; Bachir et al., 2017). The direct connection of the cytoskeleton to the nuclear skeleton through the LINC complex transduced the mechanical forces to the nucleus. These forces actively regulate various signaling pathways and genetic programs to control cell-fate decisions (Hieda et al., 2019; Bouzid et al., 2019).

In the past two decades, culture surfaces with immobilized polyamidoamine dendrimers have been developed to regulate cellular behavior based on various modifications of parameters, such as the number of dendron branches (generation number) and dendrimer density. As a

critical physical feature, dendrimer surfaces of different generation numbers have been proven to exert profound effects on cell behaviors and, thus, induce distinct cellular functions. In our previous study, we designed three types of dendrimer-immobilized surfaces, i.e., G1, G3, and G5 surfaces, and it was reported that the adhesion and morphology of hMSCs were closely related to the generation number of the dendrimer surface (Kim et al., 2010; Kim et al., 2014; Ogawa et al., 2015; Ogawa et al. 2016).

In this chapter, the migratory behavior of hMSCs on various generations of the dendrimer-immobilized surface was investigated time-dependent. With an increase in dendrimer generation number, cells exhibited highly dynamic migratory behavior, which altered the cytoskeleton and nuclear skeleton structures driven by cell-substrate interaction and regulation of extracellular matrix components. The nuclear lamin alteration due to migratory behavior on various generations of dendrimer surface in genomic regulation and epigenetic modification to regulate hMSCs fate commitment were investigated. Thus phenomena of reorganizations of the cytoskeleton and nuclear skeleton related to migratory changes on dendrimer-immobilized surface are responsible for the integrated regulation of epigenetic formations through histone modification, which leads to switching differentiation commitment of hMSCs to smooth, skeletal and cardiac muscle lineages.

1.2. Materials and methods

1.2.1. Cells and culture conditions

HMSCs derived from bone marrow were obtained from Lonza (Walkersville, MD, USA; lot no. 0000183402). The hMSCs were routinely subcultured in a growth medium (Lonza) at 37°C in a humidified atmosphere containing 5% CO_2. The cells were detached by enzymatic treatment with 0.1% trypsin / 0.02% EDTA solution (Sigma-Aldrich, St. Louis, MO, USA) after reaching 70% confluence on the culture surface. Cells with a passage number of less than five

were used in the experiments. For all experiments, hMSCs were seeded at a viable cell concentration of 5.0×10^3 cells/cm^2. The hMSCs were cultured in Dulbecco's modified Eagle's medium (DMEM; Sigma-Aldrich) supplemented with 10% fetal bovine serum and antibiotics (Life Technologies, Carlsbad, CA, USA) in 8-well plates (Nunc, Roskilde, Denmark) and T-75 flasks (Corning Inc., New York, NY, USA) with and without dendrimer-immobilized to the surface. The culture medium was changed every three days. In the control experiments carried out parallel to the experiments, hMSCs were cultured to generate floating aggregates. Briefly, cells were dissociated into single cells and seeded at 1.2×10^5 cells/mL/well (200 cells/aggregate) into 3D micro-space culture plates (Elplasia; Kuraray Co., Ltd., Tokyo, Japan) containing DMEM supplemented with 10% FBS. Beginning on the day following aggregate formation, the medium was changed every three days.

1.2.2. Preparation of dendrimer-immobilized surface

The polyamidoamine dendrimer surface was established on the polystyrene (PS) surface of 8-well plates (Nunc) or T-75 tissue culture flasks (Corning Inc.). G1, G3, and G5 surfaces were created under sterile conditions by synthesizing dendrimers over four reactions. First, hydroxyl groups were displayed by adding potassium *tert*–butoxide onto the polystyrene surface. Then, glutaraldehyde and tris(2-aminoethyl) amine solutions (pH 9.0, adjusted with 0.1 mol/L NaOH) were poured onto the surface one after another to construct a dendron structure. Every culture vessel was rinsed with sterile water, and the dendron structure construction procedures were repeated depending on the generation number applied. Finally, D-glucose was added to the surface as a final ligand.

1.2.3. Quantitative analysis of cell behaviors

The cell attachment efficiency (α_M) was estimated as the ratio of the cell concentration at 24 hours to the respective seeding density. The growth activity was defined as the apparent specific growth rate (μ) from 24 hours to 120 hours of culture, calculated as μ (h) = ln (X_{24}/X_{120})/96. In addition, the morphology was evaluated by cell roundness (R_C), which was calculated as $R_C = 2(\pi A_C)^{1/2}/l_C$, where A_C and l_C represent the area and peripheral length of each cell, respectively, and was determined using image processing software (Image Pro-plus software 7.0; Media Cybernetics, Rockville, MD, USA). The frequencies of R_C were evaluated using 150 cells under each condition. Time-lapse images were captured every 10 min at fixed positions for ten days using a BioStudio-T imaging platform (Nikon Engineering, Kanagawa, Japan) and a 60× objective lens. The mean cell migration rate (V_M) was determined from the displacement of positional centroids for 72 hours. The V_M was evaluated using more than 30 cells under each condition.

1.2.4. Immunofluorescence staining and quantification

Cells were fixed with 4% paraformaldehyde and permeabilized by incubation in PBS with 0.5% polyoxyethylene octyl phenyl ether. After masking non-specific proteins through blocking (Block Ace; Dainippon Sumitomo Pharma, Osaka, Japan), the cells were incubated with primary antibodies, anti-vinculin (Santa Cruz Biotechnology, Dallas, TX, USA), and anti-lamin A/C (Santa Cruz Biotechnology). Then, the cells were incubated with secondary antibodies, Alexa Flour 594-conjugated goat anti-mouse IgG (Life Technologies, Carlsbad, CA, USA). Nuclei were stained with 4’,6-diamidino-2-phenylindole, and dilactate (Life Technologies). Filamentous (F-actin) and monomeric actin (G-actin) were stained with fluorescence phalloidin (Life Technologies) and deoxyribonuclease-I conjugated with Alexa Fluor 488 (Life Technologies), respectively. Fluorescence images were taken using a confocal laser scanning

microscope (FV-1000; Olympus) with a 60× objective lens. Cell aggregates grown on a low-binding culture surface were collected and fixed with 4% paraformaldehyde. After washing with PBS, floating cell aggregates were soaked in a sucrose solution overnight at 4 °C, embedded in optimal cutting temperature compound (Tissue-Tek, Sakura, Japan), frozen in liquid nitrogen, and cryo-sectioned at 20 μm thickness. Staining and observation were as previously described. For G- to F-actin ratio measurements, images were captured by a confocal laser scanning microscope with a 60× objective lens. Integrated fluorescence intensity was measured for each channel by subtracting the sum projection from the background, and the G-actin to F-actin ratio was calculated. Image analysis was performed using image-processing software (Image Pro-Plus software 7.0). The G-actin to F-actin ratio was evaluated using more than 30 cells under each condition.

1.2.5. Protein extraction and western blot analysis

Total cellular protein was extracted from cells using CelLytic™ mammalian cell lysis/extraction reagent (Sigma-Aldrich, St. Louis, MO, USA). In contrast, the nuclear protein was extracted using Nuclear Extraction Kit (Abcam, Cambridge, UK). Samples were mixed with sample buffer containing 2-mercaptoethanol and boiled at 95°C for 10 min. Proteins were separated according to molecular weight by sodium dodecyl sulfate-polyacrylamide gel electrophoresis (SDS-PAGE) using 10% and 15% polyacrylamide gels, SuperSep™ (FUJIFILM Wako Pure Chemical Corporation, Osaka, Japan) and transferred to polyvinylidene fluoride membranes (Bio-Rad, Hercules, CA, USA). After masking the non-specific proteins with ECL Blocking Agent (GE Healthcare, Chicago, IL, USA) at room temperature for one hour, the membranes were incubated overnight at 4 °C with anti-myosin light chain 2 (Cell Signaling Technology, Danvers, MA, USA), anti-paxillin (Millipore, Billerica, MA, USA), anti-Rac1 (Santa Cruz Biotechnology), anti-lamin A/C (Santa Cruz Biotechnology), anti-lamin

B1 (Abcam), anti-H3K9ac, anti-H3K9me3, anti-H3K27me3, anti-histone H3 (Cell Signaling Technology), anti-desmin antibody (Abcam), anti-cardiac troponin T antibody (Abcam), anti-myosin fast skeletal muscle (Sigma-Aldrich), anti-α-smooth muscle actin (Abcam), and anti-GAPDH (Sigma-Aldrich). The membranes were then washed with Tris-buffered saline containing polyoxyethylene sorbitan 20 (TBS-T), incubated with DyLight 800 and StarBright 700 fluorescent secondary antibodies (Bio-Rad) at room temperature for one hour, and washed with TBS-T. Multiplex fluorescence was detected using a ChemiDoc Touch MP imaging system (Bio-Rad). Finally, the optical intensity of protein signals was quantified using image analysis software (Image Lab™ 6.0.1; Bio-Rad), and relative mean intensity values were calculated as the ratio of target proteins to internal control protein.

1.2.6. Quantitative reverse transcription (qRT-)PCR analysis

Total RNA was extracted from cells using the RNeasy Mini Kit (Qiagen, Hilden, Germany) according to the manufacturer's protocol. The RNA was reverse-transcribed into cDNA using a PrimeScript® RT reagent kit (Takara Bio Inc., Shiga, Japan). qRT-PCRs were conducted in 7300 Real-Time PCR systems (Applied Biosystems, Foster City, CA), using SYBR1 Green PCR Master Mix (Takara Bio Inc.). This study utilized the following specific primers according to other reports shown in **Table 1.** (Ogawa et al., 2015). Relative mRNA expression of target genes was evaluated by the $2^{-\Delta Ct}$ method and normalized to GAPDH expression.

Table 1. Sequence information for the primers used for qRT-PCR in chapter 1

No	Gene	Primer type	Primer sequence (5' → 3')
1	FN1	Forward	GGTGACACTTATGAGCGTCCTAAA
		Reverse	AACATGTAACCACCAGTCTCATGTG
2	MMP14	Forward	CCATTGGGCATCCAGAAGAGAGC
		Reverse	GGATACCCAATGCCCATTGGCCA
3	PXN	Forward	CAAACGGCCAGTGTTCTTGTC
		Reverse	TGTGTGGTTTCCAGTTGGGTA
4	RAC1	Forward	CCTGCATCATTTGAAAATGTCCG
		Reverse	CCCACTAGGATGATGGGAGTGT
5	GAPDH	Forward	CAACGGATTTGGTCGTATTGG
		Reverse	GCCATGGGTGGAATCATATTG

1.2.7. Statistical analysis

Each experiment was carried out at least three times with triplicate samples in each experiment. Representative experiments are presented, and the results are expressed as the mean ± standard deviation. Statistical significance was considered using Student's *t*-test analysis with a p-value of $p < 0.05$.

1.3. Results

1.3.1. Cellular behaviors on various generations of dendrimer immobilized surfaces

Cell morphology of hMSCs cultured on various generations of dendrimer surfaces for 3 and 10 days are shown in **Figure 6**. As a control condition for common monolayer culture, PS surfaces were used. On the other hand, low-binding culture surfaces were applied to obtain the control condition of 3D aggregate culture.

The hMSCs cultured on the G1 surface at 3 days exhibited similar morphology to culture on the PS surface. Spindle shape and elongated cells appeared in both culture conditions. When the culture period was extended to 10 days, hMSCs formed a confluent monolayer both in PS and G1 surfaces. However, from the time-lapse observation, higher cell migration and cellular protrusion were exhibited on the G1 surface compared to the culture on the PS surface.

Different from the culture on the G1 surface, hMSCs on G3 and G5 surfaces showed a stretched and more rounded shape with less connection between cells at day 3. Cells culture on the G5 surface exhibited a higher amount of round shape than on the G3 surface. The time-lapse observation also showed that temporal stretching and contracting associated with more active migration were displayed in the higher generation of dendrimer surface than on G1 and PS surface. After 10 days of culture, the cells on the G3 surface formed clustered formation of cells.

On the other hand, on the G5 surface, higher migration behavior promotes cell aggregate formation through repetitive stretching and contracting behaviors. Though similar morphology of cell aggregate achieved as aggregate generated in low-binding culture surface, the aggregate behavior is different. In a low-binding culture surface, spontaneous aggregation formed because of the designated shape of the surface providing low-binding between cell and substrate. Static migration of cells after aggregate formation appeared on the low-binding surface, while dynamic aggregate migration was exhibited on the G5 surface.

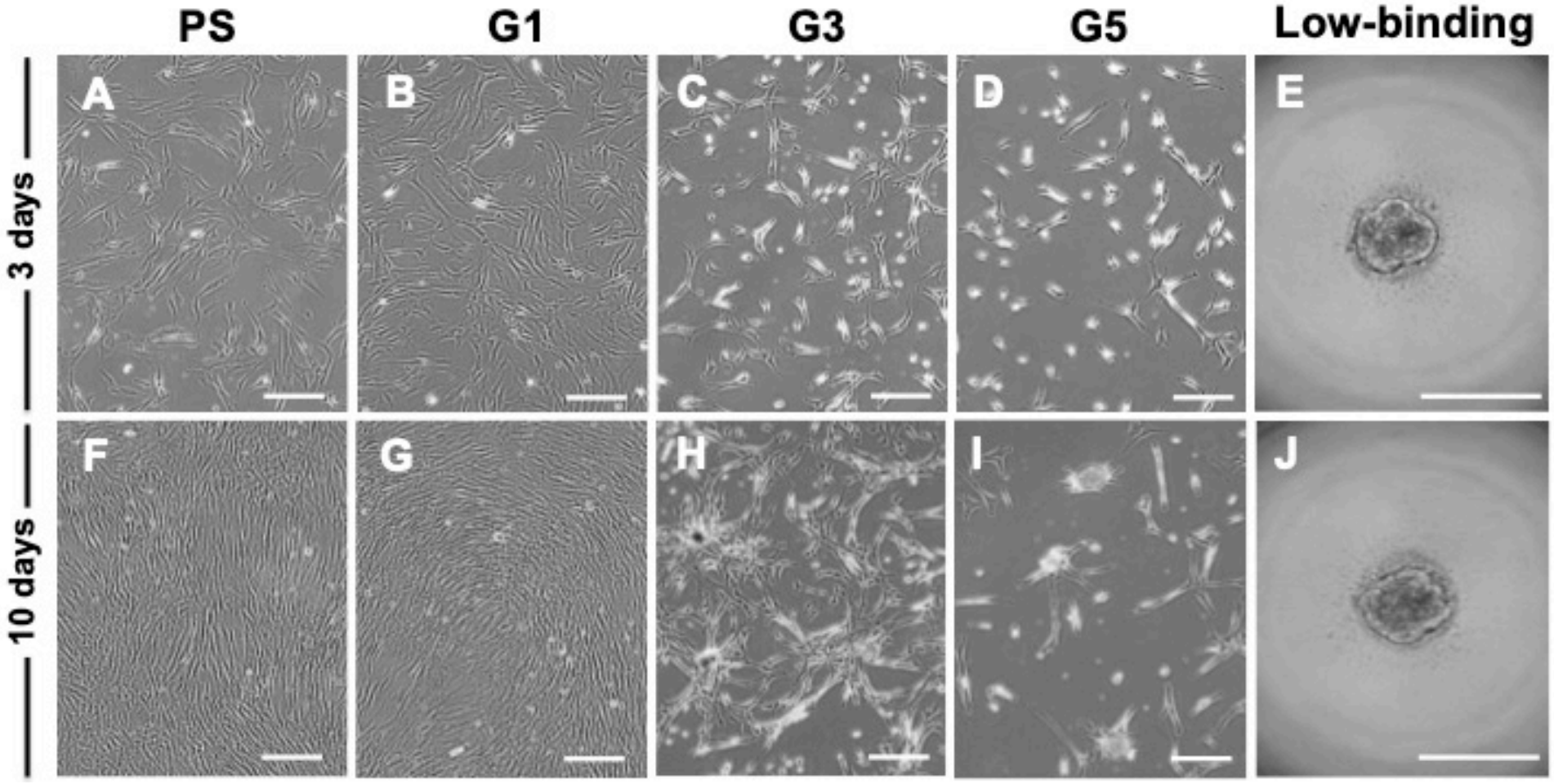

Figure 6. Morphology profiles of hMSCs cultured on PS (A, F), G1 (B, G), G3 (C, H), G5 (D, I), and low-binding (E, J) surfaces on days 3 and 10. Scale bars: 200 μm.

To examine the effects of the culture surfaces on the cellular behavior of hMSCs in detail, the cell attachment efficiency (α_M) and growth activity (μ_M) were examined in various generations of dendrimer surfaces, as shown in **Figure 7**. Although the difference was insignificant, the values of α_M and μ_M decreased with an increase in the generation number of the dendrimer surface.

The value of α_M decreased with an increase in the generation number, α_M=0.93±0.09 for the PS surface, α_M=0.90±0.07 for the G1 surface, α_M=0.90±0.08 for the G3 surface, and α_M=0.81±0.05 for G5 surface (**Fig.7 A)**. The growth activities of hMSCs were similar on PS, and G1 surfaces with the μ_M values are 1.35 $\times 10^{-2}$ h^{-1} for both culture conditions. On the other hand, μ_M values of hMSCs on the G3 and G5 surfaces were slightly decreased (μ_M = 0.93$\times 10^{-2}$ h^{-1} and 0.93$\times 10^{-2}$ h^{-1}, respectively) when compared with that on the PS and G1 surface (**Fig.7 B)**. These results indicated no significant effect of the culture surfaces on cell attachment efficiency, and a higher-generation dendrimer surface only inhibits the growth activity of hMSCs.

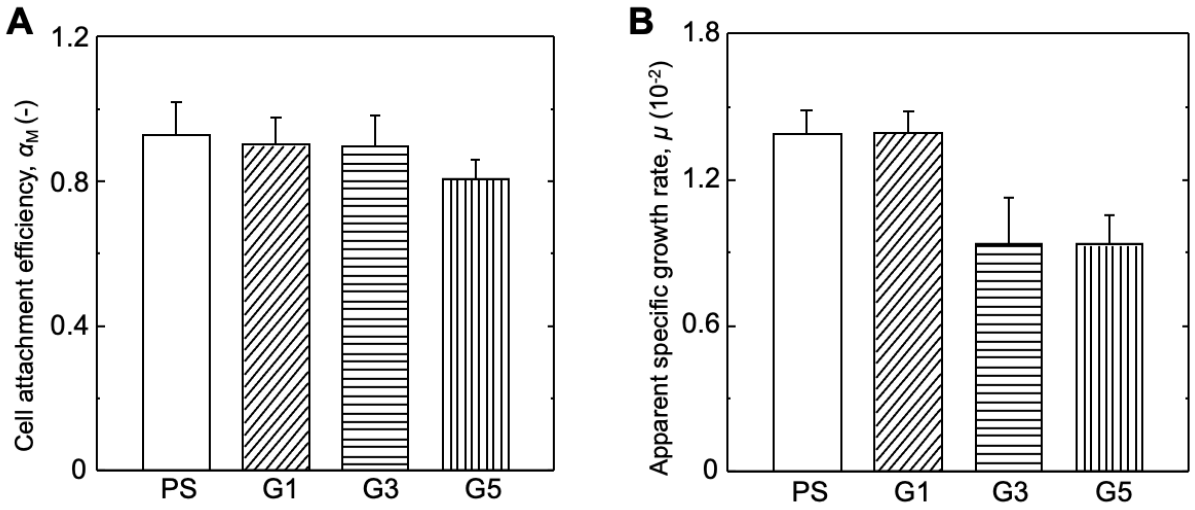

Figure 7. Cell attachment efficiency (A) and apparent specific growth rate (B) of hMSCs on PS, G1, G3, and G5 surfaces.

To further evaluation of differences in cell morphology and cell migration among the examined surfaces, the typical distributions of cell roundness (R_C) of hMSCs cultured on various generations of dendrimer-immobilized and PS surfaces on day 3 after seeding (**Figure 8)**. The R_C values of cells on the PS surface were ≤0.5, whereas R_C values on the G3 and G5 surfaces showed a broader range of $0.2 \leq R_C \leq 0.9$, indicating that stretching was suppressed in some cells. However, R_C values on the G5 surface were mainly ≥0.7, less stretched cells prevailed, and the frequency of round-shaped cells with R_C ≥0.9 drastically increased up to 0.58, which was 2.2 times higher than that on the G3 surface.

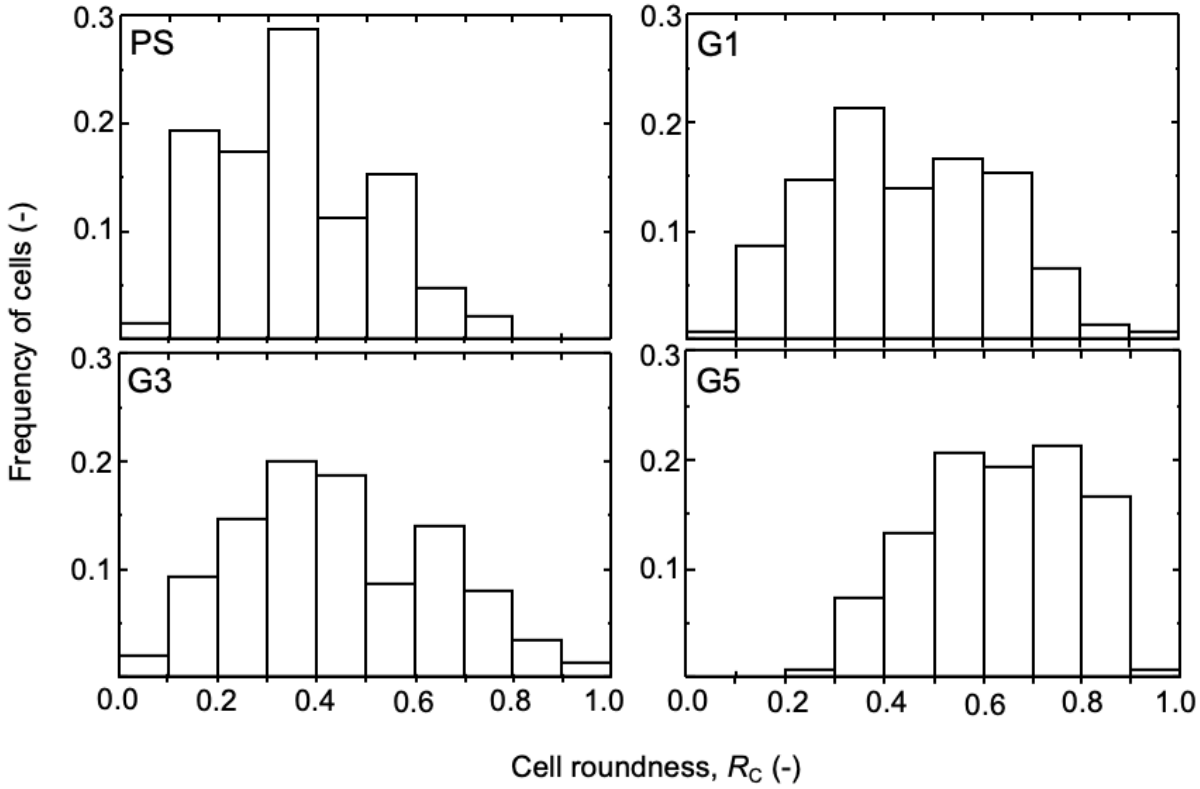

Figure 8. Cell roundness profiles of hMSCs cultured on PS, G1, G3, and G5 surfaces.

The migration rate (V_M) of hMSCs on PS and various dendrimer surfaces are shown in **Figure 9**. It is exhibited that the increase in cell migration rate was parallel with the increase in the generation number of dendrimer surfaces (V_M = 0.68 μm/h on the PS surface, V_M = 1.28 μm/h on the G1 surface, V_M = 1.81 μm/h on the G3 surface, and V_M = 2.45 μm/h on G5 surface).

V_M on the G5 surface was 1.91- and 1.35-fold higher than on the G1 and G3 surfaces, respectively, showing that a higher migration rate was achieved on the G5 surface, amongst other conditions.

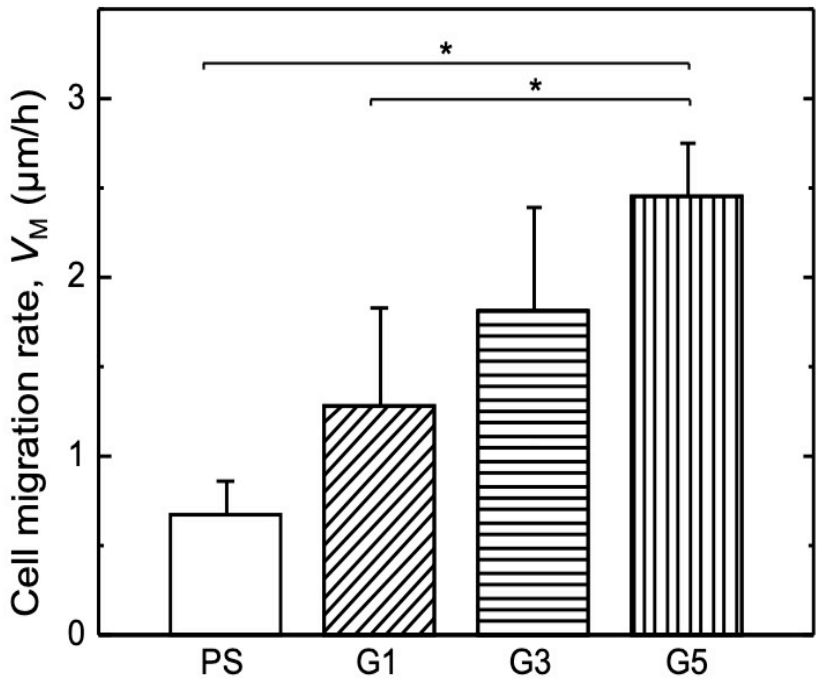

Figure 9. Cell migration rates of hMSCs cultured on PS, G1, G3, and G5 surfaces.

1.3.2. Cellular interaction with ECM

Based on cell morphology and analysis of cellular behavior parameters as mentioned above, it can be concluded that more dynamic cell behaviors were achieved in line with increasing the generation number of dendrimer-immobilized surfaces. This dynamic migration behavior of cells on the dendrimer surface is also related to the interaction between cells and ECM on the substrates.

To elucidate the cell-ECM interaction in the dendrimer surface, the expression level of fibronectin was examined, as shown in **Figure 10**. The mRNA expression of fibronectin (FN1) was analyzed by qRT-PCR on days 3 and 10. On day 3, the expression of FN1 was expressed at higher levels in the G5 surface culture compared to PS, G1, and G3 surface cultures. While the FN1 expressions were significantly decreased after 10 days of culture in most culture conditions, the FN1 expression was maintained on G5 surface culture.

When comparing aggregates that grew on the G5 surface and the low-binding culture surface, FN1 expression in cells aggregates on the low-binding culture surface was higher than that in cells cultured on the G5 surface on day 3. However, after 10 days of culture, the FN1 expression on cell aggregate in the low-binding surface was significantly decreased while on G5 surface culture maintained a similar level. This result shows a significantly lower level of FN1 expression in low-binding surface cell aggregate than cells grown on the G5 surface on day 10.

The mRNA expression of membrane-type matrix metalloproteinase 1 (MMP14), a fibronectin-degrading enzyme, was also analyzed to gain more understanding. The results shown in **Figure 11** exhibited a similar expression pattern of MMP14 over time in each culture condition. On days 3 and 10, MMP14 was expressed at higher levels in cells cultured on the G5 surface than in cells cultured on the G1, G3, and PS surfaces. MMP14 expression in cell aggregates grown in a floating manner on a low-binding surface was higher than that in cells

cultured on the G5 surface on day three but significantly lower than that in cells cultured on the G5 surface at the end of day 10.

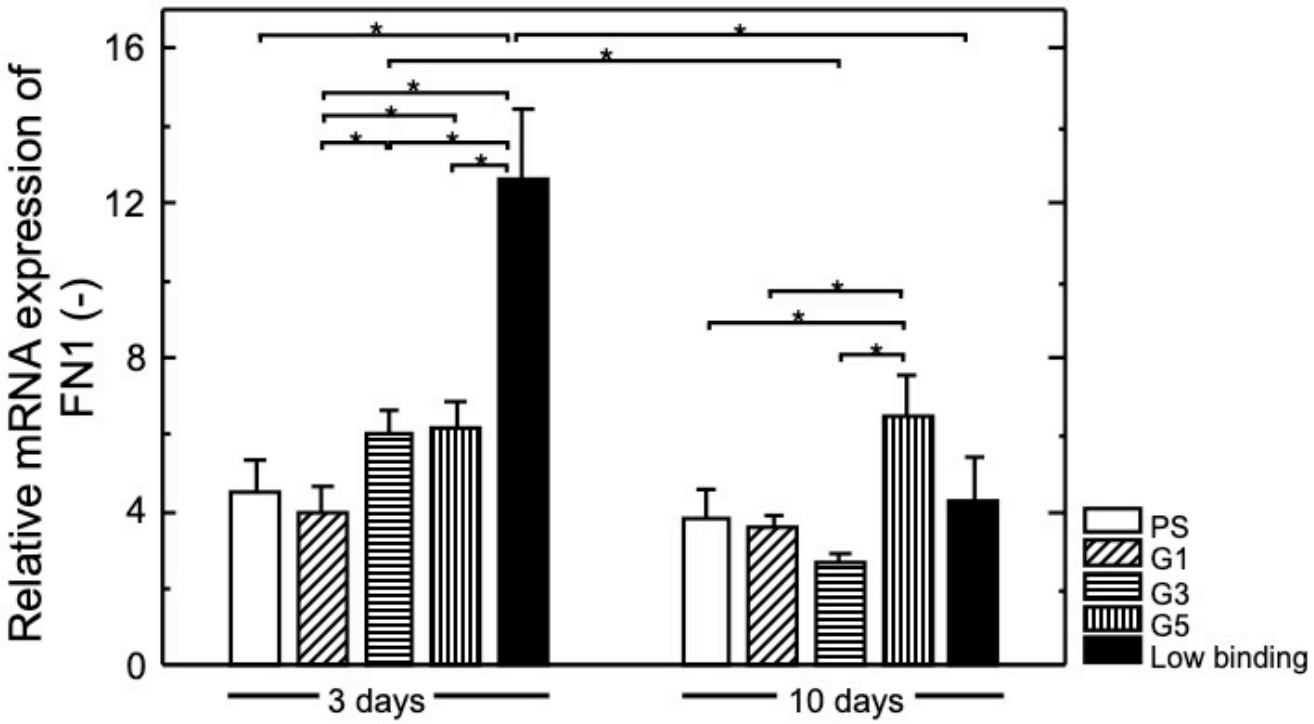

Figure 10. Relative mRNA expression of fibronectin (FN1) in hMSCs cultured on PS, G1, G3, G5, and low-binding surfaces, on days 3 and 10. Experiments were performed in triplicate, and a set of experiments was repeated three times with similar results. Statistical analysis based on Student's *t*-test, $*p < 0.05$.

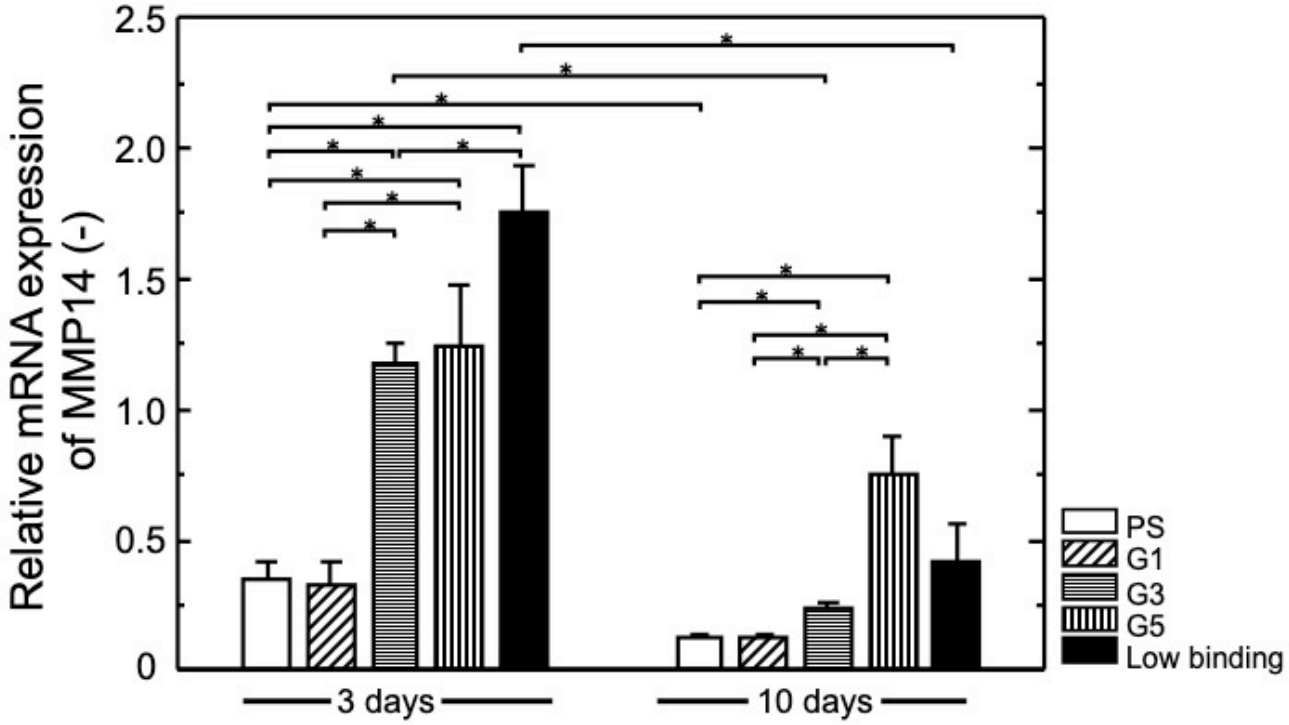

Figure 11. Relative mRNA expression of membrane-type matrix metalloproteinase 1 (MMP14), in hMSCs cultured on PS, G1, G3, G5, and low-binding surfaces, on days 3 and 10. Experiments were performed in triplicate, and a set of experiments was repeated three times with similar results. Statistical analysis based on Student's *t*-test, $*p < 0.05$.

Subsequently, we investigated the critical factor in cell-ECM interaction, the focal adhesion protein such as vinculin. As shown in **Figure 12**, the presence of vinculin protein was examined in all culture conditions to determine the interaction of cells with the substrate. Vinculin was located in the tip of actin filaments as an initial point of actin polymerization. Increasing the generation number of dendrimer surfaces exhibited fewer vinculin spots in the cells. On the G5 surface, in particular, the cells showed lamellipodia extension and immature stress fibers with punctual F-actin and fewer vinculin spots compared with those on the G1 and G3 surfaces.

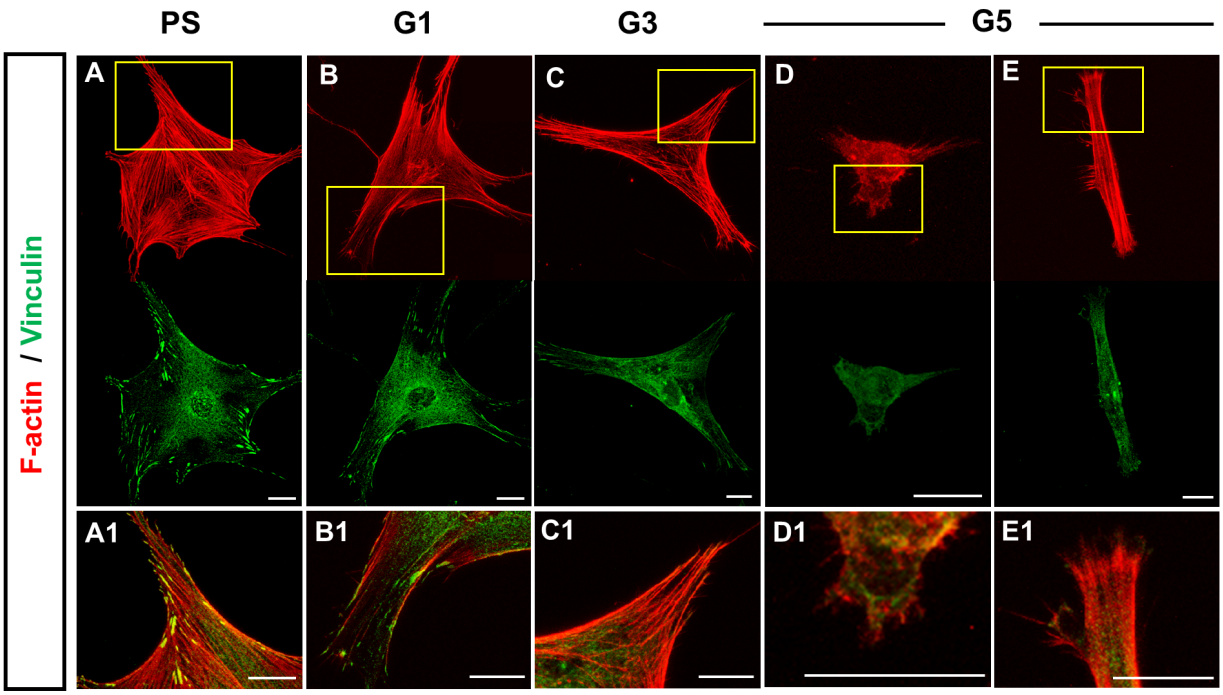

Figure 12. Fluorescence staining images of F-actin filaments (red) and vinculin (green) in hMSCs cultured on PS, G1, G3, and G5 surfaces for three days. Panels A1-E1 show the merged enlargements of demarcated box areas in panels A-E, respectively—scale bars: 20 μm.

1.3.3. Dynamic reorganization of the actin cytoskeleton on dendrimer-immobilized surface

The fluorescence staining of filamentous actin (F-actin) and globular actin (G-actin) was obtained to confirm the cytoskeletal reorganization associated with cell migration on the dendrimer-immobilized surface, as shown in **Figure 13**. The F-actin was observed both in the cytoplasm and cell periphery in the culture on the PS surface on day 3. Stress fibers were seen to develop across the cytoplasm. In the confluent monolayers on the PS surface at 10 days, the appearance of F-actin was enhanced. In contrast, cells on the dendrimer surfaces exhibited extended lamellipodia and filopodia on day 3, and actin stress fibers appeared to be less developed compared with the cells on the PS surface.

In particular, cells on the G5 surface have fewer and less pronounced stress fibers. Moreover, non-filamentous actin was concentrated at punctate structures behind the lamellipodia and along some segments of the leading edge in cells on the G5 surface, particularly after the appearance of the leading lamellipodia at the cell periphery with a noticeable decrease in filamentous actin (**Fig. 13 G1 and I1**). In addition, on the G1 surface, the perinuclear region appeared to be enriched with G-actin than F-actin (**Fig. 13 D2**). On day 10, G-actin was similarly observed in the round-shaped cells as on day 3 (**Fig. 13 P1 and P2**), whereas G-actin in the aggregated cells appeared to be located in nuclei throughout the aggregate (**Fig. 13 Q2**). Similarly, G-actin in aggregated cells on the low-binding surface appeared to be located in nuclei throughout the aggregate on days 3 and 10. Cell aggregates on the low-binding surface appeared to be enriched in non-filamentous relative to filamentous actin on days 3, and 10 (**Fig. 13 K–L and R**), and F-actin was detected only in the nuclei in the periphery of the aggregates on day 10 (**Fig. 13 R1**).

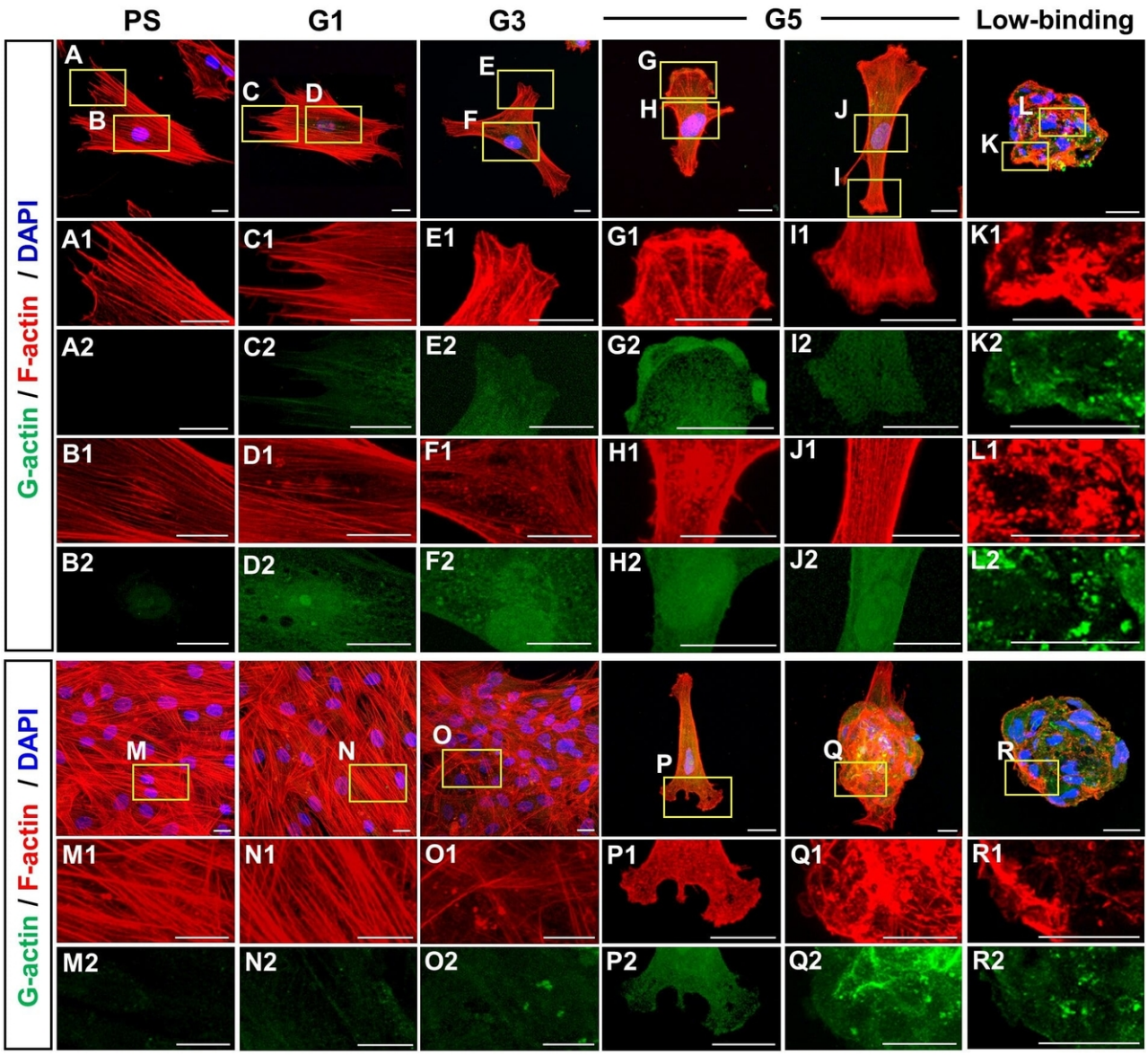

Figure 13. Fluorescence staining images of F-actin (red) and G-actin (green) structures towards nuclei (blue) in hMSCs cultured on PS, G1, G3, G5, and low-binding surfaces for 3 (A–L) and ten days (M–R). The projections of yellow-boxed areas for F-actin structures are shown in panels A1–R1 and those for G-actin are shown in panels A2–R2. Scale bars: 20 μm.

In these experiments, the ratio of G-actin to F-actin was calculated in the cells cultured on day 3. As shown in **Figure 14**, in aggregated cells cultured on the low-binding surface, the G-actin to F-actin ratio was higher than in those cultured on the G5 surface. Cell aggregates grown in low-binding culture surfaces were used as a control to gain insight into the differential

behaviors of hMSCs concerning the aggregate formation on the G5 surface. The dissociated cells spontaneously formed aggregates within 24 h without an adherent surface. These aggregates maintained their spherical morphology without cellular movement within a single aggregate over the observation period.

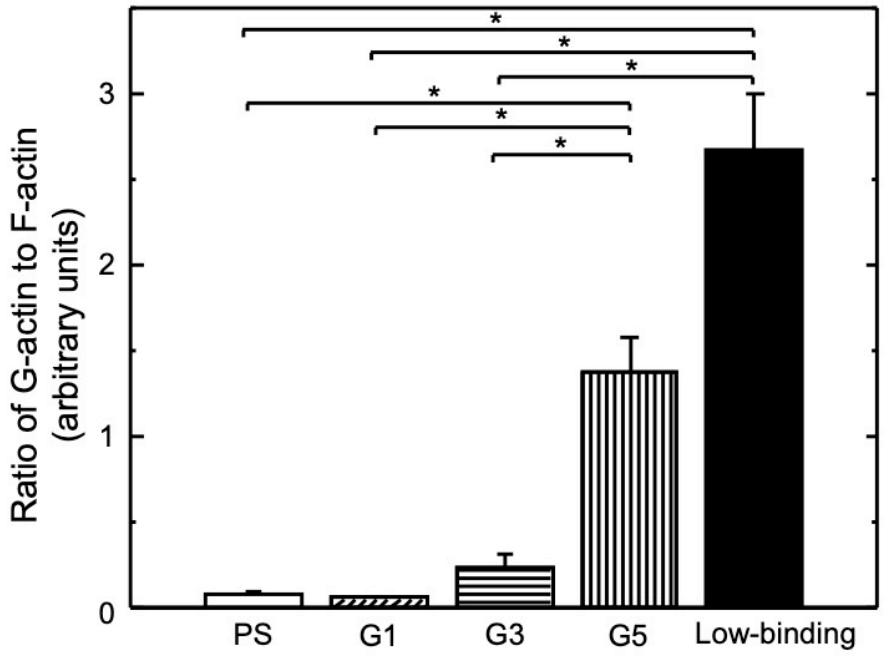

Figure 14. The ratio of G-actin to F-actin in hMSCs cultured on PS, G1, G3, G5, and low-binding surfaces for three days. Experiments were performed in triplicate, and the experiments were repeated three times with similar results. Statistical analysis based on Student's *t*-test, $*p < 0.05$.

1.3.4. Reorganization of a nuclear skeleton structure

Immunofluorescence staining of nuclear lamin A/C towards F-actin was evaluated on days 3 and 10 to assess the correlation between actin cytoskeletal tension and nuclear lamins. As shown in **Figure 15**, on day 3, cells on the PS surface exhibited a typical well-spread. They flattened morphology, with the development of bundles of tense stress fibers along both the apical and basal sides, resulting in a bean-like nuclear morphology. The actin stress fibers appeared elongated on the apical side of nuclei (**Fig. 15 A1**). However, mesh-like actin stress fibers were observed in the basal side of nuclei, while lamin A/C disappeared in the basal side

(**Fig. 15 A2**). The existence of apical actin stress fibers over the nucleus and basal-to-apical polarization of lamin A/C was maintained on the PS surface on day 10 (**Fig. 15 G1 and G2**).

In contrast with cultures on the PS surface, lamin A/C showed a rim pattern of staining around the nucleus in cells cultured on the dendrimer surfaces on days 3 and 10. Cells cultured on the G1 surface exhibited thickened or denser lamin A/C staining, although similar bean-like shapes were observed (**Fig. 15 B4 and H2**). Actin filament disruption was observed in the apical side of nuclei in cells cultured on the G1 surface, resulting in the appearance of the entire lamin A/C on the basal side (**Fig. 15 B1 and B4**). On the other hand, cells cultured on the G3 and G5 surfaces had wrinkled lamina in the rounded nucleus on day 3 (**Fig. 15 C4, D4, and E4**) and showed reduced staining of lamin A/C on day 10 (**Fig. 15 I2, J2, and K2**). For cells on the G5 surface, the formation of contractile stress fibers became pronounced, and nuclei within aggregates were more rounded and irregularly shaped, with a highly wrinkled nuclear envelope on day 10 (**Fig. 15 K2**). When comparing lamin A/C expression between aggregates on the G5 and low-binding surfaces, lamin A/C on the low-binding surface showed a thick appearance at the nuclear periphery on days 3 and 10 (**Fig. 15 F4 and L2**).

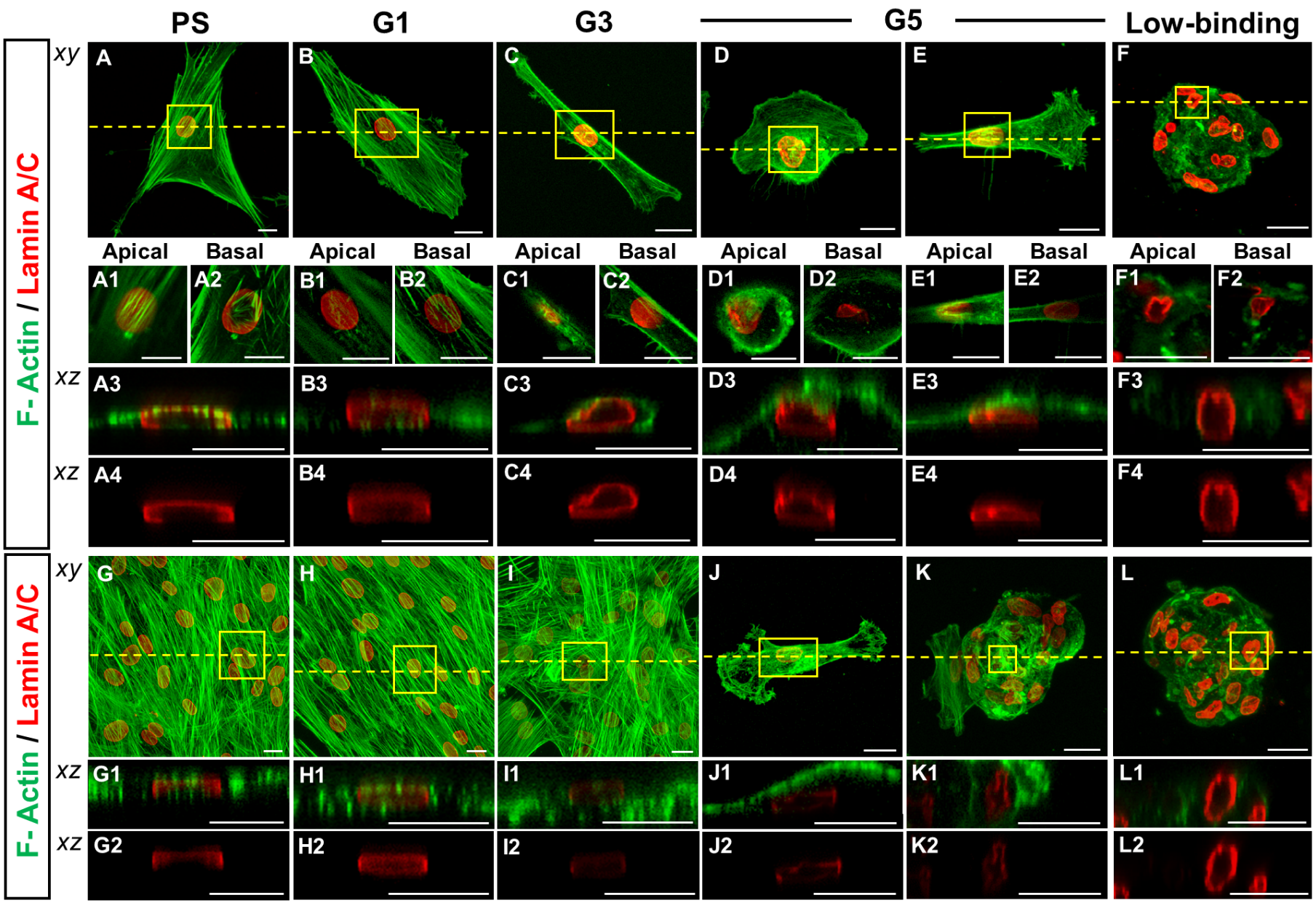
PS
G1
G3
G5
Low-binding
F- Actin / Lamin A/C
xy
xz
xz
A
B
C
D
E
F
Apical
Basal
A1
A2
B1
B2
C1
C2
D1
D2
E1
E2
F1
F2
A3
B3
C3
D3
E3
F3
A4
B4
C4
D4
E4
F4
F- Actin / Lamin A/C
xy
xz
xz
G
H
I
J
K
L
G1
H1
I1
J1
K1
L1
G2
H2
I2
J2
K2
L2

Figure 15. Fluorescence staining images of nuclear lamin A/C (red) towards F-actin (green) structures in hMSCs cultured on PS, G1, G3, G5, and low-binding surfaces for 3 (A–F) and ten days (G–L). Tomogram sections at the *xz* plane (yellow dashed lines) of the upper panels (A–L) are shown in panels A1–L1 for the interpretation of lamin A/C and actin interaction, and those in A2–L2 represent lamin A/C structures. The projections of the yellow-boxed areas for the apical side in single cells are shown in panels A3–F3 and those for the basal side are shown in A4–F4. Scale bars: 20 μm.

The levels of nucleoskeletal proteins (lamin A/C and lamin B1) were examined by western blot analysis on days 3 and 10. On day 3, cells cultured on the PS, G1, and G3 surfaces expressed higher levels of lamin A/C and lamin B1 than those cultured on the G5 surface (**Fig. 16 A**). On day 10, lamin A/C and lamin B1 levels tended to decrease with increasing generation numbers (**Fig. 16 B and C**). The lamin A/C and lamin B1 levels in cells cultured on the G3 and G5 surfaces were reduced to nearly zero at the end of culture on day 10, although they had a wrinkled nucleus with a light rim staining. When comparing aggregates that grew on the G5 and low-binding surfaces, lamin A/C and lamin B1 levels in cells cultured on the G5 surface were significantly reduced by 44.6-fold and 16.5-fold, respectively, respectively from day 3 to day 10. In contrast, the expression levels in cells cultured on the low-binding surface were maintained at the same level until day 10.

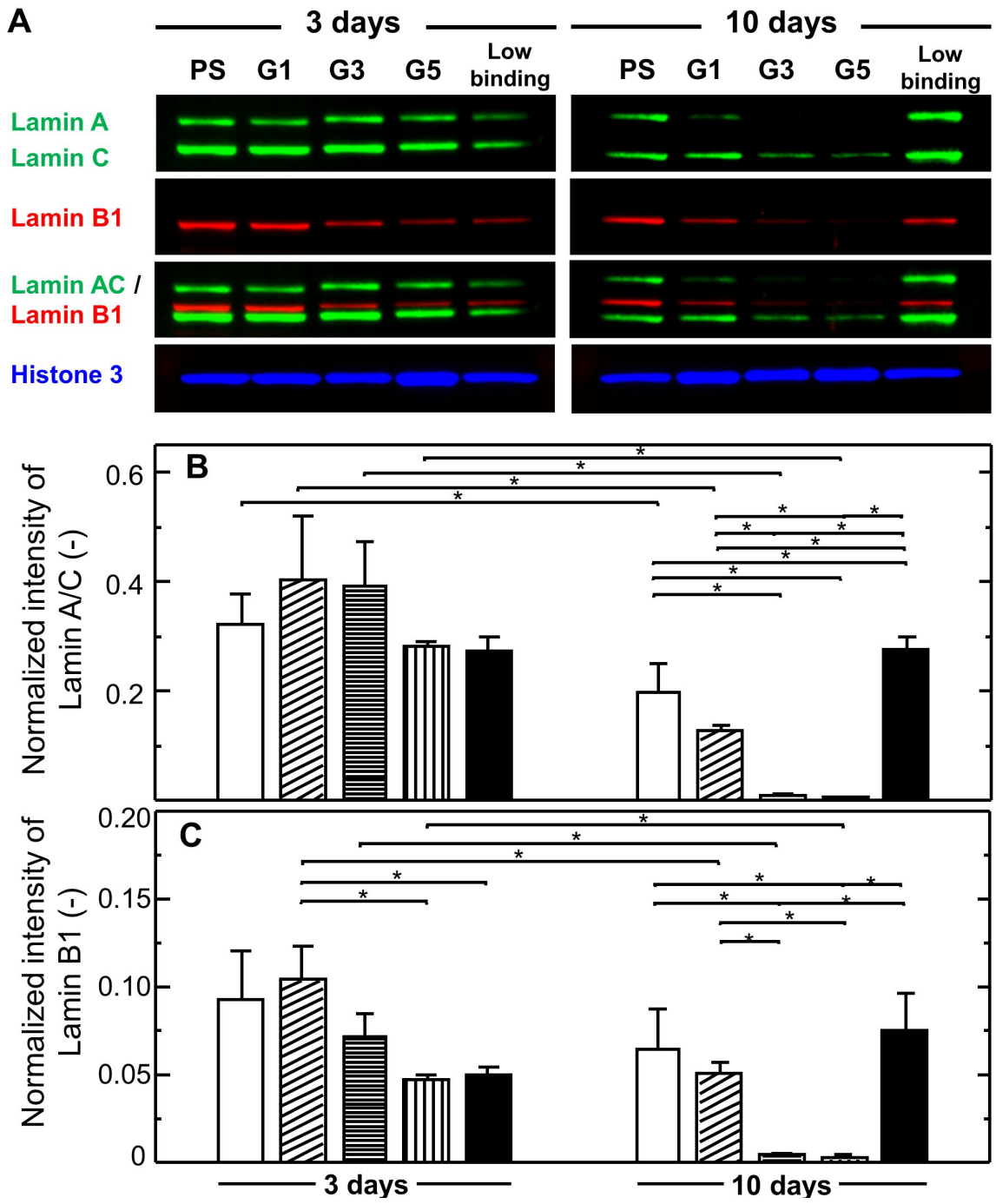

Figure 16. Western blot analysis of lamin A/C (green) and lamin B1 (red) in cells cultured on PS, G1, G3, G5, and low-binding surfaces, on days 3 and 10 (A). Semi-quantitative analysis of lamin A/C (B) and lamin B1 (C) protein intensity relative to histone three on days 3 and 10. Experiments were performed in triplicate and were repeated three times with similar results. Statistical analysis based on Student's *t*-test, $*p < 0.05$.

1.3.5. Global histone modification

The role of epigenetic chromatin markers, including two repressive histone modifications (H3K9me3 and H3K27me3) and one activating modification (H3K9ac), was investigated by western blot analysis. On day 3, H3K9me3, H3K9ac, and H3K27me3 tended to decrease with increasing generation number (**Fig. 17**). In particular, all histone modification levels in cells cultured on the G3 and G5 surfaces were reduced to nearly zero on day 3.

The H3K9me3 was highly detected on PS and low-binding surfaces at day 3, while very subtle expressions were detected on dendrimer surface cultures. After 10 days, the protein formation of H3K9me3 was significantly increased on the G1 surface culture, while in contrast, it was suppressed on the G5 surface (**Fig. 17 A**). On the other hand, H3K9ac was detected on PS, G1, and low-binding surfaces at day 3, and significant increments were found in PS and dendrimer surface after ten days (**Fig. 17 B**). Unlike H3K9me3 and H3K9ac, H3K27me3 expression was significantly increased in all conditions on day 10, and H3K27me3 levels were similar in all conditions (**Fig. 17 C**). When comparing aggregates grown on the G5 and low-binding surfaces, the H3K9me3, H3K27me3, and H3K9ac levels were higher on the low-binding surface than on the G5 surface on day three and were maintained until day 10.

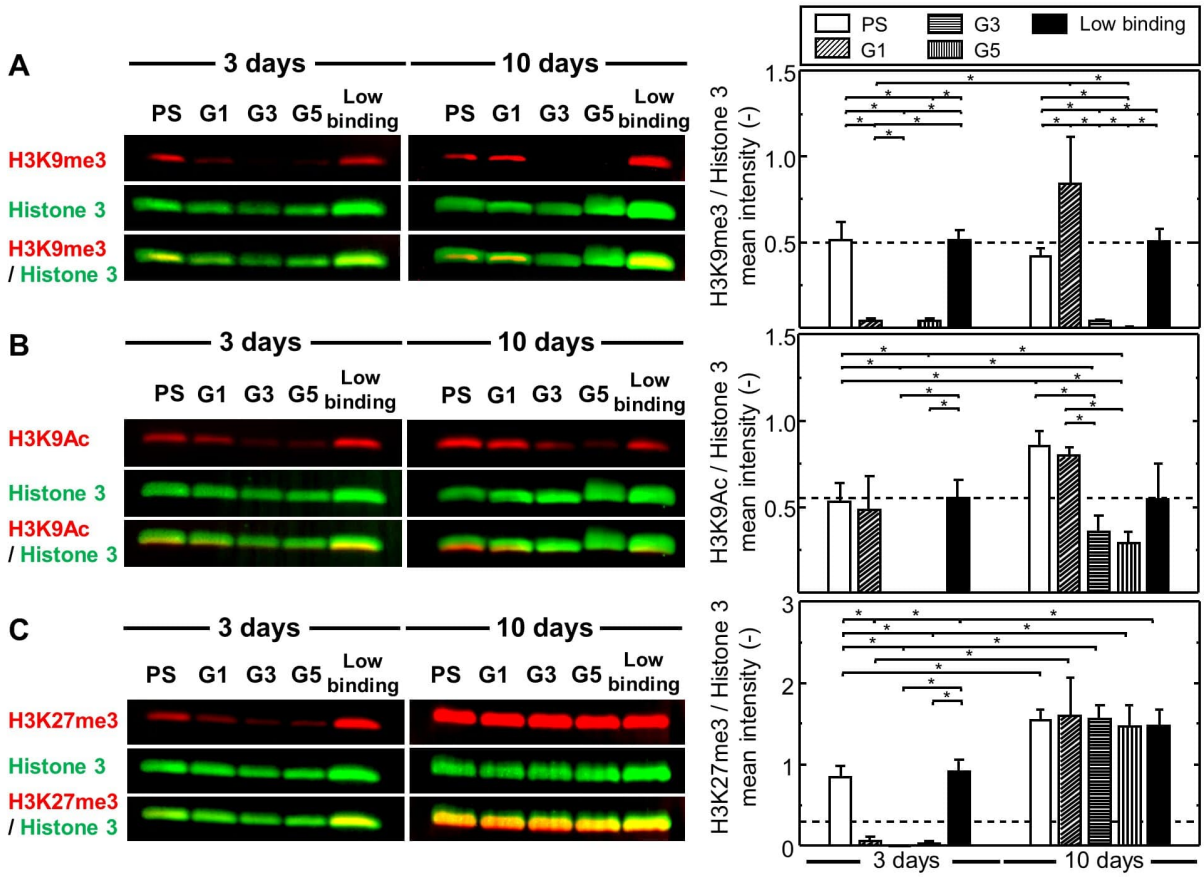

Figure 17. Western blotting and semi-quantitative protein expression analysis of H3K9me3 (A), H3K9ac (B), and H3K27me3 (C) relative to histone 3 in cells cultured on PS, G1, G3, G5, and low-binding surfaces, on days 3 and 10. Dot lines indicate the expression levels of H3K9me3, H3K9Ac, and H3K27me3 on day 0. Experiments were performed in triplicate and were repeated three times with similar results. Self-renewal and muscle lineage commitment

To confirm the phenotypes and myogenic lineage commitment capacities of hMSCs cultured on the dendrimer surfaces for 10 days, western blot analysis for an undifferentiated hMSC surface marker and different muscle lineages (cardiac, skeletal, and smooth muscle cells) markers were performed. In the western blot analysis of the MSC surface marker, CD105 (endoglin), this marker was detected in all culture conditions on days 3 and 10. CD105 at day 3 appeared higher in PS and G1 surfaces than in other conditions. After 10 days, CD105 was

significantly decreased on PS and all dendrimer surfaces, while on the low-binding surface remained unchanged (**Fig. 18 A**).

Desmin, as a common marker of muscle cells, was detected in PS and all dendrimer surfaces at day 3; it was not detected in low-binding surface culture. After 10 days, desmin was decreased by almost half value on the PS surface and completely suppressed on G3 and G5 surfaces (**Fig. 18 B**). On the other hand, smooth muscle contracting protein, α-smooth muscle actin (α-SMA), was prominently detected on PS and G1 surface culture since day 3 with a significant increment of expression, especially on the G1 surface culture after ten days. α-SMA protein marker was utterly suppressed on other culture conditions after ten days (**Fig. 18 C**).

The fast skeletal myosin heavy chain (fast skeletal MHC) was detected only in G3 and G5 surfaces on day three and maintained until day 10 (**Fig. 18 D**). On the other hand, cardiac troponin T (cTnT) expressions were detected only on the G5 surface on day three, and the expression level of cTnT increased significantly on day 10 (**Fig. 18 E**). These results confirm that hMSCs cultured on the dendrimer surfaces can successfully differentiate into cardiac, skeletal, and smooth muscle cells. Muscle lineage commitment markers were undetected for cell aggregates grown floatingly on low-binding surfaces, whereas the MSC marker was expressed (**Fig. 18 A–E**). These results confirmed that dendrimer surfaces induce significant shifts in hMSC lineage, switching to smooth, skeletal, and cardiac muscle lineages.

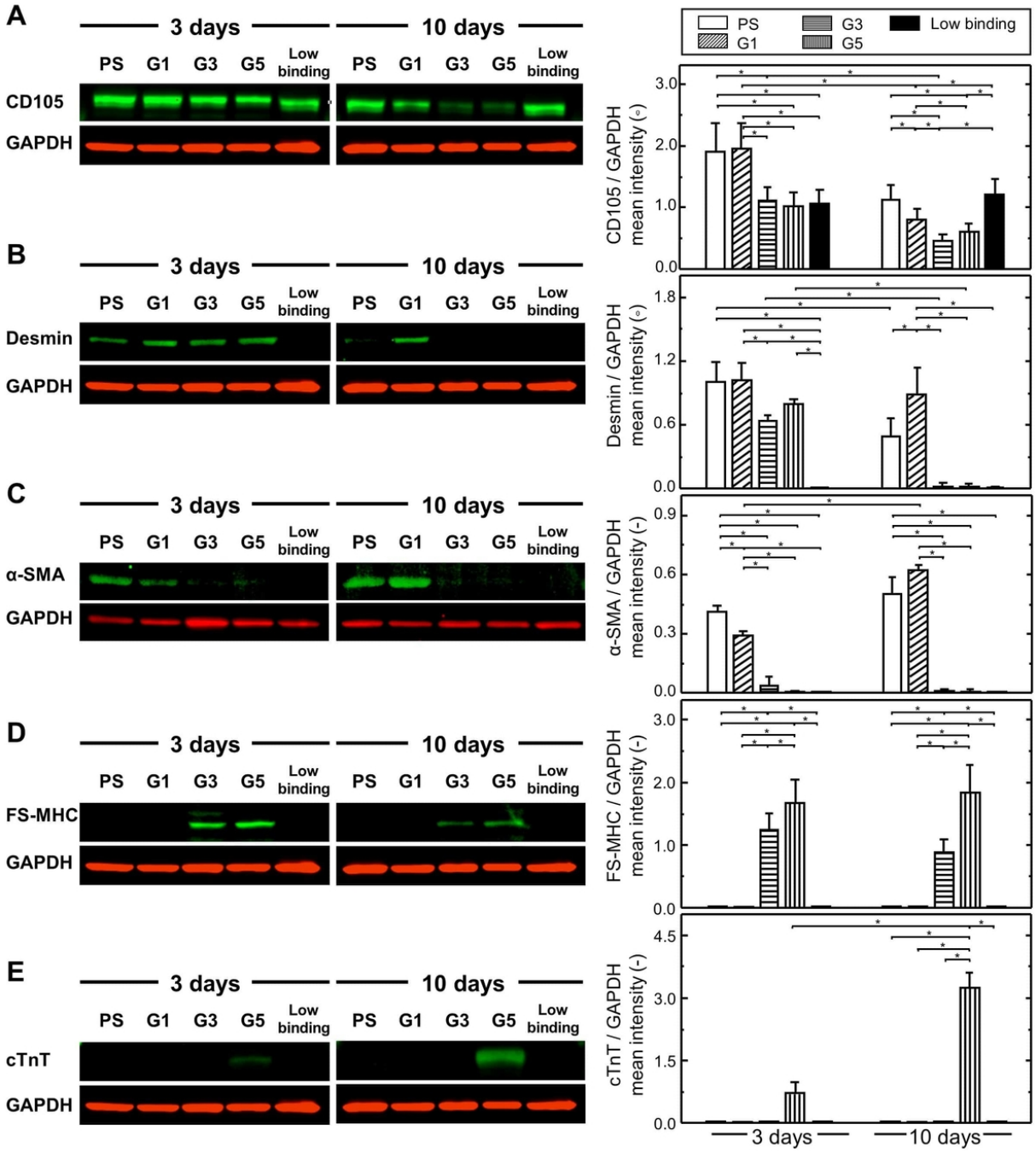

Figure 18. Western blotting and semi-quantitative protein expression analysis of endoglin (CD105) (A), desmin (B), α-smooth muscle actin (α-SMA) (C), fast skeletal MHC (FS-MHC) (D), and cardiac troponin T (cTnT) (E) relative to GAPDH in cells cultured on PS, G1, G3, G5, and low-binding surfaces, on days 3 and 10. Experiments were performed in triplicate and were repeated three times with similar results. Statistical analysis based on Student's *t*-test, $*p < 0.05$.

1.4. Discussion

The development of designated biomaterials has been widely used to study outside-in signaling events, and it is now well appreciated that material cues modulate the epigenetics status of cells (Crowder *et al.,* 2016). The cytoskeleton plays a crucial role in cell migration, and its connection with the nucleus is known to be linked with epigenetics modulation (Heo *et al.,* 2016). The ability of cells to deform is inherently linked to their mechanical properties. As reported in a study supporting these findings, de-polymerization of the actin cytoskeleton and LINC-complex disruption leads to the high accessibility of lamin A/C at the basal nuclear envelope (Kim *et al.,* 2017). The lamin A/C expression and histone methylation show a correlation in epigenetics changes during early differentiation events, giving an insight into how altered cell behaviors are transduced into nuclear biochemical signals. It has also been reported that the chromatin structure contributes directly to gene transcription and the physical properties of the nucleus (Uzer *et al.,* 2016).

This study investigates the switching of muscle lineage differentiation by epigenetic modifications driven by the migratory behavior of hMSCs on dendrimer surfaces with various generation numbers. **Figure 19** shows a possible mechanism of muscle lineage switching by cytoskeletal and nucleoskeletal reorganization related to epigenetics modification-driven migratory behavior on dendrimer surfaces.

1.4.1. Surface-driven migratory behavior of hMSCs leads to changes in connections between the nucleoskeleton and the cytoskeleton.

Based on the concept of cell stimulation through the regulation of cell behaviors, many strategies have been proposed to control switch in lineage commitment of hMSCs during in vitro cultures (Kim *et al.,* 2010; Kim *et al.,* 2014; Ogawa *et al.,* 2015; Ogawa *et al.,* 2016). In this study, the role of surface on the migratory behavior in guiding muscle lineage switching of

hMSCs has been investigated on dendrimer surfaces with different generation numbers. We found that, by increasing the generation number of dendrimer surface, dynamic migration behavior was increased, and production of cellular fibronectin was up-regulated proportionately (**Fig. 10**).

Changes in fibronectin assembly and cytoskeletal formation were responsible for the dynamic cell behaviors on the dendrimer surfaces (Ogawa *et al.,* 2015). The cell aggregate obtained at day 10 on the G5 surface exhibited the highest level of FN1 expression than other culture conditions, which signifies the higher production of cellular fibronectin secreted from cells on this surface. Furthermore, up-regulation of MT1-MMP secretion increases the degradation of fibronectin fibrils in ECM, which promotes active extension and generates phosphorylation of focal adhesion protein to develop immature stress fibers (**Fig. 11**). While cells produce MMPs to degrade the ECM as they migrate, some cells can also migrate by undergoing physical deformation and squeezing through the ECM. Secretion of cellular fibronectin is necessary to promote cell migration by assembling fibronectin fibrils on ECM (Sevilla *et al.,* 2010; Pankov & Yamada, 2002; Esparza *et al.,* 1999).

Based on understanding the direct linkage of cytoskeleton and nucleoskeleton through the LINC complex, de-polymerization of F-actin disrupts LINC complex connectivity and affects nucleoskeleton tension as well (Ihalainen *et al.,* 2015). Monomeric G-actin is the building block for F-actin but is not considered to play a direct role in the spatio-temporal control of actin dynamics in cell migration (Huang *et al.,* 2015). When the generation number increased, the cells exhibited changes in actin polymerization and de-polymerization behaviors associated with stimulated migration. Cells on the G1 surface exhibited F-actin de-polymerization in the apical site of the nucleus, remarked by the presence of G-actin monomer in a particular area. The absence of an actin cap reduced the compression in the apical site of the nucleus. It resulted in a non-polarization of nuclear lamin A/C (**Fig. 15**).

On the G5 surface, repetitive morphological changes from stretching to contracting to enhance the disassembly of F-actin stress fibers and reduce the cellular tension and compression to the nucleus. In stretching shape, cells promote active extension and the development of cellular protrusions, generating a profound tension towards the nucleus. The spontaneous contraction of cells after stretching then puts the nucleoskeleton in a super-relaxed condition (**Fig. 15**). Those repetitions of stretching and contracting during dynamic migration on the G5 surface not only cause perturbation of nucleoskeleton and promote relaxation of lamin A/C but also degrade nuclear lamin protein in nucleus (**Fig.15**). Cell aggregate formation during dynamic migration on G5 surface displayed vast de-polymerization of F-actin, similarly to cell aggregate obtained from low-binding culture surface. However, in the basal part of cell aggregate on the G5 surface, some cells maintain attachment to the substrate, resulting in repetitive aggregate coalescence and cell-cell dissociation within the aggregate.

The present study's results indicate that the surface-driven migratory behavior level varies concerning the cytoskeleton and nucleoskeleton during active cell migration. It was also demonstrated that changing the generation number of dendrimers could promote the morphological change of cells, accompanied by the dynamic cytoskeletal formation of cells on the culture surface. The possible processes for the nuclear lamina-cytoskeleton organization of hMSCs associated with dynamic behaviors were considered as, by increasing the dendrimer generation number, active cell migration with repetitive stretching and contracting increase, resulting in the suppression of vinculin and undeveloped stress fibers (**Fig. 12**).

In particular, cells on the G5 surface changed their morphology due to repetitive stretching and contracting, spontaneous aggregation through cell division, also coalescence of migrating cells. The particular dynamic migratory behaviors were maintained in aggregate forms. During this dynamic migration behavior, the cells exhibited changes in actin polymerization and depolymerization manners associated with stimulated migration on the G5 surface (**Fig. 15**).

1.4.2. Alternation of migration-driven epigenetic mechanism switches their transition from a self-renewal state to three forms of smooth, skeletal, and cardiac muscle lineages in hMSCs

Mechanical forces exerted from the substrate into the nucleus through cell-substrate interaction, and cytoskeleton reorganization on dendrimer surfaces culture are assumed to be affected by genomic regulation inside nuclei (Steensel & Balmont, 2017). Lamin A/C, as a part of the nucleoskeleton, forms functional associations with polynucleosomes, histones, and DNA, known as lamin-associated domains (LADs) (Dahl *et al.,* 2011). LADs consist mainly of silence genes and are enriched by the typical heterochromatin histone modification such as H3K9me3 and H3K27me3 (Uzer *et al.,* 2016; Dahl *et al.,* 2011; Steensel & Balmont, 2017). H3K9me3 and H3K27me3 play an essential role in stem cell differentiation to prevent cellular reprogramming and silencing of lineage-specific genes from maintaining cellular identity (Guelen et al*.,* 2008).

In stem cell reprogramming, H3K9me3 has a function to maintain an undifferentiated state and prevent specific-lineage commitment by repressing activation of transcription factors and reorganized chromatin into packed heterochromatin. Unlike H3K9me3, H3K27me3 plays a role in facultative silencing, which applies cell-type-specific repression (Becker et al*.,* 2016), enabling it to present not only in the undifferentiated state but also during differentiation. It remains unclear how gene expression patterns are switched from stem cell-specific to lineage-restricted expression and whether epigenetic modifier-mediated chromatin dynamics underlie differentiation-dependent transcription changes.

In this study, fast skeletal MHC and cTnT expressions, used as markers for skeletal muscle cells and cardiomyocytes, were not detected in the cells on the PS and G1 surfaces. Fast skeletal MCH markers were expressed in G3 and G5 surface cultures, although prominently seen in the cells on the G5 surface. On the other hand, cTnT only appeared in the G5 surface culture. It was

found that cells on a higher generation of dendrimer surface have increased nuclear deformation and decreased protein levels of lamin A/C and lamin B1 during culture. Furthermore, analysis of two repressive (H3K9me3 and H3K27me3) and one activating (H3K9ac) modifications revealed that suppression of H3K9me3 was maintained from the early to late phase of culture on the G3 and G5 surface. At the same time, H3K27me3 and H3K9ac were suppressed early but significantly up-regulated after a prolonged culture period. On the other hand, less disruption of nuclear lamin was found in the G1 surface linked to the up-regulation of H3K9ac since the early period of culture and significant up-regulation of H3K9me3 after a prolonged culture period. The differences in histone modification regulation between the G1 surface and the higher generation number of dendrimer surfaces are presumed to be related to the expression of smooth muscle cells marker, desmin, and α-SMA, particularly in the G1 surface (**Fig. 15**).

Though the direct connection between different patterns of histone modifications regulation and switching of muscle lineages differentiation needs to be clarified by further investigation, this study has significantly contributed to understanding the mechanotransduction mechanism involving cell-ECM interaction to cytoskeleton-nucleoskeleton interaction and genome regulation inside the nucleus based on cellular response to biomaterials modification. Based on these new insights into how the physical environment on the designed surface influences cell behavior, our findings might contribute to a better understanding of mechanical control mechanisms in the interaction of cells with their extracellular environment. Such knowledge is expected to be essential in developing future material strategies for creating artificial cell-instructive niches.

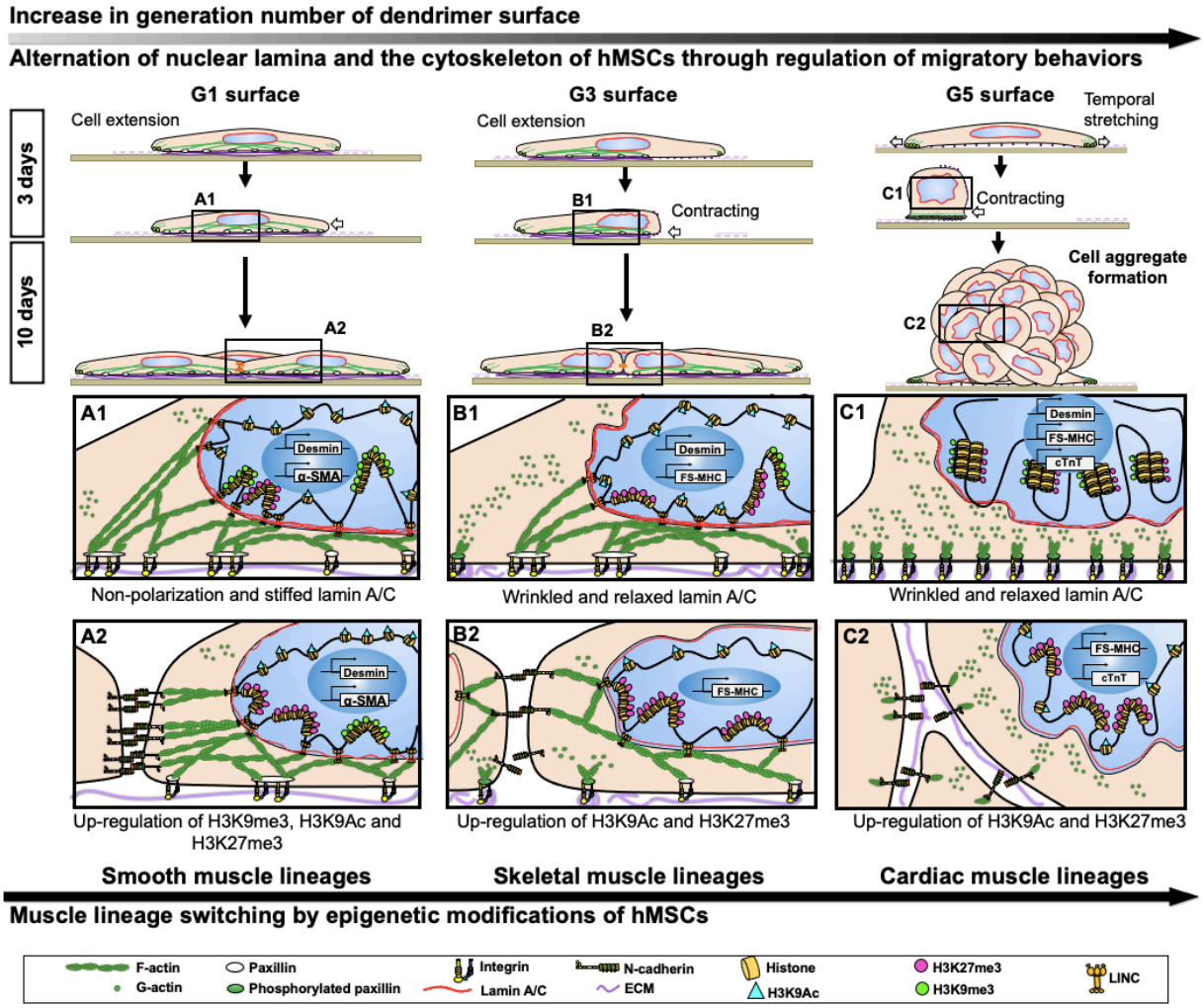

Figure 19. Schematic drawing showing the possible mechanism of muscle lineage switching by cytoskeletal and nucleoskeletal reorganization related to migratory behavior on dendrimer surfaces.

1.5. Summary

This chapter examined the migratory behavior of hMSCs in various generations of dendrimer-immobilized surfaces to understand the dynamic migratory behavior due to cell-substrate interaction. Regulation of extracellular matrix component and focal adhesion complex as a cell response to mechanical forces derived by immobilized dendrimer in the substrate leads to alteration of cytoskeleton and nucleoskeleton structures. Nucleoskeleton deformation in hMSCs culture related to the regulation of global histone modification in H3K9me3, H3K27me3, and H3K9ac. Thus phenomena of reorganizations of the cytoskeleton and nuclear skeleton related to migratory changes on dendrimer-immobilized surface are responsible for the integrated regulation of epigenetic formations through histone modification, which leads to switching differentiation commitment of hMSCs to smooth, skeletal and cardiac muscle lineages.

Chapter 2

Enhancement of cardiomyogenic commitment through migration-driven epigenetic memory maintenance during the aggregate-based passage

2.1. Introduction

In a stem cell study, Conrad Hal Waddington initially proposed epigenetics analysis of stem cell fate in the early 1900s, entitled the "*epigenetic landscape*". The epigenetic landscape concept describes the determination mechanism of stem cell fate regarding the epigenetic changes as methylation, acetylation, or phosphorylation in genetics materials which then lead to transcription of specific gene expression related to differentiation commitment (Mathews *et al.,* 2009). Epigenetics defines various gene expression changes that may occur without alteration in the DNA sequence (Gibney & Nolan, 2010). Such modifications in genomic levels can alter gene expression and, therefore, the properties and behavior of the cells (Handy *et al.,* 2011).

Inter-connection between the nuclear skeleton and chromatin within nuclei, which is linked through the nuclear membrane and LINC complex, transducing mechanical forces from outside nuclei and affecting the regulation of chromatin structures (Dahl *et al.,* 2011; Hieda *et al.,* 2019; Bouzid *et al.,* 2019). The direct link between nuclear architecture and cellular differentiation suggests that chromatin organization might be necessary for stable lineage commitment (Ahmed *et al.,* 2010; Boland *et al.,* 2014). Post-translational modifications of histones, including acetylation and methylation of conserved lysine residues, are also dynamically regulated by chromatin structure, putting histone modifications one of the mechanisms in epigenetic memory formation (Bowman & Poirier, 2015).

Epigenetic memory is defined as modifications in genomic levels of cells that do not alter their DNA sequence and have been inherited from the cell from which it descends (Bird, 2002). In the mechanism of epigenetic change, histone modification plays an essential role in epigenetic memory regulation. Histones become modified by acetylation and methylation and are amenable to mono-, di- and tri-methylated, adding to the complexity of histone modifications (Handy *et al.,* 2011). H3K27me3 marks dynamically regulated genes and is easily reversible, enabling switched-on and off states in response to developmental signals, holding an important role in epigenetic changes (Lafos et al*.,* 2011; Duncan *et al.,* 2014). Methylation and acetylation of H3K9 are also crucial in, specifically, the epigenetic changes of MSCs during differentiation (Perez-Campo & Riancho, 2015). Overall, these histone modifications have been found to correspond to regulate chromatin modifications and gene transcription during developmental stages and cellular differentiation (Wu *et al.,* 2006).

The intrinsic and extrinsic signals that are generated within the cell or in its microenvironment are likely to serve as the triggers to initiate a cascade of events that will convert the "ready state" epigenetic marks into the active epigenetic marks defining the properties and functional status of the cell at the various stages of development. These phenomena could be described as epigenetic memory formation (Handy *et al.,* 2011; Bowman & Poirier, 2015, Wu *et al.,* 2006). Accumulative signals of epigenetic memory factors during the culture process of stem cells by serial passaging in a prolonged period were assumed to maintain the epigenetic changes and enhance the cellular transcription within cells.

According to the previous chapter in this study, through an understanding of migratory behavior changes and regulation of epigenetic memory driven by culture process on the dendrimer-immobilized surface, to enhance the differentiation commitment of hMSCs toward cardiomyogenic lineage, a suitable culture process needs to be addressed. Based on the finding in the previous chapter of the study, the migration-driven aggregates behaviors on the G5 surface

play a role as a factor of epigenetic memory formation, and the prolonged accumulation of epigenetic changes triggers tried to be achieved by serial passages of cell aggregates. In hypothesis, higher constitutive deformation of the cytoskeleton and nuclear skeleton structure and accumulation of epigenetic changes could maintain the epigenetic memory and promote the enhancement of hMSCs differentiation commitment into the cardiomyogenic lineage.

2.2. Materials and methods

2.2.1. Cells and culture conditions

HMSCs derived from bone marrow grown in an MSC growth medium were obtained from Lonza (lot no. 0000183402). hMSCs were routinely subcultured an in hMSC growth medium (Lonza) at 37°C in a humidified atmosphere containing 5% CO_2. When reaching 70% confluence on the culture surface, the cells were detached by enzymatic treatment with 0.1% trypsin / 0.02% EDTA solution (Sigma-Aldrich). Cells with a passage number of less than five were used in the experiments. For all experiments, hMSCs were seeded at a viable cell concentration of 5.0×10^3 cells/cm^2. The hMSCs were cultured in Dulbecco's modified Eagle's medium (DMEM; Sigma-Aldrich) supplemented with 10% fetal bovine serum and antibiotics (Life Technologies) in 8-well plates (Nunc) and T-75 flasks (Corning Inc.) with and without dendrimer-immobilized to the surface. The culture medium was changed every three days. To activate or inhibit cell migration, hMSCs were exposed to a medium with 50 μg/mL Rac1 activator HMG-1 (Sigma-Aldrich) or 5 μg/mL Rac1 inhibitor NSC23766 (Calbiochem, Merck) from day 3 to day 10.

To understand the effect of passaged culture in this experiment, hMSCs from the initial culture in the surface with or without dendrimer-immobilized were subcultured through two different passage conditions **(Fig. 20)**. Single cell-based passaging was applying enzymatic detachment to obtain single cells hMSCs and then reseeded into new culture surface. In the

aggregate-based passaging, cell aggregates were collected through tapping and directly reseeded into the new surface without breaking the aggregates. In the serial passage culture experiments, hMSCs were cultured for 40 days and passaged every ten days of culture **(Fig. 21)**.

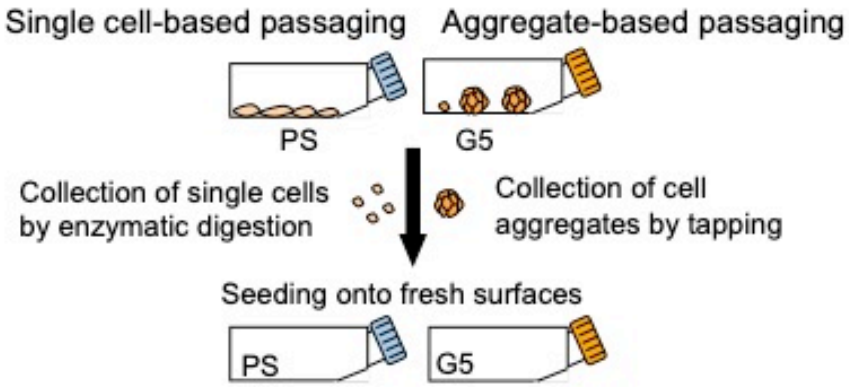

Figure 20. Schematic diagram showing the passaged hMSCs culture process conditions

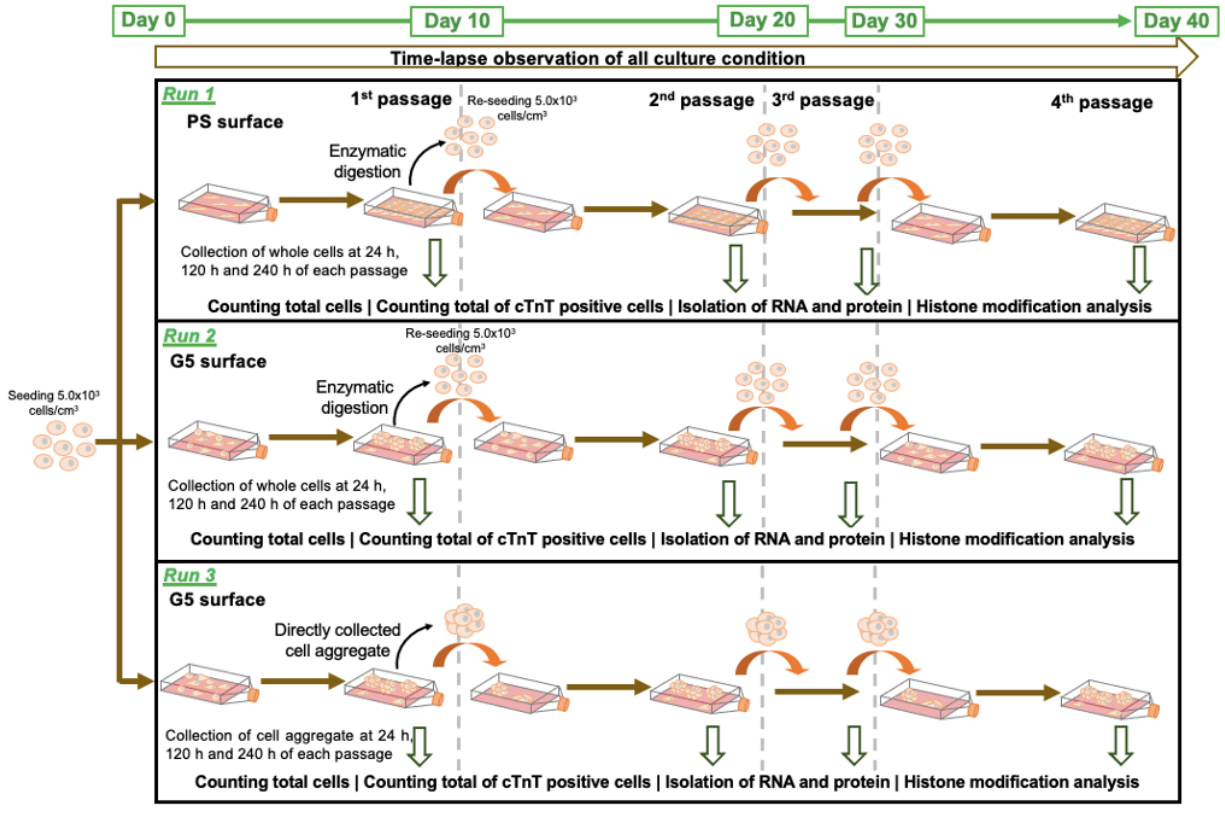

Figure 21. Schematic diagram showing the serial passage culture process of hMSCs

2.2.2. Preparation of dendrimer-immobilized surface

The polyamidoamine dendrimer surface was established on the polystyrene (PS) surface of 8-well plates (Nunc) or T-75 tissue culture flasks (Corning Inc.). G5 surfaces were created under sterile conditions by synthesizing dendrimers over four reactions. First, hydroxyl groups were displayed by adding potassium *tert*–butoxide onto the polystyrene surface. Then, glutaraldehyde and tris(2-aminoethyl) amine solutions (pH 9.0, adjusted with 0.1 mol/L NaOH) were poured onto the surface one after another to construct a dendron structure. Every culture vessel was rinsed with sterile water, and the dendron structure construction procedures were repeated five times. Finally, *D*-glucose was added to the surface as a final ligand.

2.2.3. Determination of the cell growth and cardiomyogenic potential of aggregates

To determine the total cell number (X_T), after ten days of culture, hMSCs were detached through an enzymatic reaction, and the viable cell number was determined using trypan blue exclusion and counted on a hemocytometer. The cells then continue to be re-seeded into the new surface with the fixed seeding density at 5.0×10^3 cells/cm^2 (X_0) and cultured for another ten days before undergoing the next passage cycle. The ratio of total cell number (X_T/X_0) was calculated at the end of every passage.

To evaluate the induction of cardiomyogenic differentiation of hMSCs, after specific periods of culture, cells were obtained through an enzymatic reaction. They re-seeded with a low seeding density number on the PS surface. The cells were then stained using nuclei stain and antibodies against cTnT, as mentioned previously. The images were captured using IN Cell Analyzer 2000 (GE Healthcare, Uppsala, Sweden) using 10× magnification of the objective lens. Signal intensities of fluorescence for cTnT and DAPI were obtained by excitation at the corresponding wavelengths of 488 and 358 nm, respectively. The ratio of cTnT-positive cell number (X_P) towards DAPI-positive cell number (X_T) was calculated.

2.2.4. Immunofluorescence staining

Cells were fixed with 4% paraformaldehyde and permeabilized by incubation in PBS with 0.5% polyoxyethylene octyl phenyl ether. After masking non-specific proteins through blocking (Block Ace; Dainippon Sumitomo Pharma), the cells were incubated with primary antibodies, anti-CD105 (Santa Cruz), anti-cardiac troponin T antibody (Abcam), and anti-Lamin A/C antibody (Santa Cruz). Then, the cells were incubated with secondary antibodies, Alexa Flour 594-conjugated goat anti-mouse IgG (Life Technologies). Nuclei were stained with 4',6-diamidino-2-phenylindole dilactate (Life Technologies). Filamentous (F-actin) were stained with fluorescence 488-phalloidin (Life Technologies). Fluorescence images were taken using a confocal laser scanning microscope (FV-1000; Olympus) and a 60× objective lens.

2.2.5. Protein extraction and western blot analysis

Total cellular protein was extracted from cells using RIPA Buffer lysis/extraction reagent (Sigma-Aldrich). In contrast, the nuclear protein was extracted using Nuclear Extraction Kit (Abcam). Samples were mixed with sample buffer containing 2-mercaptoethanol and boiled at 95°C for 10 min. Proteins were separated according to molecular weight by sodium dodecyl sulfate-polyacrylamide gel electrophoresis (SDS-PAGE) using 10% and 15% polyacrylamide gels, SuperSep TM (FUJIFILM Wako Pure Chemical Corporation) and transferred to polyvinylidene fluoride membranes (Bio-Rad). After masking the non-specific proteins with ECL Blocking Agent (GE Healthcare) at room temperature for one hour, the membranes were incubated overnight at 4 °C with anti-lamin A/C (Santa Cruz Biotechnology), anti-lamin B1 (Abcam), anti-H3K9ac, anti-H3K9me3, anti-H3K27me3 anti-histone H3 (Cell signaling Technology), anti-cardiac troponin T antibody (Abcam), anti-Endoglin CD105 (Santa Cruz Biotechnology) and anti-GAPDH (Sigma-Aldrich). The membranes were then washed with Tris-buffered saline containing polyoxyethylene sorbitan 20 (TBS-T), incubated with DyLight

800 and StarBright 700 fluorescent secondary antibodies (Bio-Rad) at room temperature for one hour, and washed with TBS-T. Multiplex fluorescence was detected using a ChemiDoc Touch MP imaging system (Bio-Rad). Finally, the optical intensity of protein signals was quantified using image analysis software (Image Lab TM 6.0.1; Bio-Rad), and relative mean intensity values were calculated as the ratio of target proteins to internal control protein.

2.2.6. Quantitative reverse transcription (qRT-)PCR analysis

Total RNA was extracted from cells using the RNeasy Mini Kit (Qiagen) according to the manufacturer's protocol. The RNA was reverse-transcribed into cDNA using a PrimeScript® RT reagent kit (Takara Bio Inc). qRT-PCRs were conducted in 7300 Real-Time PCR systems (Applied Biosystems), using SYBR1 Green PCR Master Mix (Takara Bio Inc.). This study utilized the following specific primers according to other reports shown in **Table 2** (Ogawa *et al.,* 2015). Relative mRNA expression of target genes was evaluated by the $2^{-\Delta Ct}$ method and normalized to GAPDH expression.

Table 2. Sequence information for the primers used for qRT-PCR

No	Gene	Primer type	Primer sequence (5' → 3')
1	GATA4	Forward	TCCCAGACGTTCTCAGTCAG
		Reverse	GGAGCTGGTCTGTGGAGACT
2	NKX2.5	Forward	ACCCTGAGTCCCCTGGATTT
		Reverse	TCACTCATTGCACGCTGCAT
3	MYH7	Forward	ACAAGCTGCAGCTAAAGGTC
		Reverse	TCAAGATGTGGCAAAGCTAC
4	TNNT2	Forward	TTCACCAAAGATCTGCTCCTCGCT
		Reverse	TTATTACTGGTGTGGAGTGGGTGTGG
5	GAPDH	Forward	CAACGGATTTGGTCGTATTGG
		Reverse	GCCATGGGTGGAATCATATTG

2.2.7. Statistical analysis

Each experiment was carried out at least three times with triplicate samples in each experiment. Representative experiments are presented, and the results are expressed as the mean ± standard deviation—statistical analysis using one-way ANOVA with Tukey's *post hoc*, $p < 0.05$ and 0.001.

2.3. Results

2.3.1. Migration-driven epigenetics formation on the dendrimer-immobilized surface

To understand the histone modifications derived from migration behavior, the hMSCs were cultured on PS and G5 surfaces with the addition of migration agents. Rac1 activator (HMG-1) was added to induce active migration, and Rac1 inhibitor was exposed to inhibit cell migration. The results show a significant increase of repressive histone modification, H3K9me3, during exposure to Rac1 inhibitor both in PS and G5 surface culture. On the opposite, a lower expression of H3K9me3 was obtained both in PS and G5 surfaces by adding the Rac1 activator (**Fig. 22 A**).

On the other hand, activating histone modification marker, H3K9ac, was down-regulated both in PS and G5 surface under the addition of Rac1 inhibitor. The addition of Rac1 activator to enhance active migration in PS and G5 surface resulted in a similar level of H3K9ac expression in both conditions. It also exhibited the up-regulation of H3K9ac expression in both culture conditions with Rac1 activator compared to culture with the addition of Rac1 inhibitor (**Fig. 22 B**).

The other repressive histone modification, H3K27me3, was down-regulated compared to normal conditions after adding Rac1 activator and inhibitor on hMSCs cultured in PS surface. In addition to the Rac1 activator and Rac1 inhibitor on PS surface culture, both exhibited a similar level of the H3K27me3 expression. On the other hand, the addition of Rac1 inhibitor during culture on the G5 surface resulting in down-regulation of H3K27me3, while the addition of Rac1 activator on G5 surface culture significantly increases the level of H3K27me3 (**Fig. 22 C**).

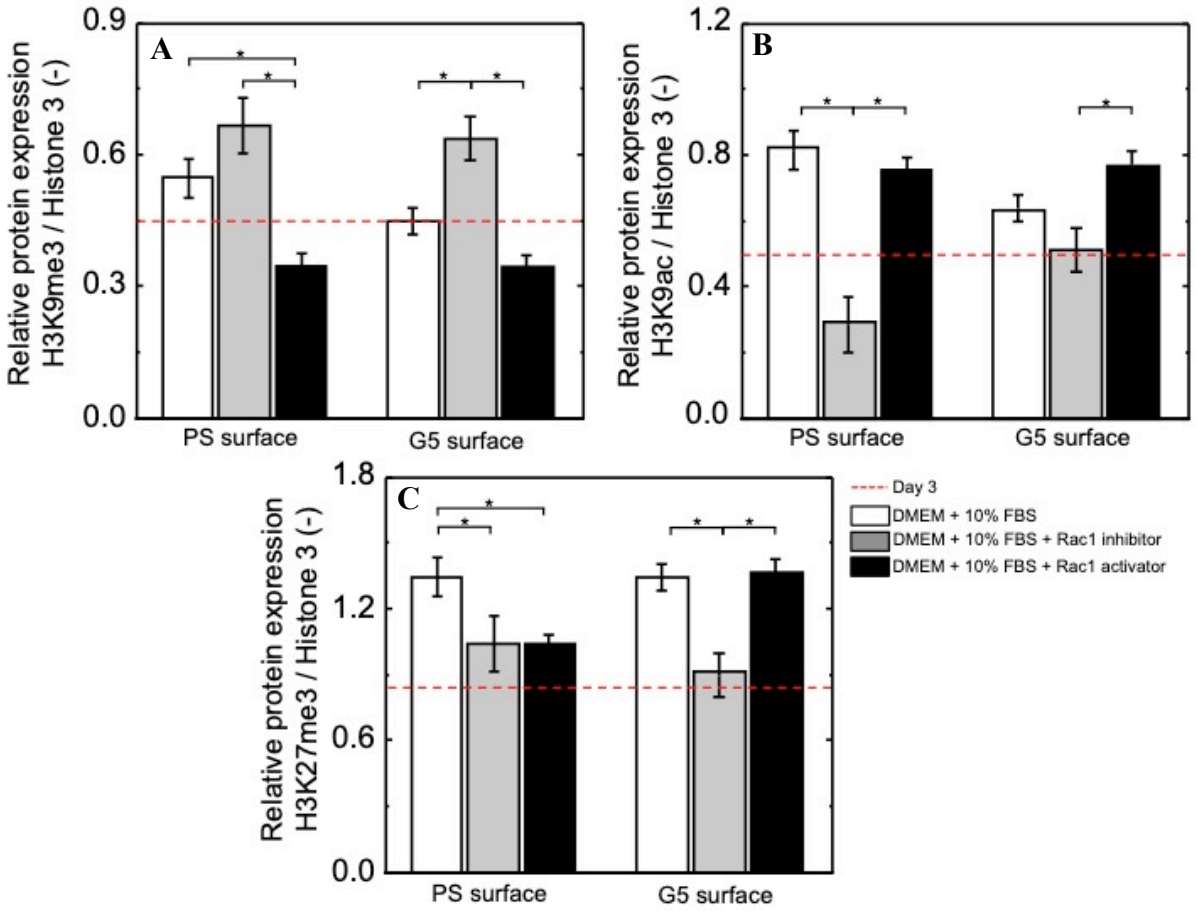

Figure 22. Migration-driven of (A) H3K9me3, (B) H3K9ac, and (C) H3K27me3 formation in addition to Rac1 activator and inhibitor.

2.3.2. Effect of dendrimer surface and passage methods on morphology and cardiomyogenic differentiation potential of hMSCs

To investigate the effect of a G5 surface on the cardiomyogenic differentiation potential of hMSCs, the cells were subcultured after 10 days on the fresh surface using two different methods. The experimental scheme is depicted in **Figure 23 C**. In the initial culture, hMSCs were grown on PS and G5 surfaces for ten days. Cells on the G5 surface maintained a round shape and participated in cell aggregation, in contrast to the cells keeping stretched-shaped morphology on the PS surface (**Fig. 23 A**). On day 10, the cells were attached to the surface after initial seeding and displayed consequent morphological changes (**Fig. 23 A**).

HMSCs from the initial culture then dissociated into single cells through enzyme digestion and re-seeded into fresh G5 and PS surfaces. After culturing for 20 days, cells on the G5 surface repeated similar behavior as in the initial culture; the loosely attached cells then re-formed cell aggregates by the end of the subculture period (**Fig. 23 D**). However, the cells on the PS surface exhibited spindle-shaped fibroblastic cells; they were confluent by the end of the subculture period. After the subculture, there were no significant morphological differences (**Fig. 23 D**).

In aggregate cell-based passaging, cell aggregates from the initial culture on the G5 surface were collected through tapping. The collected cell aggregates were then re-seeded onto the G5 and PS surfaces. Right after re-seeded, the harvested cell aggregates adhered to the surface and initiated to disperse as single cells migrated out actively from cell aggregates, then during the culture period, re-formed cell aggregates again through active migration (**Fig. 23 D**). However, the cell aggregates that subcultured on the PS surface adhered and the cells out-spread from the aggregates. After ten days post-subculture, the cells proliferated and formed a confluent monolayer (**Fig. 23 D**).

To investigate whether the cells grown on G5 and PS surfaces maintained the cardiomyogenic differentiation potential following subcultures, we confirmed the expression of typical MSC marker (CD105) and cardiomyogenic marker (cTnT) at the initial attachment. Immunofluorescence staining revealed that these cell aggregates on the G5 surface exhibited the expression of cTnT and not expressing the CD105 marker (**Fig. 23 B**). However, hMSCs on the PS surface were positive for CD105 and negative for cTnT. Further confirmation of these markers' expression was conducted by western blot analysis (**Fig. 23 E**). Cells on G5 surfaces at 10 days showed higher levels of cTnT expression than those on the PS surface. However, cells on the G5 surface significantly reduced the protein levels of CD105 compared to those on the PS surface. At 10 days after single cell-based passaging, the protein level of cTnT in the cells subcultured onto the G5 surface was increased, whereas the level of CD105 was reduced.

The levels of cTnT on the G5 surface increased by about 1.34-fold for 10 days after the subculture compared with those 10 days before the subculture. When comparing two passage methods in aggregates grown on the G5, cTnT levels were 1.19-fold higher than those in single cell-based passaging. In addition, the expression of CD105 was decreased in the culture on G5 surfaces with both passage methods. These results concluded that the highest level of cTnT was found in aggregate-based passage cultures compared to that passaged cells as single cells, suggesting that the migration-driven aggregate behavior on the G5 surface leads to lineage commitment toward a cardiomyogenic fate.

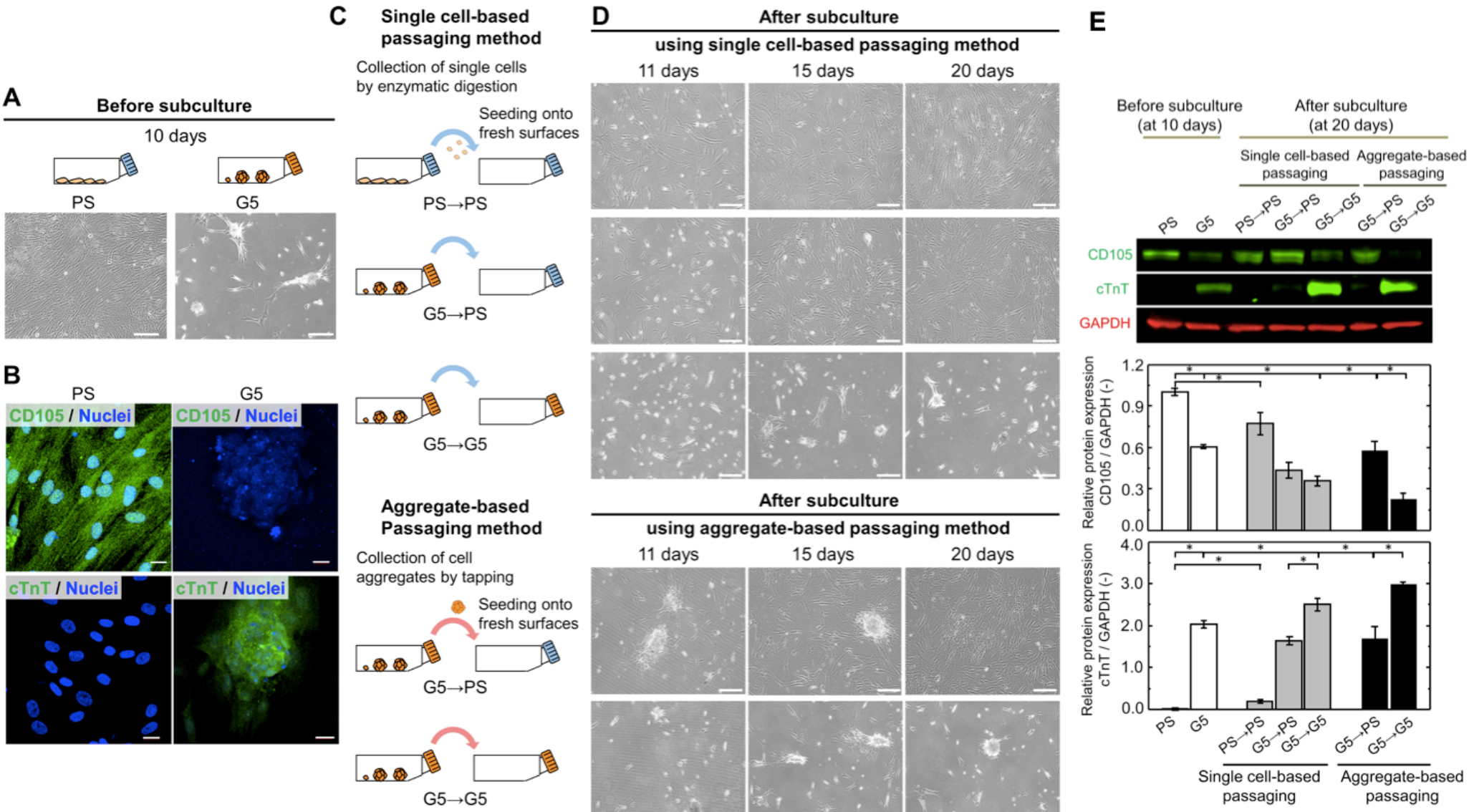
A
Before subculture
10 days
PS
G5
B
PS
G5
CD105 / Nuclei
CD105 / Nuclei
cTnT / Nuclei
cTnT / Nuclei
C
Single cell-based passaging method
Collection of single cells by enzymatic digestion
Seeding onto fresh surfaces
PS→PS
G5→PS
G5→G5
Aggregate-based Passaging method
Collection of cell aggregates by tapping
Seeding onto fresh surfaces
G5→PS
G5→G5
D
After subculture
using single cell-based passaging method
11 days
15 days
20 days
After subculture
using aggregate-based passaging method
11 days
15 days
20 days
E
Before subculture (at 10 days)
After subculture (at 20 days)
Single cell-based passaging
Aggregate-based passaging
PS
G5
PS→PS
G5→PS
G5→G5
G5→PS
G5→G5
CD105
cTnT
GAPDH
Relative protein expression CD105 / GAPDH (-)
Relative protein expression cTnT / GAPDH (-)
Single cell-based passaging
Aggregate-based passaging

Figure 23. Dynamic cell behavior of passaged hMSCs on G5 and PS surfaces. (A) Cell morphologies on G5 and PS surface at 10 days of initial culture before passaging. (B) Immunofluorescence staining of hMSCs marker (CD105) and cardiomyogenic marker (cTnT) in passaged cells cultured on G5 and PS surfaces. Scale bar, 20 μm. (C) Schematic diagram of single cell-based and aggregate-based passaging methods onto PS and G5 surfaces. (D) Cell morphologies on PS and G5 surfaces at days 11, 15, and 20 after re-seeding using single cell-based and aggregate-based passaging methods. Scale bar, 200 μm. (E) Western blotting images and quantitative analysis of western blotting results towards CD105 and cTnT normalized to GAPDH on the G5 and PS surfaces. White bars indicate cells cultured on G5 and PS surfaces at 10 days of initial culture before passaging, grey bars indicate cells cultured on G5 and PS surfaces for 10 days after single cell-based passaging, and black bars indicate cells cultured on G5 surface after aggregate-based passaging. Experiments were performed in triplicate and were repeated three times with similar results. Statistical analysis using one-way ANOVA with Tukey's post hoc analysis, $*p < 0.05$ and $**p < 0.001$.

2.3.3. Nucleoskeletal organization of hMSCs during the long-term serial passage

To understand the correlation between actin cytoskeletal formation and nuclear lamins on G5 and PS surfaces, the observation of F-actin and lamin A/C using fluorescence staining was conducted one day after passaging. The flattened and well-spread morphology was observed in the cells from PS surface culture, accompanied by the development of bundles of tensed stress fibers, which elongated in the apical side of nuclei, resulting in the polarization of lamin A/C from basal to apical (**Fig. 24 A**). In contrast, lamin A/C polarization was not found on the culture from the G5 surface; the staining results exhibited a rim pattern of lamin A/C around the slightly relaxed and rounded nuclei. In cells cultured a day after the subculture, the lamin A/C showed a similar staining pattern as before the subculture, regardless of the passaging methods (**Fig. 24 A**).

The levels of nuclear lamins proteins (lamin A/C and lamin B1) were examined by western blot analysis of cells on day 10 after the initial culture, and 10 days after passage, the intensity of lamin A/C and lamin B1 were then calculated relative to GAPDH. Cells on G5 surfaces at 10 days contained much lower levels of lamin A/C and lamin B1 than on PS surfaces (**Fig. 24 B**). The lamin A/C and lamin B1 levels on the G5 surface culture were 3.83-fold and 3.75-fold lower than those cultured on the PS surface. At 10 days after single cell-based passaging, the lamin A/C and lamin B1 levels on the G5 surface were increased by about 2.44-fold and 1.34-fold, respectively, compared with those 10 days before subculture. When comparing two passage methods for aggregates on the G5 surface, lamin A/C and lamin B1 levels were suppressed until nearly zero in the aggregate-based passage culture.

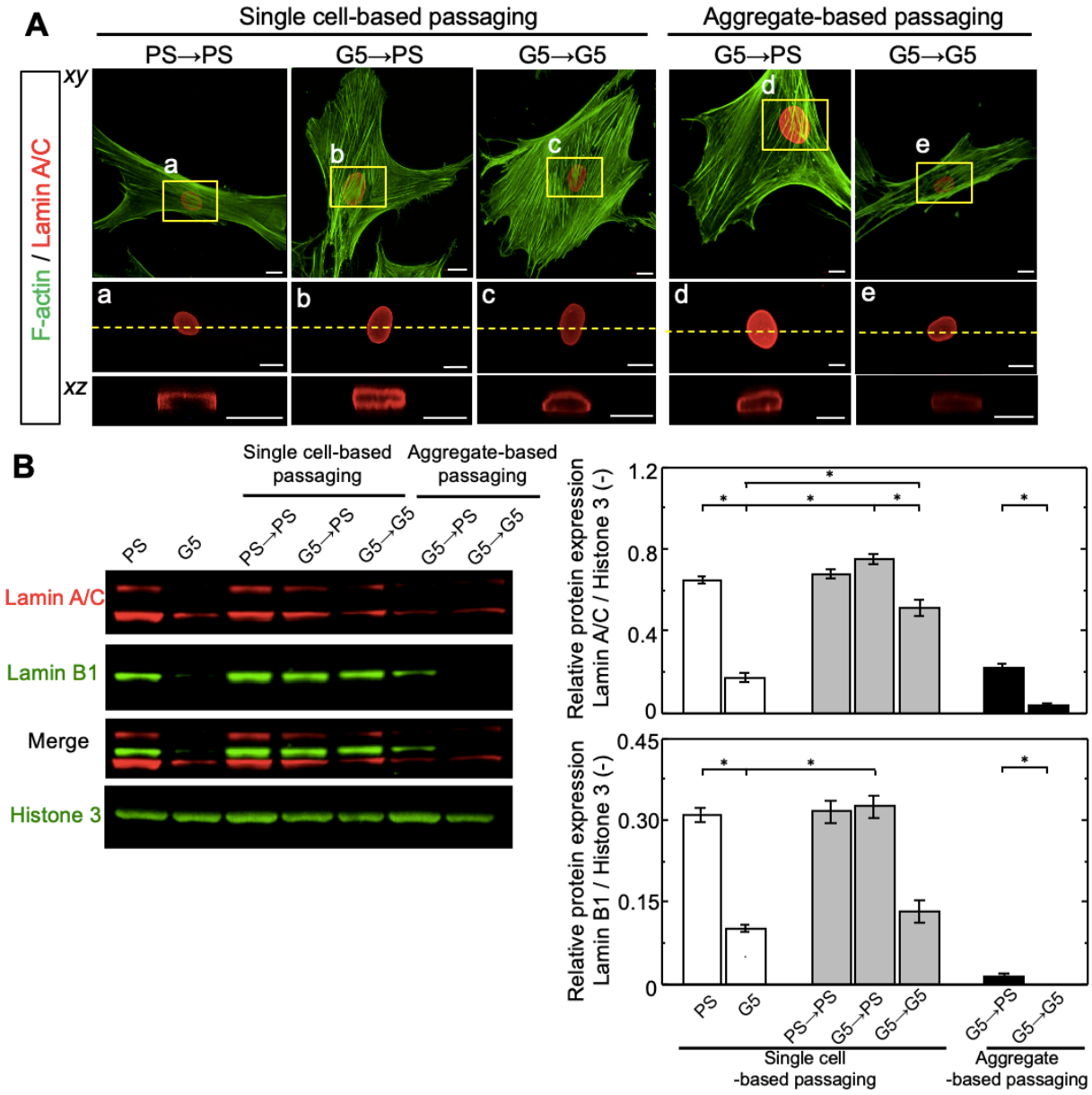

Figure 24. Nuclear lamin expression of passaged hMSCs on G5 and PS surfaces. (A) Immunofluorescence staining of F-actin (green) and lamin A/C (red) in passaged cells cultured on G5 and PS surfaces. Scale bar, 20 μm. (B) Western blotting images and quantitative analysis of western blotting results towards lamin A/C and lamin B1 normalized to histone 3 on the G5 and PS surfaces. White bars indicate cells cultured on G5 and PS surfaces at 10 days of initial culture before passaging, grey bars indicate cells cultured on G5 and PS surfaces for 10 days after single cell-based passaging, and black bars indicate cells cultured on G5 surface after aggregate-based passaging. Experiments were performed in triplicate and were repeated three times with similar results. Statistical analysis using one-way ANOVA with Tukey's post hoc analysis, *$p < 0.05$ and **$p < 0.001$.

Subsequently, the lamin A/C and lamin B1 levels in cells cultured on the G5 and PS surfaces were investigated during repeated passages at one and 10 days of culture. The lamin A/C and lamin B1 levels in cells cultured on the G5 surface were gradually reduced from 1 to 10 days (**Fig. 25**). Following single cell-based passaging, the lamin A/C and lamin B1 levels increased temporarily on the G5 surface one day after the subculture (day 11). However, these levels gradually decreased from 11 to 20 days. The patterns of lamin A/C and lamin B1 expression were repeated during the third passage in single cell-based passage methods in the G5 surface. Cells cultured on the PS surface exhibited patterns similar to lamin A/C and lamin B1 expression.

On the other hand, these levels on the PS surface were 1.49-fold and 3.53-fold higher than those cultured on the G5 surface 10 days after the third passage (day 40). When the cells on the G5 surface were subcultured on the G5 surface following aggregate-based passaging, lamin A/C and lamin B1 levels decreased gradually after the first passage. They were suppressed to nearly zero by the end of the third passage.

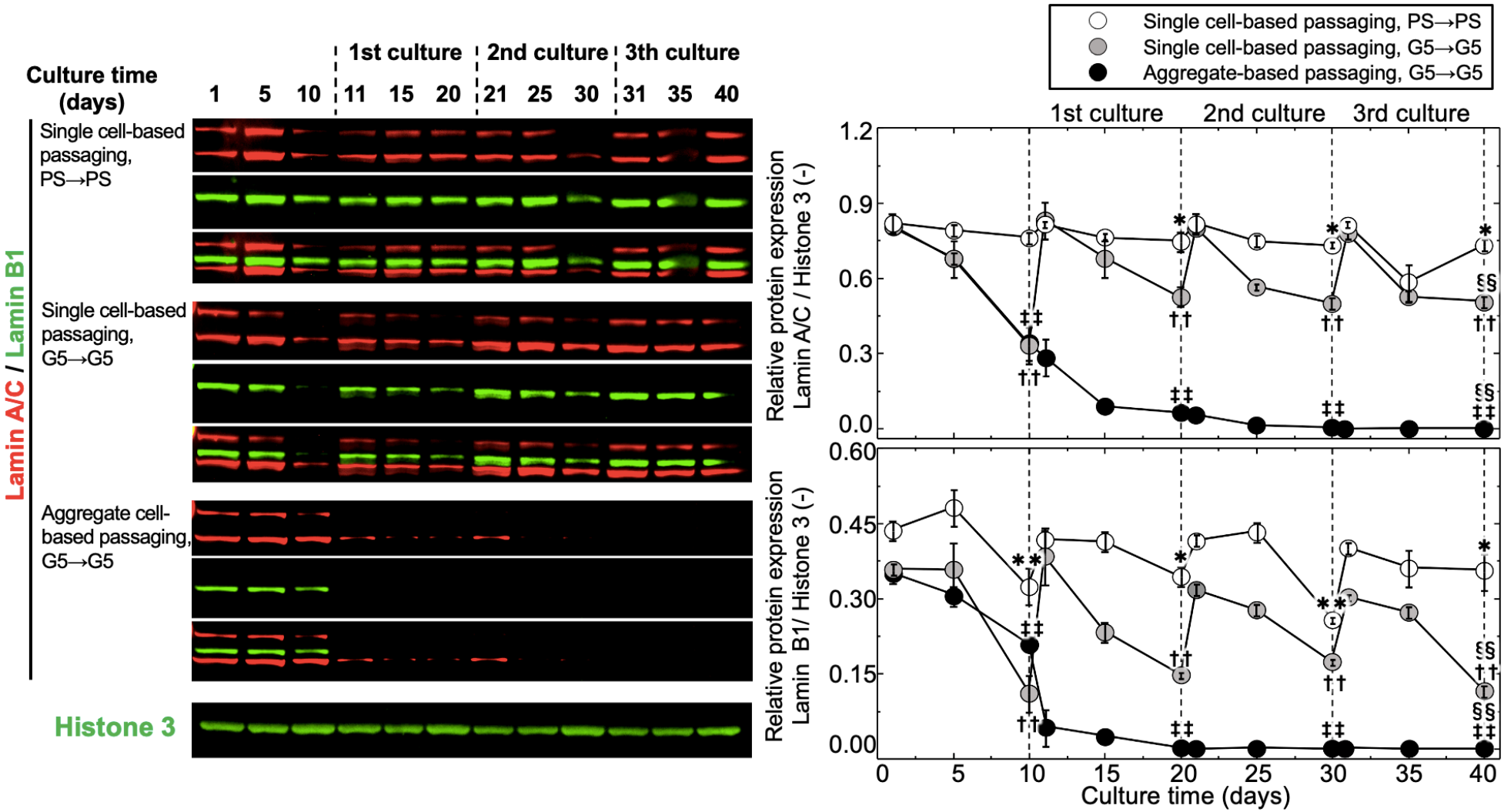
Culture time (days)
1st culture
2nd culture
3th culture
1 5 10 11 15 20 21 25 30 31 35 40
Lamin A/C / Lamin B1
Single cell-based passaging, PS→PS
Single cell-based passaging, G5→G5
Aggregate cell-based passaging, G5→G5
Histone 3
Single cell-based passaging, PS→PS
Single cell-based passaging, G5→G5
Aggregate-based passaging, G5→G5
1st culture
2nd culture
3rd culture
Relative protein expression Lamin A/C / Histone 3 (-)
Relative protein expression Lamin B1/ Histone 3 (-)
Culture time (days)

Figure 25. Nuclear lamin of hMSCs cultured on G5 and PS surfaces during long-term serial passage. Quantitative data shows the normalized intensity of lamin A/C and lamin B1 to histone 3 images. White circles indicate passaged cells from PS to PS surface through single cell-based passaging, grey circles indicate passaged cells from G5 to G5 surface through single cell-based passaging, and black circles indicate passaged cells from G5 to G5 surface through aggregate-based passaging. Experiments in each analysis were performed in triplicate and were repeated three times with similar results. Statistical analysis using one-way ANOVA with Tukey's post hoc, $p < 0.05$ and 0.001. (*) Significant differences of time-dependent effect at the end of every passage towards initial culture at day 1 in single cell-based passaging from PS to PS surface (white circles). (*) $p < 0.05$ and (**) $p < 0.001$. (†) Significant differences of time-dependent effect at the end of every passage to initial culture at day 1 in single cell-based passaging from G5 to G5 surface (grey circles). (†) $p < 0.05$ and (††) $p < 0.001$. (‡) Significant differences of time-dependent effect at the end of every passage towards initial culture at day 1 in single aggregate-based passaging from G5 to G5 surface (black circles). (‡) $p < 0.05$ and (‡‡) $p < 0.001$. (§) Significant differences of single cell-based and aggregate-based passaging conditions on the G5 surface towards the control condition on the PS surface at the end of the third passage (40 days). (§) $p < 0.05$ and (§§) $p < 0.001$.

2.3.4. Histone modification of hMSCs during the long-term serial passage

To investigate whether histone modifications play a role in the cardiomyogenic differentiation capacity of hMSCs, western blot analysis for global histone modification markers, including two types of repressive markers (H3K9me3 and H3K27me3) and one activating modification marker (H3K9ac) in the cells cultured on PS and G5 surface were obtained. By calculating the relative intensity of H3K9me3, H3K27me3, and H3K9ac towards Histone 3, there was a significant difference in the cells on G5 and PS surfaces in terms of changes in passage numbers and passage methods.

Cells on G5 surfaces at 10 days showed a higher level of H3K9me3 and a lower level of H3K9ac than cells on the PS surface (**Fig. 26**). When cells on the G5 surface were subcultured on G5 and PS surfaces following single cell-based passaging, the H3K9me3 level on the G5 surface was decreased by about 1.1-fold at day 10 compared to the initial culture. In contrast, the H3K9me3 level on the PS surface was increased by approximately 1.8-fold compared to the initial culture. In the case of H3K9ac modifications, the cells on G5 and PS surfaces significantly increased the expression levels of H3K9ac at 10 days of culture after single-cell passage for 5.4-time fold and 3.7-time fold, respectively. In the case of H3K27me3 level modifications on the G5 surface, the expression level of H3K27me3 in cells passaged on the G5 surface remained almost the same level at 10 days of culture, while the H3K27me3 level in cells passaged on PS surface increased by about 1.7-fold compared with those before subculture. When comparing two passage methods for aggregates on the G5 surface, the levels of H3K9ac and H3K27me3 were 1.0-fold and 1.3-fold lower in the aggregation-based passaging. At the same time, H3K9me3 was suppressed to almost zero in aggregate-based passage culture.

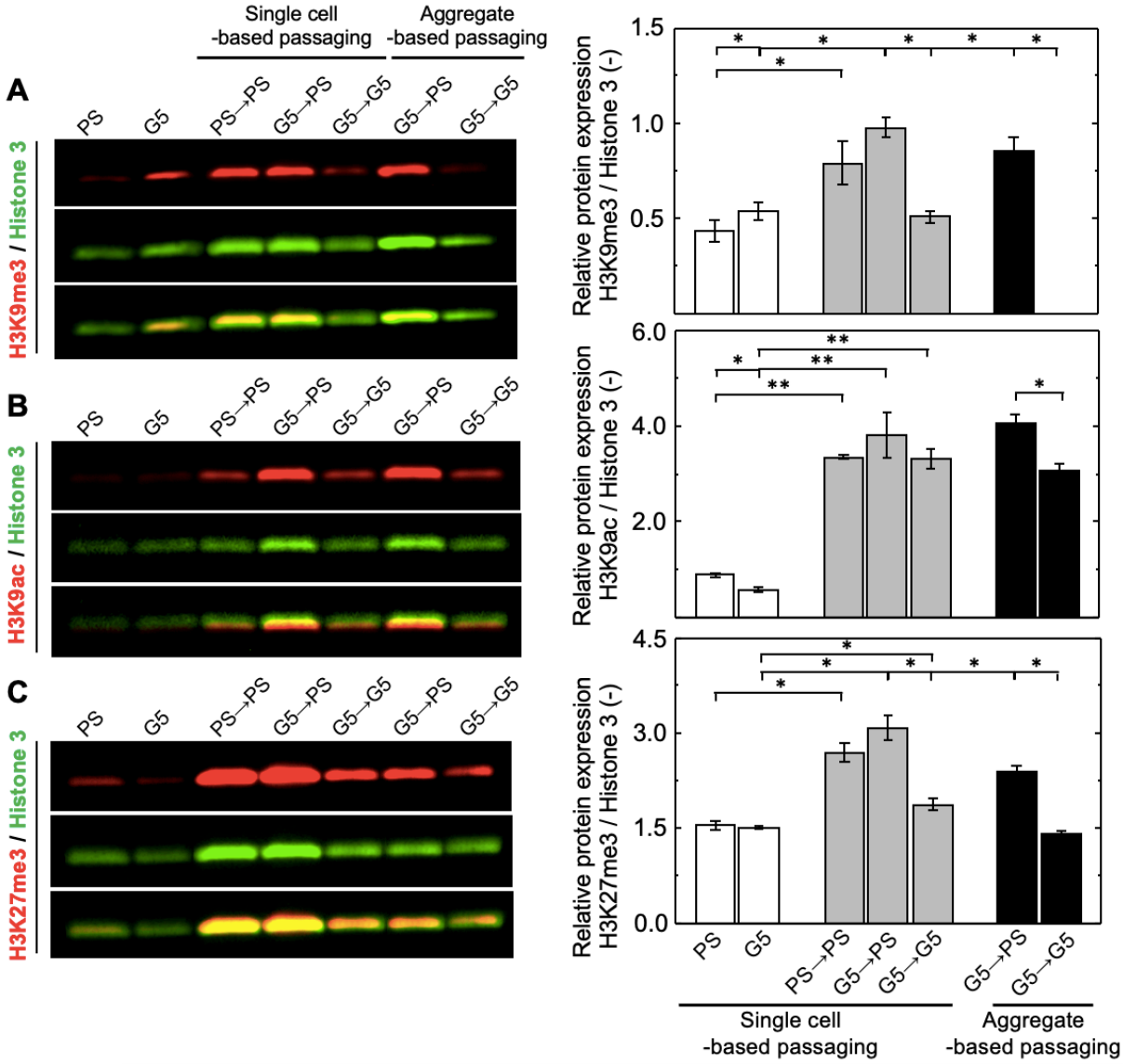

Figure 26. Global histone modification of passaged hMSCs on G5 and PS surfaces. Western blotting images and quantitative analysis of western blotting results towards (A) H3K9me3, (B) H3K9ac, and (C) H3K27me3, normalized to histone 3 on the G5 and PS surfaces. White bars indicate cells cultured on G5 and PS surfaces at 10 days of initial culture before passaging, grey bars indicate cells cultured on G5 and PS surfaces for 10 days after single cell-based passaging, and black bars indicate cells cultured on G5 surface after aggregate-based passaging. Experiments were performed in triplicate and were repeated three times with similar results. Statistical analysis using one-way ANOVA with Tukey's post hoc analysis, *$p < 0.05$ and **$p < 0.001$.

Subsequently, the levels of H3K9me3, H3K9ac, and H3K27me3 in cells cultured on the G5 and PS surfaces at one and 10 days in every passage were investigated for global histone modifications by western blotting analysis (**Fig. 27**). When the cells on the G5 surface were subcultured following single cell-based passaging, the H3K9me3 levels were maintained at the same level until three passages (day 40). However, the levels of H3K9ac and H3K27me3 gradually increased from one to 10 days of the initial culture before the subculture, followed by a transient decrease one day after the first passage (day 11) and a gradual increase from 11 to 20 days. This pattern was repeated for three passages in the single cell-based passage method. A similar expression pattern was observed in the levels of H3K9ac and H3K27me3 expression in cells passaged on the PS surface repeated during three passages.

When the cells on the G5 surface were subcultured on the G5 surface following aggregate-based passaging, the levels of H3K9me3 were reduced to nearly zero at 10 days after the first passage (day 20). This level was maintained until three passages. In the case of H3K9ac and H3K27me3 modifications, the levels of H3K9ac were found to increase gradually until three passages, whereas the levels of H3K27me3 increased gradually in the 10 days before passage. This expression level was maintained during three passages. The cells passaged on the G5 surface sustained the enrichment of H3K9ac during three passages, while those cultured on the PS surface significantly enhanced the enrichment of H3K9me3 and H3K27me3 with increasing passage numbers. At 10 days after the third passage (day 40), the H3K9ac levels in the cells cultured on the G5 surface were 2.02-fold higher than those cultured on the PS surface, while the levels of H3K27me3 in cells cultured on the G5 surface were 2.07-fold lower than those cultured on PS surface.

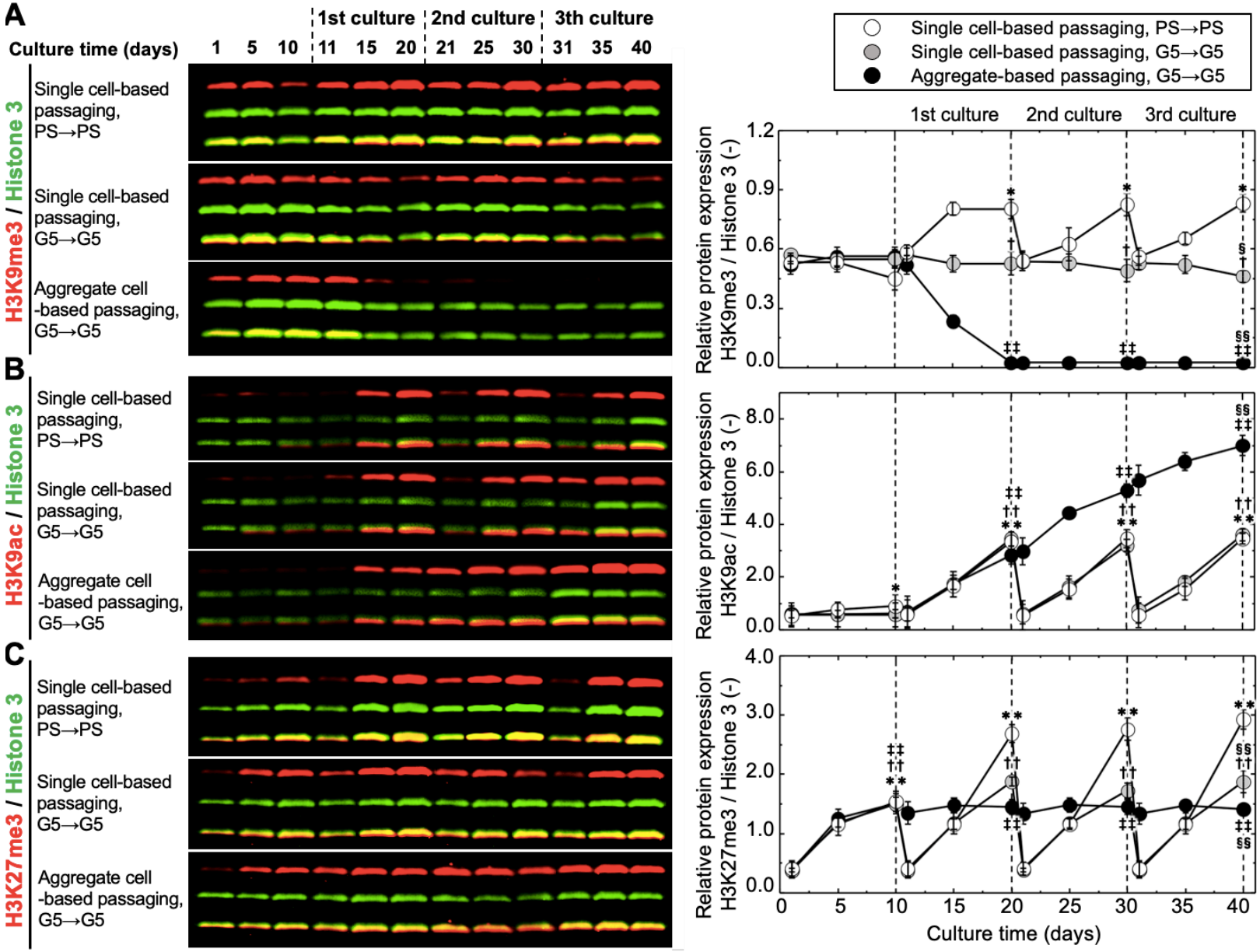
A
B
C
1st culture
2nd culture
3th culture
Culture time (days)
1 5 10 11 15 20 21 25 30 31 35 40
H3K9me3 / Histone 3
H3K9ac / Histone 3
H3K27me3 / Histone 3
Single cell-based passaging, PS→PS
Single cell-based passaging, G5→G5
Aggregate cell -based passaging, G5→G5
Single cell-based passaging, PS→PS
Single cell-based passaging, G5→G5
Aggregate-based passaging, G5→G5
Relative protein expression H3K9me3 / Histone 3 (-)
Relative protein expression H3K9ac / Histone 3 (-)
Relative protein expression H3K27me3 / Histone 3 (-)
Culture time (days)

Figure 27. Global histone modification of hMSCs cultured G5 and PS surfaces during long-term serial passage. Quantitative data shows normalized intensities of (A) H3K9me3, (B) H3K9ac, and (C) H3K27me3 to histone 3 in western blotting images. White circles indicate passaged cells from PS to PS surface through single cell-based passaging, grey circles indicate passaged cells from G5 to G5 surface through single cell-based passaging, and black circles indicate passaged cells from G5 to G5 surface through aggregate-based passaging. Experiments in each analysis were performed in triplicate and were repeated three times with similar results. Statistical analysis using one-way ANOVA with Tukey's post hoc, $p < 0.05$ and 0.001. (*) Significant differences of time-dependent effect at the end of every passage towards initial culture at day 1 in single cell-based passaging from PS to PS surface (white circles). (*) $p < 0.05$ and (**) $p < 0.001$. (†) Significant differences of time-dependent effect at the end of every passage to initial culture on day one at single cell-based are passaging from G5 to G5 surface (grey circles). (†) $p < 0.05$ and (††) $p < 0.001$. (‡) Significant differences of time-dependent effect at the end of every passage towards initial culture at day 1 in single aggregate-based passaging from G5 to G5 surface (black circles). (‡) $p < 0.05$ and (‡‡) $p < 0.001$. (§) Significant differences of single cell-based and aggregate-based passaging conditions on the G5 surface towards the control condition on the PS surface at the end of the third passage (40 days). (§) $p < 0.05$ and (§§) $p < 0.001$.

2.3.5. Growth characteristics and cardiomyogenic differentiation potential of hMSCs during the long-term serial passage

To identify whether long-term passage on the G5 surface alters the growth characteristics and cardiomyogenic potential of hMSCs, the ratio of adherent cells to seeded cells (X_T/X_0) and the ratio of cTnT-positive cells to adherent cells (X_P/X_T) were measured under two passage methods. As shown in **Figure 26 A**, the X_T/X_0 gradually decreased on the PS surface over time while it was maintained in the G5 surface culture. At the end of three passages 40 days, the X_T/X_0 was 5.0 on the PS surface, which was higher than that on the G5 surface. The X_T/X_0 on the

G5 surface was less than half the level observed in the PS surface culture. No significant difference was found in the comparison of the two passage methods.

Furthermore, the ratio of $cTnT^+$ cells to total cell numbers (X_P/X_T) for aggregate on the G5 surface at ten days showed a higher level ($X_P/X_T = 0.18$) compared to those on the PS surface ($X_P/X_T = 0.06$). The X_P/X_T exhibited an increase in culture on the G5 surface, and the level of X_P/X_T on the G5 surface reached 0.60 at the end of three passages at 40 days, which was 9.5-fold higher compared with on PS surface. Comparing the X_T/X_0 of two passaging methods to G5 surfaces, the X_T/X_0 in collected aggregates from the G5 surface was 0.60 at 40 days, which was 1.44-fold higher than for X_T/X_0 containing single cells after enzyme treatment (**Fig. 26 A**).

Subsequently, the cardiomyogenic potential of hMSCs cultured on the G5 surface at 10 days in every passage was evaluated by quantitative RT-PCR analysis for cardiomyogenic differentiation markers (GATA4, NKX2.5, MYH7, and TNNT2). The mRNA expression levels of GATA4, NKX2.5, MYH7, and TNNT2 were markedly increased in cells on the G5 surface compared to that on the PS surface by 10 days after the third passage (day 40) (**Fig. 26 B**). When comparing the two passage methods for aggregates on the G5 surface, although the levels of TNNT2 between the two passage methods on the G5 surface were not significantly different, the other gene markers showed significant differences. The expression levels of GATA4, NKX2.5, and MYH7 were higher in the aggregate-based passage cultures 10 days after the third passage (day 40) than in the single cell-based passage cultures (1.52-fold, 1.93-fold, and 5.96-fold, respectively). These results indicate that aggregate formation on the G5 surface and aggregate-based passaging culture are useful methods for directing hMSCs toward cardiomyogenic differentiation.

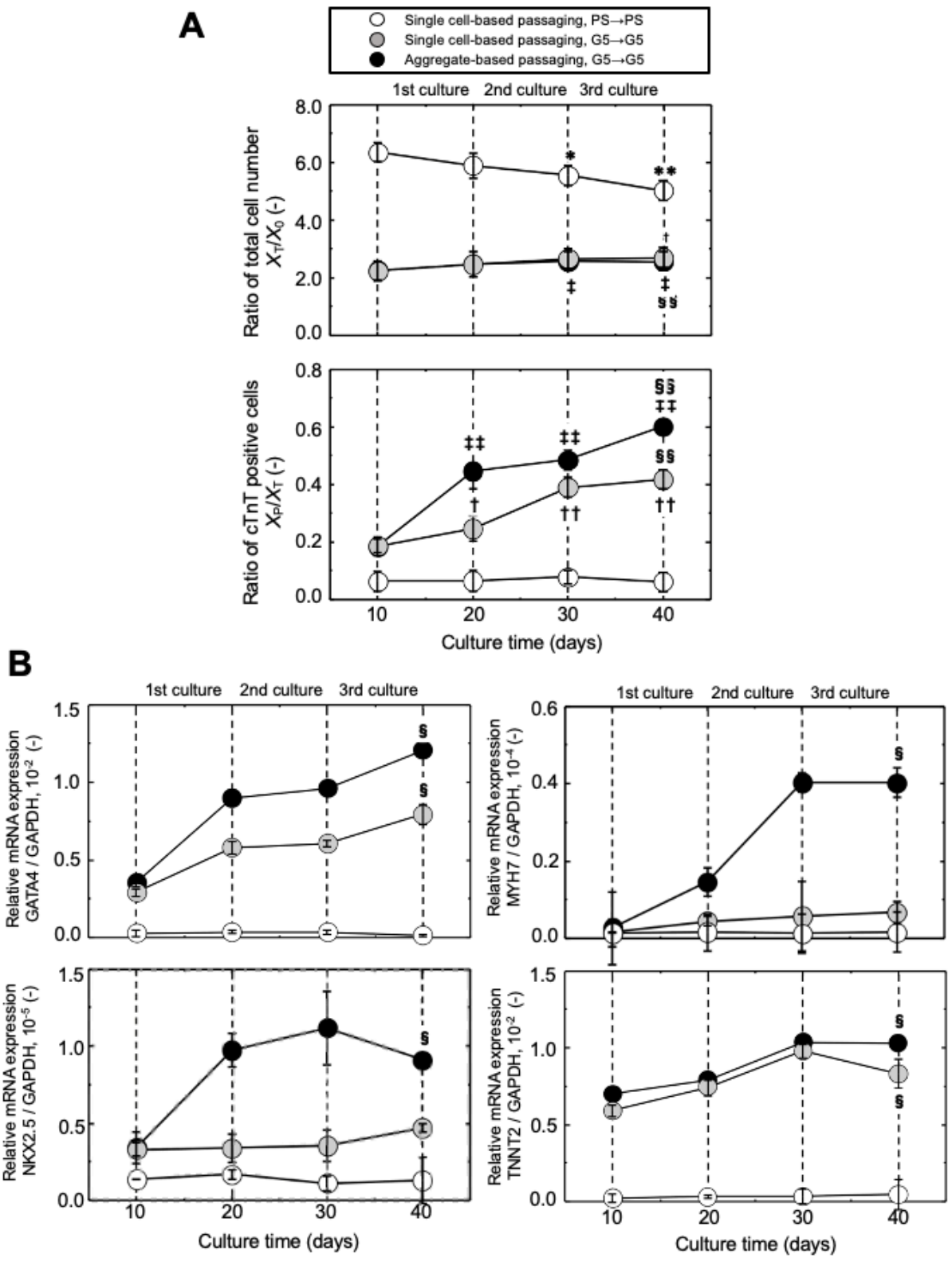
A
Single cell-based passaging, PS→PS
Single cell-based passaging, G5→G5
Aggregate-based passaging, G5→G5
1st culture
2nd culture
3rd culture
Ratio of total cell number
X_T/X_0 (-)
Ratio of cTnT positive cells
X_P/X_T (-)
Culture time (days)
B
Relative mRNA expression
GATA4 / GAPDH, 10^{-2} (-)
MYH7 / GAPDH, 10^{-4} (-)
NKX2.5 / GAPDH, 10^{-5} (-)
TNNT2 / GAPDH, 10^{-2} (-)
Culture time (days)

Figure 28. Growth and cardiomyogenic differentiation potential of hMSCs cultured G5 and PS surfaces during long-term serial passage. (A) Time profiles of ratio total cell numbers (X_T/X_0) and the ratio of cTnT positive cells (X_P/X_T) values. (B) Analysis of qPCR analysis of early cardiomyogenic differentiation gene markers (GATA4 and NKX2.5) and late cardiomyogenic differentiation gene markers (MYH7 and TNNT2) normalized to GAPDH. White circles indicate passaged cells from PS to PS surface through single cell-based passaging, grey circles indicate passaged cells from G5 to G5 surface through single cell-based passaging, and black circles indicate passaged cells from G5 to G5 surface through aggregate-based passaging. Experiments in each analysis were performed in triplicate and were repeated three times with similar results. Statistical analysis using one-way ANOVA with Tukey's *post hoc*, $p < 0.05$ and 0.001. (*) Significant differences of time-dependent effect at the end of every passage (10, 20, 30, 40 days) in single cell-based passaging from PS surface to PS surface (open circles). (*) $p < 0.05$ and (**) $p < 0.001$. (†) Significant differences of time-dependent effect at the end of every passage to initial culture on day ten at single cell-based passaging from G5 surface to G5 surface (grey circles). (†) $p < 0.05$ and (††) $p < 0.001$. (‡) Significant differences of time-dependent effect at the end of every passage towards initial culture at day 10 in single aggregate-based passaging from G5 to G5 surface (closed circles). (‡) $p < 0.05$ and (‡‡) $p < 0.001$. (§) Significant differences of single-based and aggregate-based passaging conditions on the G5 surface towards the control condition on the PS surface at the end of the third passage (40 days). (§) $p < 0.05$ and (§§) $p < 0.001$.

2.4. Discussion

This study investigated the enhancement of cardiomyogenic differentiation through repeated migration-driven epigenetic memory formation and maintenance during aggregate-based passage on a G5 surface. Cell aggregates grown on the G5 surface showed dynamic changes in morphology associated with repetitive stretching and contracting during migration. In addition, they exhibited altered cytoskeletal formation and nuclear lamina, leading to epigenetic modifications and cardiac transcription factors. The spontaneous aggregate formation and migratory behaviors of aggregates affect the organization of cadherin-based and integrin-based adhesion complexes within aggregates, thereby regulating intracellular signaling in cell fate decisions (Ogawa et al., 2016). In aggregate-based subculture on the G5 surface, the formation, maintenance, and enhancement of behavior-driven epigenetic modification can easily be achieved rather than cells detached by enzymatic detachment. This study suggests that the method proposed is a valuable improvement on current techniques for inducing cardiomyocyte differentiation. The current hypothesis was summarized based on the results of this study, shown in **Figure 29.**

2.4.1. Repetitive regulation of the nuclear lamins and cytoskeleton via aggregate migration on the G5 surface involved in the maintenance of epigenetic memory formation

The dynamic migration on the G5 surface was initiated through the cell-substrate interaction and regulation of extracellular-matrix adsorption. The change in fibronectin adsorption through the accumulation of matrix metalloproteinase-1 (MMP1) activated the phosphorylation of focal adhesion protein and altered the cytoskeleton structures (Ogawa et al., 2015). The repetitive stretching and active migration due to low attachment to the substrate lead to cell aggregate formation on the G5 surface. The migration-driven aggregate behavior

maintained until the later duration of culture exhibited repeated collision and cell slipping within the aggregate (Kim et al., 2014; Ogawa et al., 2016).

In that regard, active cell migration is efficient in disrupting cell-cell contacts by dissociating the N-cadherin/ß-catenin complex at the adherens junction (Kim et al., 2010; Ogawa et al., 2016). It was also demonstrated that the migratory behaviors on the G5 surface could affect the ß-catenin signaling pathway and histone modification, which play a crucial role in cardiomyogenic differentiation (Ogawa et al., 2016). Besides, this dynamic behavior on the G5 surface and alteration of actin cytoskeleton structure, which is directly linked to the nucleus, affected the reorganization of the nuclear skeleton structure, causing nuclear lamina deformation and influencing the regulation of epigenetic modification inside nuclei. For example, cell migration on a culture surface affects the morphology and location of the nuclei within the cell aggregate, inducing actomyosin forces that push on and pull the nucleus.

The lamina-associated domains contain regions enriched with typical heterochromatin histone modifications, such as H3K9me3 and H3K27me3, which are associated with cell fate decisions (Wu et al., 2014; Nava et al., 2020). Other studies have found that alterations in the nuclear lamin, such as depletion of lamin A/C and lamin B1, affect chromatin histone modifications by decreasing heterochromatin-related histone modifications, such as H3K9me3, and the upregulation of histone acetylation (Becker et al., 2016). Interestingly, down-regulation of H3K9me3 affected the loosening up of the chromatin and activating gene transcription, commonly found during the differentiation process of stem cells (Lochs et al., 2019; Becker et al., 2016). In the first chapter of the study, an epigenetic modification associated with alteration in cytoskeletal and nuclear skeleton structure played a pivotal role in the switching of myogenic lineage commitment of hMSCs during culture on different generation numbers of dendrimer surfaces.

Consistent with this role, the current study also demonstrated that nuclear lamina disruption was higher in cells on the G5 surface and was associated with epigenetic modification (**Fig. 24**). Cells on the G5 surface maintained a trend of increased H3K9ac, unchanged H3K27me3, and decreased H3K9me3 at 10 days of culture after the first subculture, which contributes to cardiomyogenic differentiation (**Fig. 26**). Higher nuclear lamin disruption in aggregate-based passage culture on the G5 surface shows a similar pattern with suppression of H3K9me3 and up-regulation of H3K9ac. At the same time, H3K27me3 maintained a stagnant expression level until 40 days. Several studies also mentioned that the alteration in nuclear lamina, such as depletion of lamin A/C and lamin B1 in particular, affected chromatin histone modification through decreasing the heterochromatin-related histone modification such as H3K9me3 and up-regulated the acetylation in histone modification (Stephens et al., 2018; Ankam et al., 2018; Shevelvov et al., 2019).

Based on these findings, it was concluded that the nuclear response of migration-driven aggregate behavior leads to the enhancement of modified epigenetic memory, promoting the differentiation of hMSCs into the cardiomyogenic lineage via repetitive migration behaviors on the G5 surface. This phenomenon of the formation and maintenance of the histone modification during MSC culture on the G5 surface is defined as aggregation behavior-driven epigenetic memory. The meaning of enhancement here is that the cardiomyogenic differentiation abilities of hMSCs with later passages cultured on the G5 surface were higher than those with earlier passages.

2.4.2. Maintenance of epigenetic memory formation during aggregate-based subculture on the G5 surface could enhance the cardiomyogenic differentiation of hMSCs

To identify the mechanism most likely responsible for cell aggregate formation and migration behavior, the status of the nucleoskeleton organization and histone modification of

collecting cells by aggregate and single cell-based passage methods were compared. A technique commonly used for subculturing hMSCs involves enzymatically dissociating the cells from the surface attachment digestion, usually with trypsin, to obtain individual cells, which are then seeded onto fresh culture surfaces for further growth (Huang et al., 2014). This method may injure the internal system of cells by degrading polyribosomes and causing damage to the cell surface (Dey et al., 2011).

In this context, cells passaged as cell aggregates on the G5 surface have less damage to the nuclear lamina-cytoskeleton interactions than those passaged with trypsinization and, thus, are more likely to maintain subsequent nucleoskeletal organization and histone modifications. Higher nuclear lamin disruption in aggregate-based passage cultures on the G5 surface showed a similar pattern, with H3K9me3 suppression and H3K9ac upregulation in this culture condition (**Fig. 25 and 27**)

Our novel approach could be improved the *in vitro* differentiation of hMSCs toward cardiomyocyte-like cells by up to 60% after the third passage (40 days), exhibiting high efficiency and reproducibility for cardiomyocyte enrichment. For aggregate-based passage culture, the X_P/X_T value on the G5 surface increased 1.44-fold higher than that for single-cell-based passage culture. Furthermore, the aggregate-based passage method on the G5 surface induces significant changes in the expression of early and late cardiac differentiation markers (GATA4, NKX2.5, MYH7, and TNNT2) carried by these epigenetic variations in comparison with single-cell-based passages.

The up-regulation of early and late cardiomyogenic genes markers is also related to the epigenetic formation during culture on the G5 surface. Several studies mentioned that enhancement of H3 acetylation on MSCs increased the expression of early cardiac differentiation markers, GATA4 and NKX2.5. At the same time, the knockdown of enzymes related to histone deacetylation, such as HDAC1, facilitates the expression of cardiac-specific

genes such as GATA4, NKX2.5, MYH7, and TNNT (Guo et al., 2018; Lu et al., 2014; Wang et al., 2013).

The GATA4 and NKX2.5 genes also play a role as transcription factors in the canonical pathway of cardiac differentiation (Bhuvanalaksmi et al., 2017; Oyama et al., 2014; Armiñán et al., 2009; Xu et al., 2016). At the same time, the down-regulation of H3K9me3 was assumed to have a direct relationship with the up-regulation of these two early cardiac differentiation markers, as found in this study.

Based on these findings, it was concluded that the repetitive regulation of the nuclear lamina and cytoskeleton via aggregate migration on the G5 surface is involved in the maintenance and enhancement of histone modifications and is therefore facilitated by the transition from a multipotent state to cardiomyogenic commitment in MSCs subcultured on the G5 surface. These results indicate that aggregate-based passaging can more easily maintain epigenetic memory than cells detached by enzymatic detachment and suggests that the method proposed is a useful improvement on current techniques for inducing cardiomyocyte differentiation.

In conclusion, we found that migration-driven aggregate behaviors on the dendrimer surface caused epigenetic memory formation and maintenance through repeated aggregate migratory behaviors during the aggregate-based passage, leading to a switch towards enhanced cardiomyogenic fate commitment and facilitated differentiation. Using the aggregate-based passage method, the nuclear response of migration-driver aggregate behavior leads to the maintenance of epigenetic modifications and thus can. Therefore, the differentiation commitment of hMSCs into cardiomyogenic lineage can be promoted through repetitive migration behaviors on the G5 surface. Maintenance of aggregate formation during aggregate-based passage method on the G5 surface could initiate epigenetic memory formations, which enhance the cardiomyogenic commitment through regulation of specific histone modification

markers, H3K9me3, H3K9ac, and H3K27me3. Finally, this study revealed that the G5 surfaces provide a more efficient culture method based on the regulation of migratory behavior-driven epigenetic mechanisms under the aggregate-based passage of hMSCs as a culture strategy for guiding the proper cardiomyogenic lineage differentiation process in the stem cell culture system.

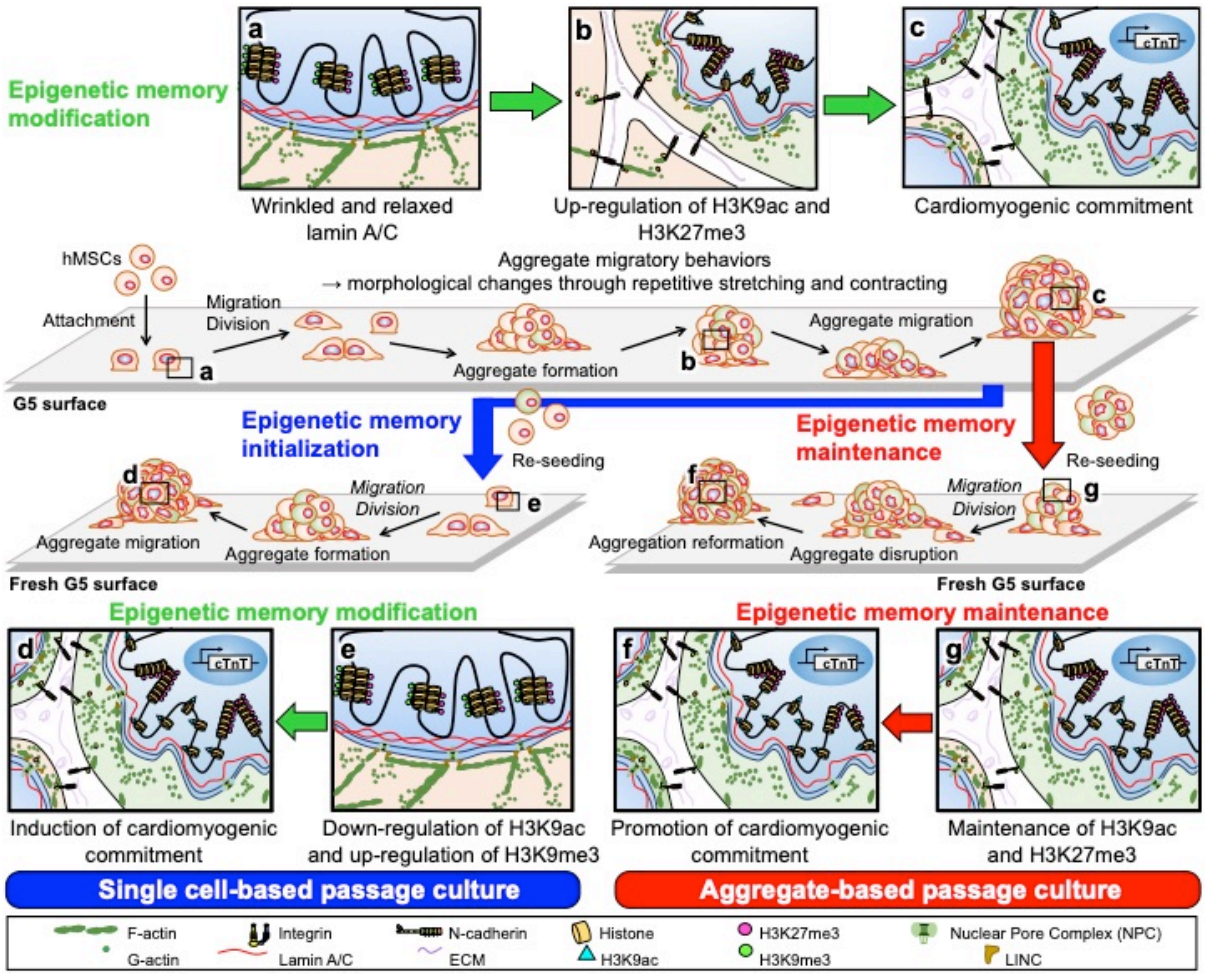

Figure 29. Schematic illustration of the working hypothesis of enhancement in cardiomyogenic commitment in passaged hMSCs on a dendrimer-immobilized surface due to maintenance of epigenetic memory through migration-driven aggregate behaviors.

2.5. Summary

The dynamic migratory behavior of human mesenchymal stem cells (hMSCs) significantly impacts the epigenetic profiles that determine fate choice and lineage commitment. However, the changes in cell behavior responsible for the formation and maintenance of epigenetic memory still need to be fully understood. This study investigated the mechanism underlying the cardiomyogenic differentiation of hMSCs via epigenetic memory formation on the surface of fifth-generation (G5) immobilized polyamidoamine dendrimer cultures. The repressive histone modification marker H3K9me3 and repressive marker H3K27me3 were found to be suppressed and upregulated, respectively, while histone modification marker H3K9ac was activated in G5 surface cultures. Cells displayed increased and decreased cardiac troponin T (cTnT) and undifferentiated markers (CD105) after ten days, respectively. Upon reseeding on new G5 surfaces, histone methylation levels were sustained at the end of three passages. However, the memory effect during a single cell-based passage on the PS surface was repeated after the initialization and reformation during three passages.

Furthermore, the expression of early and late cardiomyogenic differentiation markers, such as GATA4, NKX2.5, MYH7, and TNNT2, was upregulated by the end of the third passage, especially during aggregate-based passaging on the G5 surface. Thus, repetitive aggregate migratory behavior during aggregate-based passage led to a greater degree of histone methylation and gene expression changes suggestive of cardiomyogenic differentiation, which persevered in the long term. Thus, the repetitive induction of aggregate migratory behavior during repeated passage on the G5 surface results in migration-driven epigenetic memory encrypted through the maintenance of an altered nuclear structure. These findings emphasize the need for a robust and stable hMSC differentiation process.

Chapter 3

General conclusion

3.1. Research summary

Continuing the development of research using the dendrimer-immobilized surface for hMSCs-directed differentiation, this research provides further information about the mechanisms of mechanotransduction and its role in epigenetic memory modification inside nuclei considered important in stem cell fate decisions. In a previous study, the development of a dendrimer-immobilized surface to regulate the migratory behavior of hMSCs and resulted in differentiation commitment towards myogenic lineage has been clarified (Kim et al., 2010). The study continued with the elucidation of the G5 surface to directed differentiation of hMSCs towards cardiomyogenic lineage due to cell-substrate interaction, which causes the regulation of ECM and intracellular pathway specifically in Wnt/ß-catenin signaling in the activation of cardiomyogenic protein markers (Ogawa et al., 2016).

The elucidation of cardiomyogenic lineage commitment of hMSCs in the dendrimer-immobilized surface was continued by studying the mechanotransduction process in the regulation of epigenetics memory formation, which plays a role in the up-regulation of cardiomyogenic specific genes and protein markers. This current research position completed the study of the dendrimer-immobilized surface potential to direct hMSCs differentiation commitment toward cardiomyogenic lineage, as mentioned in the schematic diagram below (**Fig. 30).**

Reorganizations of the cytoskeleton and nuclear skeleton related to migratory changes on dendrimer-immobilized surface are responsible for the integrated regulation of epigenetic formations through histone modification, which leads to switching differentiation commitment

of hMSCs to smooth, skeletal and cardiac muscle lineages. The constitutive alteration of cytoskeleton and nuclear skeleton structure through cell aggregate passage culture in G5 surface generated memory of epigenetic regulation and increased the cardiomyogenic commitment potential of hMSCs. The prolonged migration-driven aggregate behavior through serial passages of the cell aggregates resulted in higher constitutive deformation of the cytoskeleton and nuclear skeleton structures which affected the maintenance of epigenetic memory and activated cardiomyogenic-specific genes transcription. The migration-driven aggregate behavior also promotes intracellular signaling. The higher efficiency of cardiomyocyte-like cells obtained through this process shows that serial passages of cell aggregate on the dendrimer-immobilized surface could enhance the cardiomyogenic commitment of hMSCs.

This study provides an understanding of the role of epigenetic modification through migratory-cell behavior related to cellular mechanotransduction provided by a suitable designed surface using dendrimer-immobilized to induce differentiation commitment of hMSCs towards cardiomyogenic lineage. Moreover, integrating improved culture processes and appropriate microenvironmental cues could enhance the efficiency of hMSCs differentiation commitment toward specific cell lineages.

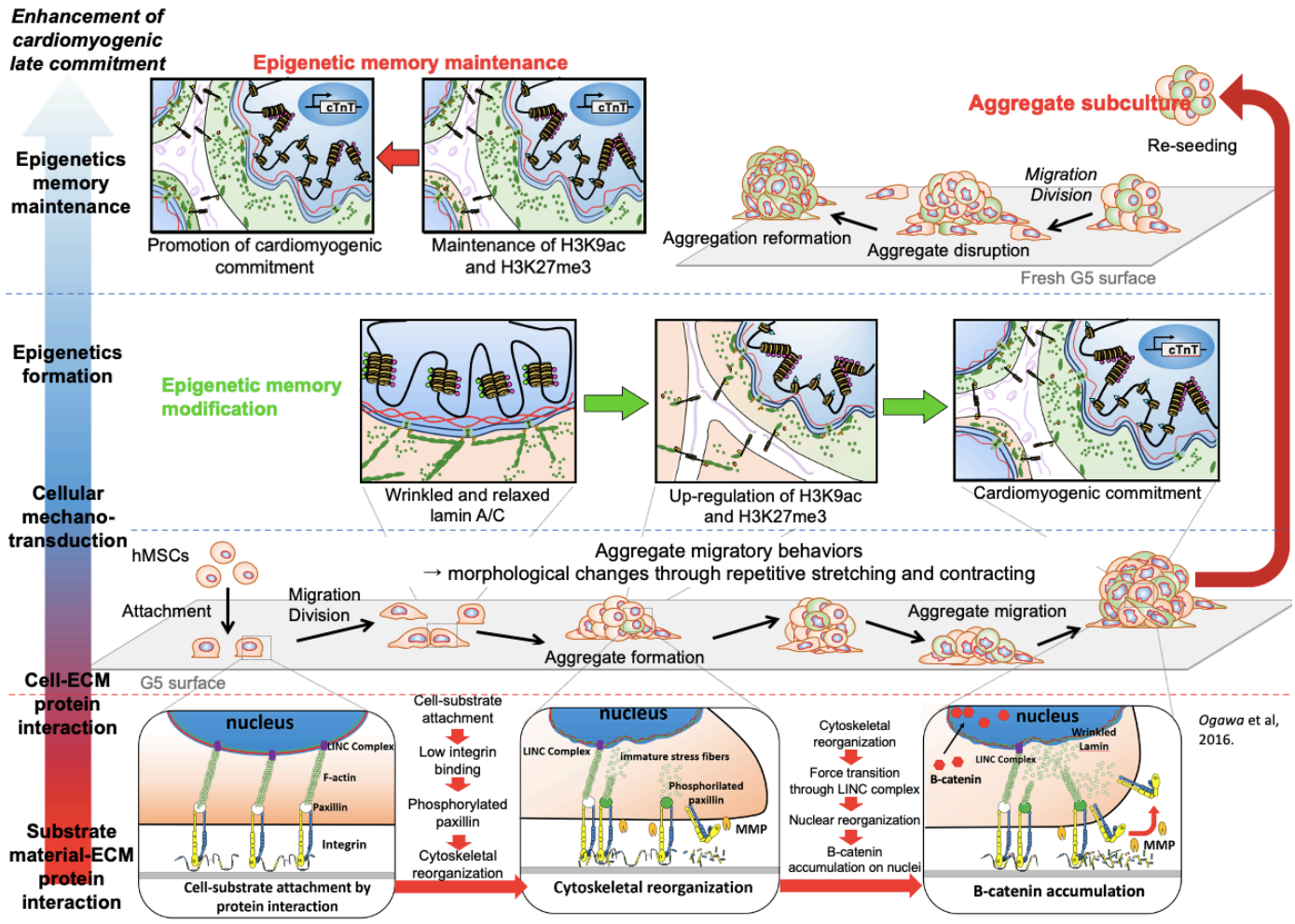

Figure 30. The general conclusion illustration of comprehensive study in cardiomyogenic commitment during passaged culture of hMSCs on a dendrimer-immobilized surface.

3.2. Future prospective

From the findings in this study, the mechanotransduction mechanism during culture of hMSCs on dendrimer surface has mainly elucidated. The role of cytoskeleton and nucleoskeleton reorganization has been proven to play a role in epigenetic formation derived by behavioral changing during active migration on the dendrimer surface. However, the direct link between the alteration of nucleoskeleton structure and chromatin structure related to epigenetic modification remains unclear. On the other hand, the determination of histone modification in specific gene promoters could enhance the deeper understanding instead of the evaluation of global histone modification as obtained in this research.

Although the endogenous stimulation from the microenvironment can direct the differentiation of hMSCs towards cardiomyogenic lineage, the degree of commitment has yet to reach the mature stage of cardiomyocytes. Our refined hypothesis, after gathering data and findings about epigenetic memory formation, concludes that the addition of exogenous stimulation from differentiation factors was required to enhance the degree of commitment to reach the maturation process. In the preliminary data (**Fig. 31**), the TGF-ß1 was applied to provide exogenous stimulation to directed differentiation toward cardiomyogenic lineage. Stand-alone, the TGF-ß1 addition also faces problems in differentiation efficiency and cost-related during the process of differentiation hMSCs towards cardiomyocytes. A combination of endogenous and exogenous stimulation was assumed to promote a synergistic effect, resulting in mature differentiation of hMSCs.

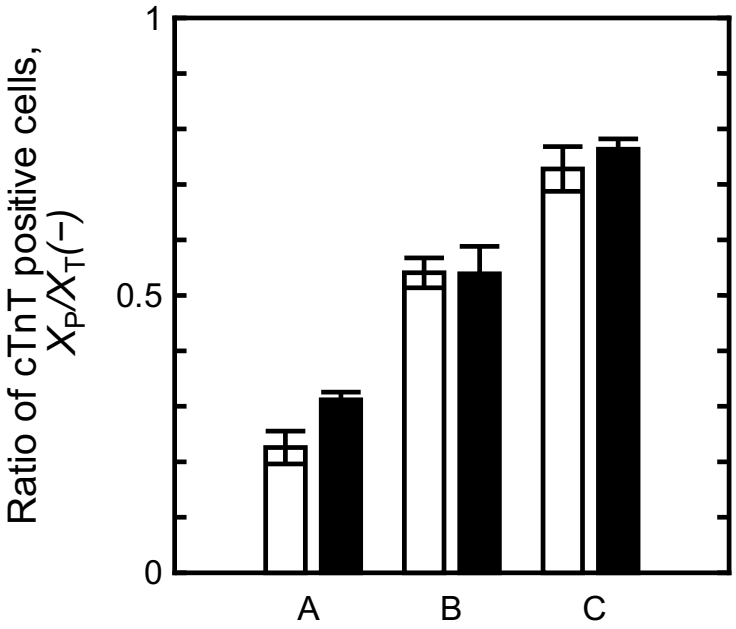

Figure 31. The ratio of $cTnT^+$ cells in hMSCs cultured on the G5 surface in culture conditions when exposed to medium without (A) and with Rac1 activator (B) from day 3 to day 10, and (C) passage culture with Rac1 activator from day 3 to day 20, and without (open bars) and with TGF-ß1 (closed bars) from day 20 to day 30, by co-immunostaining with cTnT and DAPI after re-seeding to the PS surface by collecting all cells with enzymatic treatment at day 30. Vertical bars indicate the standard deviations (n = 3). Statistical significance was according to one-way analysis of variance (ANOVA) and Tukey-Kramer posthoc test (*$p < 0.01$ and **$p < 0.05$).

Regarding those considerations, to extend the findings of the related study, the following research is considered promising concerning the application of stem cell engineering:

1. Investigation of chromatin structures and localization of LINC complex

The LINC complex and lamin-associated domains (LADs), as a direct link between cytoskeleton – nucleoskeleton – chromatin, were considered to play an essential role during the alteration of cytoskeleton and nucleoskeleton during active migration of hMSCs on dendrimer surface. By investigating the presence of LINC complex and levels of LADs during culture, the missing mechanism during transduction of mechanical forces could be elucidated. On the other

hand, the chromatin structure, which is also directly connected to the nucleoskeleton through LADs, could give a whole image of the direct mechanism of forces transduction into the nucleus and specifically investigate the deeper relation between nucleoskeleton alteration and regulation of global histone modification. Knowing those matters, the complete mechanism pathway of mechanotransduction phenomena could be obtained.

2. *Investigation of histone modification in specific gene promoter-related cardiomyogenic genes*

In the current study, the global histone modification markers were used to understand the epigenetic formation during the induction of cardiomyogenic differentiation through active migration on the dendrimer surface. However, this understanding could be extended through elucidation of the histone modification markers in the specific promoter of cardiomyogenic genes through further experiments, for example, using Chip-qPCR. The level of histone modification markers through methylation or acetylation in the specific promoters of cardiomyogenic genes could give a clear image and understanding of related gene activation in real-time, so the differentiation stage could also be investigated. Another consideration is that the investigation of histone modification in specific promoters of cardiomyogenic genes could focus the determination of the differentiation process only into the cardiomyogenic lineage and reduce the possibility of general trans-differentiation into another lineage with a high potential to have occurred in the differentiation process of hMSCs.

3. *Investigation of TGF-ß1addition in the passaged culture of hMSCs on a dendrimer-immobilized surface*

The synergistic effects between endogenous stimulation using dendrimer immobilized surface and exogenous stimulation through the addition of TGF-ß1 should be elucidated during

the passage cultured of hMSCs on a dendrimer-immobilized surface. The results of a preliminary experiment using the addition of TGF-ß1 show the significant impact in the up-regulating expression of cTnT marker, exhibited differentiation direction of hMSCs towards cardiomyogenic lineage. However, this synergistic effect between dendrimer-immobilized surface and TGF-ß1 needs to be elucidated in the future development of these experiments and to establish the most efficient methods in directed differentiation of hMSCs towards cardiomyogenic lineage. Similar parameters, such as histone modification and cardiomyogenic markers, must be clarified during further experiments.

Nomenclature

α	Attachment efficiency	[-]
μ	Specific growth rate	[h-1]
V_M	Migration rate	[μm/h]
R_C	Cell roundness	[-]
Ct	Cycle threshold value	[cycle]
X_0	Cell density at the seeding	[cells/cm2]
X_{24}	Cell density after seeding for 24 h	[cells/cm2]
X_T	Cell density after planting for t h	[cells/cm2]
X_P/X_0	Ratio of positive cell	[-]
X_T/X_0	Ratio of total cell number	[-]

Abbreviations

3D	Three dimensional
A_C	Area length
ANOVA	Analysis of variance
C	Celsius
CD105	Endoglin
cDNA	Coding deoxyribonucleic acid
Chip-qPCR	Chromatin immunoprecipitation – quantitative polymerase chain reaction
CO_2	Carbon dioxide
cTnT	Cardiac Troponin T
CVDs	Cardiovascular disease
D-glucose	Dextrose glucose
DAPI	4,6-diamidino-2-phenylindole
DMEM	Dulbecco's modified Eagle's medium
DNA	Deoxyribonucleic acid
ECL	Enhanced chemiluminescence
ECM	Extracellular matrix
EDTA	Ethylenediaminetetraacetic acid
F-actin	Filamentous actin
FA	Focal adhesion
FBS	Fetal bovine serum
FN1	Fibronectin 1
FS-MHC	Fast skeletal myosin heavy chain

G-actin	Globular actin
G1	First generation
G3	Third generation
G5	Fifth generation
GAPDH	Glyceraldehyde 3-phosphate dehydrogenase
GATA4	GATA Binding Protein 4 gene
H3	Histone 3
H3K27me3	Histone H3 trimethylation at lysine 27
H3K9ac	Histone H3 acetylation at lysine 9
H3K9me3	Histone H3 trimethylation at lysine 9
HDAC1	Histone deacetylase 1
HMG-1	High-mobility group protein 1
hMSCs	Human mesenchymal stem cells
l_C	Peripheral length
IgG	Immunoglobulin G
LADs	Lamina-associated domains
LINC	Linker of nucleoskeleton and cytoskeleton
MMP1	Matrix metalloproteinase-1
MMP14	Matrik metallopeptidase gene
mRNA	Messenger ribonucleic acid
MSCs	Mesenchymal stem cells
MT1-MMP	Membrane-type 1 matrix metalloproteinase
MYH7	Myosin heavy chain β gene
N-cadherin	Neural cadherin
NaOH	Sodium hydroxide

NE	Nuclear envelope
NKX2.5	NK2 Homeobox 5 gene
NPC	Nuclear Pore Complex
PBS	Phosphate buffer saline
PCR	Polymerase chain reaction
pH	Potential of hydrogen
PS	Polystyrene
PXN	Paxillin gene
qRT-PCR	Quantitative real-time reverse transcription–polymerase chain reaction
Rac1	Rac Family Small GTPase 1 protein
RAC1	Rac Family Small GTPase 1 gene
R_C	Cell roundness
RIPA	Radioimmunoprecipitation
RNA	Ribonucleic acid
SDS-PAGE	Sodium dodecyl sulfate-polyacrylamide gel electrophoresis
TBS-T	Tris-buffered saline with poly-oxyethylene sorbitan 20
TGF-ß1	Transforming growth factor beta 1
TNNT2	Cardiac troponin T gene
V_M	Migration rate
WHO	World Health Organization
Wnt	Wingless and Int-1
α-SMA	Alpha smooth muscle actin
α_M	Attachment rate
ß-catenin	Beta-catenin protein
μ_M	Specific growth rate

References

Ahmed, K., Dehghani, H., Rugg-Gunn, P., Fussner, E., Rossant, J., Bazzet-Jones, D. P. Global Chromatin Architecture Reflects Pluripotency and Lineage Commitment in the Early Mouse Embryo. *PLoS ONE.* 5(5): e10531 (2010).

Al-Rekabi Z, Pelling AE. Cross-talk between matrix elasticity and mechanical force regulates myoblast traction dynamics. *Phys Biol.* 10 (6): 066003 (2013).

Ankam, S., Teo, B. K. K., Pohan, G., Ho, S. W. L., Lim, C. K., Yim, E. K. F. Temporal changes in nucleus morphology, lamin A/C and histone methylation during nanotopography-induced neuronal differentiation of stem cells. *Front Bioeng Biotechnol.* 6 (69) (2018).

Arney, K.L. and Fisher, A.G. Epigenetic aspects of differentiation. *J Cell Sci.* 117 4355–4363 (2004).

Armiñán, A., Gandía, C., Bartual, M., García-Verdugo, J. M., Lledó, E., Mirabet, V., Llop, M., Barea, J., Montero, J. A., and Sepúlveda, P. Cardiac differentiation is driven by NKX2.5 and GATA4 nuclear translocation in tissue-specific mesenchymal stem cells, *Stem Cell Dev.* 18: 907-918 (2009).

Bachir, A. I., Horwitz, A. R., Nelson, J., Bianchini, J. M. Actin-Based Adhesion Modules Mediate Cell Interactions with the Extracellular Matrix and Neighboring Cells. *Cold Spring Harb Perspect Biol.* 9: a023234 (2017).

Baksh, D., Song, L., Tuan, R. S. Adult mesenchymal stem cells: characterization, differentiation, and application in cell and gene therapy. *J Cell Mol Med.* 8(3):301-16 (2004).

Bannister, A., Kouzarides, T. Regulation of chromatin by histone modifications. *Cell Res.* 21: 381–395 (2011).

Becker, J. S., Nicetto, D., Zaret, K. S. H3K9me3-dependent heterochromatin: a barrier to cell

fate changes. *Trends Genet.* 32 (1): 29–41 (2016).

Bird, A. DNA methylation patterns and epigenetic memory. *Genes & Dev.* 16: 6-21 (2002).

Bieback, K., Wuchter, P., Besser, D., Franke, W., Becker, M., Ott, M., Pacher, M., Ma, N., Stamm, C., Klüter, H., Müller, A., Ho, A. D. Mesenchymal stromal cells (MSCs): science and f(r)iction. *J Mol Med (Berl).* 90 (7): 773–782 (2012).

Boland, M. J., Nazor, K.L., Loring, J. F. Epigenetic Regulation of Pluripotency and Differentiation. *Circulation Research.* 115(2): 311-324 (2014).

Bouzid, T., Kim, E., Riehl, B.D. et al. The LINC complex, mechanotransduction, and mesenchymal stem cell function and fate. *J Biol Eng.* 13 (68) (2019).

Bowman, G. D., and Poirier, M. G. Post-Translational Modifications of Histones That Influence Nucleosome Dynamics. *Chem Rev.* 115 (6): 2274–2295 (2015).

Burridge, P.W., Holmstrom, A., Wu, J.C. Chemically Defined Culture and Cardiomyocyte Differentiation of Human Pluripotent Stem Cells. *Curr Protoc Hum Genet.* 87 (1): 21.3.1–21.3.15 (2015).

Bhuvanalakshmi, G., Arfuso, F., Kumar, A. P., Dharmarajan, A., and Warrier, S. Epigenetic reprogramming converts human Wharton's jelly mesenchymal stem cells into functional cardiomyocytes by differential regulation of Wnt mediators. *Stem Cell Res Ther.* 8: 185 (2017).

Briand, N. and Collas, P. Lamina-associated domains: peripheral matters and internal affairs. *Genome Biol.* 21 (85) (2020).

Caplan, A. I., and Correa, D. The MSC: an injury drugstore. *Cell Stem Cell*. 9 (1): 11-5 (2011).

Changede, R. and Sheetz, M. Integrin and cadherin clusters: A robust way to organize adhesions for cell mechanics. *Bioessays.* 39 (1): 1-12 (2017).

Christophersen, N. S., Helin, K. Epigenetic control of embryonic stem cell fate. *J Exp Med.* 207(11):2287-95 (2010).

Cimmino, C., Rossano, L., Netti, P.A., Ventre, M. Spatio-temporal control of cell adhesion: toward programmable platforms to manipulate cell functions and fate. *Front Bioeng Biotechnol.* 6 (190) (2018).

Costa, A. R., Sousa, S. C., Costa, R. P., Mateus, J. C., Lopes, C. D.F., Costa, A. C., Rosa, D., Machado, D., Pajuelo, L. The membrane periodic skeleton is an actomyosin network that regulates axonal diameter and conduction. *eLife.* 9:e55471 (2020).

Conway, A., Vazin, T., Spelke, D. P., Rode, N. A., Healy, K. E., Kane, R. S., Schaffer, D. V. Multivalent ligands to control stem cell behavior in vitro and in vivo. *Nat Nanotechnol.* 8(11): 831–838 (2013)

Crowder, S.W., Leonardo, V., Whittaker, T., Papathanasiou, P., Stevens, M. M. Material cues as potent regulators of epigenetics and stem cell function. *Cell Stem Cell.* 18: 39–52 (2016).

Cruz Walma, D. A. and Yamada, K. M. The extracellular matrix in development. *Development*. 147 (10): dev175596 (2020).

Dahl, K.N., Kallnowski, A. Nucleoskeleton mechanics at a glance. *J Cell Sci.* 124: 675–678 (2011).

Dey, S., Kellam, B., Alexander, M. R., Alexander, C., Rose, F. R. A. J. Enzyme-passage free culture of mouse embryonic stem cells on thermo-responsive polymer surfaces. *J Mater Chem.* 21: 6883-6890 (2011).

Driscoll, T.P., Cosgrove, B.D., Heo, S-J., Shurden, Z.E., Mauck, R.L. Cytoskeletal to nuclear strain transfer regulates Yap signaling in mesenchymal stem cells. *Biophys J.* 108 (12): 2783–2793 (2015).

Duncan, E. J., Gluckman, P. D., Dearden, P. K. Epigenetics, Plasticity, and Evolution: How do we link epigenetic change to phenotype? *J. Exp. Zool. (Mol. Dev. Evol).* 322B:208-220 (2014).

Engler, A. J., Sen, S., Sweeney, H. L., Discher, D. E. Matrix Elasticity Directs Stem Cell Lineage Specification. *Cell.* 126 (4): 677-689 (2006).

Esparza, J., Vilardell, C., Calvo, J., Juan, M., Vivas, J., Urbano-Marquez, A., Yague, J., Cid, M.C. Fibronectin upregulates gelatinase B (MMP-9) and induces coordinated expression of gelatinase A (MMP-2) and its activator MT1-MMP (MMP-14) by human T lymphocyte cell lines. A process repressed through RAS/MAP kinase signaling pathways. *Blood.* 94 (8): 2754–2766 (1999).

Gattazzo, F., Urciuolo, A. and Bonaldo, P. Extracellular matrix: a dynamic microenvironment for stem cell niche. *Biochim. Biophys. Acta* 1840, 2506-2519 (2014).

Geiger, B., Spatz, J.P. and Bershadsky, A.D. Environmental sensing through focal adhesions. *Nat Rev Mol Cell Biol.* 10:21–33 (2009).

Gerlitz, G. and Bustin, M. Efficient cell migration requires global chromatin condensation. *Journal of Cell Science.* 123: 2207-2217 (2010).

Gibney, E. and Nolan, C. Epigenetics and gene expression. *Heredity*. 105: 4–13 (2010).

Guelen, L., Pagie, L., Brasset, E., Meuleman, W., Faza, M.B., Talhout, W., Eussen, B.H., Klein, A.D., Wessels, L., Laat, W.D., Stenseel, B.V. Domain organization of human chromosomes revealed by mapping of nuclear lamina interactions. *Nature.* 453: 948–951 (2008).

Guo, X., Bai, Y., Zhang, L., Zhang, B., Zagidullin, N., Carvalho, K., Du, Z., Cai, B. Cardiomyocyte differentiation of mesenchymal stem cells from bone marrow: new regulators and its implications. *Stem Cell Res Ther.* 9 (44) (2018).

Handy, D. E., Castro, R. and Loscalzo, J. Epigenetic Modifications: Basic Mechanisms and Role in Cardiovascular Disease. *Circulation.* 123 (19): 2145-2156 (2011).

Heo, S-J., Thorpe, S. D., Driscoll, T.P., Duncan, R.L., Lee, D.A., Mauck, R.L. Biophysical regulation of chromatin architecture instills a mechanical memory in mesenchymal

stem cells. *Sci Rep.* 5: 16895 (2015).

Heo, S-J., Driscoll, T.P., Thorpe, S.D., Nerurkar, N.L., Baker, B.M., Yang, M.T., Chen, C.S. Lee, D.A. Mauck, R.L. Differentiation alters stem cell nuclear architecture, mechanics and mechanosensitivity. *elife.* 5: e18207 (2016).

Hieda, M. Signal Transduction across the Nuclear Envelope: Role of the LINC Complex in Bidirectional Signaling. *Cells.* 8(2) (2019).

Hocking, D.C., Sottile, J., Langenbach, K.J. Stimulation of integrin-mediated cell contractility by fibronectin polymerization. *J Biol Chem.* 275 (14): 10673–10682 (1999).

Howard, S., Deroo, T., Fujita, Y., Itasaki, N. A positive role of cadherin in Wnt/β-catenin signaling during epithelial-mesenchymal transition. *PLoS ONE.* 6 (8): e23899 (2011).

Huang, S., Xu, L., Sun, Y., Wu, T., Wang, K., Li, G. An improved protocol for isolation and culture of mesenchymal stem cells from mouse bone marrow. *J Orthop Transl.* 3: 26-33 (2015).

Hwang, N.S., Varghese, S., Elisseeff, J. Controlled differentiation of stem cells. *Adv Drug Deliv Rev.* 60 (2): 199–214 (2007).

Ihalainen, T.O., Aires, L., Herzog, F.A., Schwartlander, R., Moeller, J., Vogel, V. Differential basal-to-apical accessibility of lamin A/C epitopes in the nuclear lamina regulated by changes in cytoskeletal tension. *Nat Mater.* 14 (12): 1252–1262 (2015).

Janmey, P. A. and Miller, R.T. Mechanisms of mechanical signaling in development and disease. *J Cell Sci.* 124(1):9-18 (2011).

Kaminski, A., Fedorchak, G.R., Lammerding, J., The cellular mastermind(?)-mechanotransduction and the nucleus. *Prog Mol Biol Transl Sci.* 126:157–203 (2014).

Kechagia, J.Z., Ivaska, J. and Roca-Cusachs, P. Integrins as biomechanical sensors of the microenvironment. *Nat Rev Mol Cell Biol*. 20(8):457-473 (2019).

Keung, A. J., Kumar, S., and Schaffer, D. V. Presentation Counts: Microenvironmental

Regulation of Stem Cells by Biophysical and Material Cues. Annu. Rev. Cell Dev. Biol. 26:533–556 (2010).

Kim, J-K., Louhghalam, A., Lee, G., Schafer, B.W., Wirtz, D., Kim, D-H. Nuclear lamin A/C harnesses the perinuclear apical actin cables to protect nuclear morphology. *Nat Comm.* 8 (1): 2123 (2017).

Kim, M.-H., Kino-oka, M., Saito, KA., Sawa, Y. and Taya, M. Myogenic induction of human mesenchymal stem cells by culture on the dendrimer-immobilized surface with D-glucose display. *J Biosci Bioeng.* 109 (1): 55–61 (2010).

Kim, M.-H., Kino-oka, M., Maruyama, N., Saito, A., Sawa, Y. and Taya, M. Cardiomyogenic induction of human mesenchymal stem cells by altered Rho family GTPase expression on the dendrimer-immobilized surface with D-glucose display. *Biomaterials.* 31 (30): 7666–7677 (2010).

Kim, M.-H. and Kino-oka, M. Switching between self-renewal and lineage commitment of human induced pluripotent stem cells via cell-substrate and cell-cell interactions on a dendrimer-immobilized surface. *Biomaterials.* 35 (22): 5670–5678 (2014).

Kim, M.-H., Ogawa, Y., Yamada, K., Taya, M. and Kino-oka, M. Directed differentiation of human mesenchymal stem cells toward a cardiomyogenic fate commitment through the formation of cell aggregates. *Biochem Eng J.* 84: 53–58 (2014).

Kumar, A., Placone, J.K., Engler, A.J. Understanding the extracellular forces that determine cell fate and maintenance. *Development.* 144 (23): 4261–4270 (2017).

Ladoux, B., Nelson, W.J., Yan, J., Mege, R.M. The mechanotransduction machinery at work at adherens junction. *Integr Biol.* 7 (10): 1109–1119 (2015).

Lafos, M., Kroll, P., Hohenstatt, M. L., Thorpe, F. L., Clarenz, O., & Schubert, D. Dynamic Regulation of H3K27 Trimethylation during Arabidopsis Differentiation. *PLoS Genets.* 7(4): e1002040 (2011).

Li, D., Zhou, J., Chowdhury, F., Cheng, J., Wang, N. and Wang, F. Role of mechanical factors in fate decisions of stem cells. *Regenerative Medicine.* 6 (2): 229-240 (2011).

Lochs, S. J. A., Kefalopoulou, S., Kindm, J. Lamina associated domains and gene regulation in development and cancer. *Cells.* 8 (271): 1-15 (2019).

Lu, D.-F., Wang, Y., Su, Z.-Z., Zeng, Z.-H., Xing, X.-W., He, Z.-Y., Zhang, C. Knockdown of the HDAC1 promotes the directed differentiation of bone mesenchymal stem cells into cardiomyocytes. *PLos ONE.* 9 (3): e92179 (2014).

Mammoto, A., Mammoto, T. and Ingber, D. E. Mechanosensitive mechanisms in transcriptional regulation. *J Cell Sci.* 125 (13): 3061-3073.(2012).

Mathews, L. A., Crea, F. and Farrar, W. L. Epigenetic Gene Regulation in Stem Cells and Correlation to Cancer. *Differentiation.* 78 (1): 1-17 (2009).

Martino, F., Perestrelo, A.R., Vinarsky, V., Pagliari, S., Forte, G. Cellular mechanotransduction: from tension to function. *Front Physiol.* 9 (824) (2018).

McCain, M. L., Lee. H., Aratyn-Schaus. Y., Kléber, A. G. and Parker, K. K. Cooperative coupling of cell-matrix and cell-cell adhesions in cardiac muscle. *Proc Natl Acad Sci*. 109(25):9881-6 (2012).

Miroshnikova, Y.A., Nava, M.M., Wickstrom, S.A. Emerging roles of mechanical forces in chromatin regulation. *J Cell Sci.* 130: 2243–2250 (2017).

Mohanty, S., Bose, S., Jain, K.G., Bhargava, B., and Airan, B. TGFβ1 contributes to cardiomyogenic-like differentiation of human bone marrow mesenchymal stem cells. *Int J Cardiol*. 163(1): 93-9 (2013).

Mui, K. L., Chen, C. S. and Assoian, R. K. The mechanical regulation of integrin–cadherin crosstalk organizes cells, signaling and forces. J Cell Sci. 129 (6): 1093-1100 (2016).

Muncie, J.M. and Weaver, V.M. The physical and biochemical properties of the extracellular matrix regulate cell fate. *Curr Top Dev Biol.* 130: 1–37 (2018).

Nathan, A.S., Baker, B.M., Nerurkar, N.L., Mauck, R.L., Mechano-topographic modulation of stem cell nuclear shape on nanofibrous scaffolds. *Acta Biomater.* 7 (1): 57–66 (2011).

Nava, M. M., Miroshnikova, Y. A., Biggs, L. C., Niessen, C. M., Dahl, K. N., Wickstrom, S. A. Heterochromatin-driven nuclear softening protects the genome against mechanical stress-induced damage. *Cell.* 181: 800–817 (2020).

Ninova, M., Tóth, K. F. and Aravin, A. A. The control of gene expression and cell identity by H3K9 trimethylation. *Development.* 146(19) (2019)

Ogawa, Y., Kim, M.-H., Kino-oka, M. Changes in human mesenchymal stem cell behaviors on dendrimer-immobilized surfaces due to mediation of fibronectin adsorption and assembly. *J Biosci Bioeng.* 120 (6): 709–714 (2015).

Ogawa, Y., Kim, M.-H., Kino-oka, M. Migration-driven aggregate behaviors of human mesenchymal stem cells on a dendrimer-immobilized surface direct differentiation toward a cardiomyogenic fate commitment. *J Biosci Bioeng.* 122 (5): 627–632 (2016).

Oyama, K., El-Nachef, D., Zhang, Y., Sdek, P., MacLellan, R. Epigenetic regulation of cardiac myocyte differentiation. *Front Genet.* 5 (375) (2014).

Pankov, R. and Yamada, K.M. Fibronectin at a glance. *J Cell Sci* .115: 3861–3863 (2002).

Park, J., Kim, P., Helen, W., Engler, A. J., Levchenko, A. and Kim, H. Control of stem cell fate and function by engineering physical microenvironments. *Integr Biol (Camb).* 4(9): 1008-1018 (2012).

Pérez-Campo, F. M. and Riancho, J. A. Epigenetic Mechanisms Regulating Mesenchymal Stem Cell Differentiation. Curr Genomics. 16(6): 368-383 (2015).

Ren, J., Huang, D., Li, R., Wang, W., Zhou, C. Control of mesenchymal stem cell biology by histone modification. *Cell Biosci.* 10 (11) (2020).

Salmeron-Sanchez, M. and Altankov, G. Cell-protein-material interaction in tissue engineering, in D. Eberli (Ed.), *Tissue Engineering. InTech, Vukovar, Croatia*. pp. 77–102. (2010)

Segal, T., Salmon-Divon, M., Gerlitz, G. The Heterochromatin Landscape in Migrating Cells and the Importance of H3K27me3 for Associated Transcriptome Alterations. *Cells.* 7 (205) (2018).

Sevilla, C.A., Dalecki, D., Hocking, D.C. Extracellular matrix fibronectin stimulates the self-assembly of microtissues on native collagen gels. *Tissue Eng Part A.* 16 (12): 3805–3819 (2010).

Shevelyov, Y. Y. and Ulianov, S. V. The nuclear lamina as an organizer of chromosome architecture. *Cells.* 8 (136) (2019).

Shi, F. and Sottile, J. MT1-MMP regulates the turnover and endocytosis of extracellular matrix fibronectin. *J Cell Sci.* 124: 4039–4050 (2011).

Shivasankar, G.V. Mechanosignaling to the cell nucleus and gene regulation. *Annu Rev Biophys.* 40: 361–378 (2011).

Steensel, B.V. and Belmont, A.S. Lamina-associated domains: links with chromosome architecture, heterochromatin and gene repression. *Cell.* 169 (5): 780–791 (2017).

Stephens, A. D., Liu, P. Z., Banigan, E. J., Almassalha, L. M., Backman, V., Adam, S. A., Goldman, R. D., and Marko, J. F. Chromatin histone modifications and rigidity affect nuclear morphology independent of lamins. *Mol Biol Cell.* 29 (2) (2018).

Sun, Z., Guo, S. S. and Fassler, R. Integrin-mediated mechanotransduction. *J. Cell Biol.* 215, 445–456 (2016)

Szczesny, S.E., Mauck, R.L. The nuclear option: evidence implicating the cell nucleus in mechanotransduction. *J Biomech Eng.* 139 (2) (2017).

Tee, W. and Reinberg, D. Chromatin features and the epigenetic regulation of pluripotency states in ESCs. *Development*. 141: 2376 – 2390 (2014).

Tijore, A., Cai, P., Nai, M.H., Zhuyun. L., Yu, W., Tay, C.Y., Lim, C.T., Chen, X. and Tan, L.P. Role of Cytoskeletal Tension in the Induction of Cardiomyogenic Differentiation

in Micropatterned Human Mesenchymal Stem Cell. *Adv Healthc Mater.* 4(9): 1399-407 (2015).

Trisciuoglio, D., Di-Martile, M. and Del-Bufalo, D. Emerging Role of Histone Acetyltransferase in Stem Cells and Cancer. *Stem Cells Int.* 2018:8908751 (2018).

Toma, J.G., Akhavan, M., Fernandes, K.J., Barnabe-Heider, F., Sadikot, A., Kaplan, D.R., and Miller, F.D. Isolation of multipotent adult stem cells from the dermis of mammalian skin. *Nat Cell Bio.* 3: 778–784 (2001).

Uhler, C., and Shivasankar, G.V. Regulation of genome organization and gene expression by nuclear mechanotransduction. *Nat Rev.* 18 (12): 717–727 (2017).

Uzer, G., Rubin, C.T., Rubin, J. Cell mechanosensitivity is enabled by the LINC nuclear complex. *Curr Mol Bio Rep.* 2 (1): 36–47 (2016).

Wahane, S., Halawani, D., Zhou, X. and Zou, H. Epigenetic Regulation of Axon Regeneration and Glial Activation in Injury Responses. *Front Genet.* 10:640 (2019).

Wang, J., Jia, S.T., Jia, S. New insights into the regulation of heterochromatin. *Trends Genet.* 32 (5): 284–294 (2016).

Wang, M., Yu, Q., Wang, L., Gu, H. Distinct patterns of histone modifications at cardiac-specific gene promoters between cardiac stem cells and mesenchymal stem cells. *Am J Physiol Cell Physiol.* 304 : C1080 - C1090 (2013).

Wu, J., Kent, I. A., Shekhar, N., Chancellor, T. J., Mendonca, A., Dickinson, R. B., Lele, T. P. Actomyosin pull to advance the nucleus in migrating tissue cell. *Biophys J.* 106: 7–15 (2014).

Xu, H., Yi, Q., Yang, C., Wang, Y., Tian, J., and Zhu, J. Histone modifications interact with DNA methylation at the GATA4 promoter during differentiation of mesenchymal stem cells into cardiomyocyte-like cells. *Cell Prolif.* 49: 315-329 (2016).

Yim, E.K., Sheetz, M.P. Force-dependent cell signaling in stem cell differentiation. *Stem Cell*

Res Ther. 3 (5): 41 (2012).

Zhang, P., Zhang, C., Li, J., Han, J., Liu, X., and Yang, H. The physical microenvironment of hematopoietic stem cells and its emerging roles in engineering applications. *Stem Cell Res Ther* 10 (327) (2019).

List of publication

1. **Ayuningtyas, F.D.,** Kim, M.H. and Kino-oka, M. Muscle lineage switching by migratory behavior-driven epigenetic modifications of human mesenchymal stem cells on a dendrimer-immobilized surface. *Acta Biomater*. 106:170-180 (2020).
2. Kim, M.H., **Ayuningtyas, F.D.** and Kino-oka, M. Novel approach to enhance aggregate migration-driven epigenetic memory which induces cardiomyogenic differentiation on a dendrimer-immobilized surface. *J Biosci and Bioeng.* 132(4):390-398 (2021).

Conference Papers

- **Ayuningtyas, F.D.,** Kim, M.H. and Kino-oka, M. Reorganization of the nuclear lamina and cytoskeleton of human mesenchymal stem cells on a dendrimer-immobilized surface. Proceedings of ISCT 2018, May 2nd-5th 2018, *Cytotherapy*, 20(5): S28 (2018).
- **Ayuningtyas, F.D**., Kim, M.H. and Kino-oka, M. Role of the cytoskeleton and nuclear skeleton reorganization in cardiomyogenic differentiation of human mesenchymal stem cells on the dendrimer-immobilized surface. Proceedings of JIISC 2018, October 28^{th,} 2018.

Acknowledgment

I want to express my gratitude to all who make it possible for me to complete this dissertation. First and foremost, I would like to express my most significant appreciation to my supervisor, Professor Masahiro Kino-oka, who allowed me to conduct my doctoral study at the Bioprocess System Engineering Laboratory, Graduate School of Engineering, Osaka University. I also feel very grateful for his guidance throughout the research work, with valuable and constructive suggestions during my study. He gave me a fundamental motivation that will be useful in research work and life. Also, to the Associate professor, Dr. Mee-Hae Kim as my supervisor for her guidance and help in getting me through the whole study process. She always forces me to improve every day and gives me a great example as a successful woman scientist, which will be very useful for me in the future. I am very grateful for their outstanding support and patience from the day I started my study until now. I also express my gratitude to Prof. Kazuhito Fujiyama and Prof. Hajime Watanabe as sub-supervisor for their constructive comments and suggestion, which were very helpful for me in improving the quality of this dissertation.

I also express my gratitude to the whole staff in the BPSE laboratory and Assistant Professor Ikki Horiguchi for his kind help and support for me in the laboratory. Also, for the secretaries and former secretary in the BPSE laboratory, Ms. Mitsuko Wakamatsu, Ms. Tomoko Nishimura, Ms. Junko Hanashima, Ms. Imaizumi Junko, Ms. Megumi Fukui, for all the help and supports since before I arrived in Japan until now. Thank you to Dr. Yuuki Ogawa, my former senpai, for his patience and kindness; he taught me many things initially and motivated me until I returned to Japan to pursue a Ph.D. I am also very thankful for the very kind help of Ms. Shoko Tajima in my experiments and her presence as a good friend here. For all students in BPSE Laboratory, especially Win, Nan, Trang, New, AD, Ali, Matsumoto, and all the other

students whom I couldn't mention one by one, thank you very much for the great friendship and support during my study here, I will miss you all.

I express my most profound appreciation to Indonesia Endowment Fund for Education (LPDP) scholarship for awarding me financial support during my study in Japan. I also want to express my gratitude to my former supervisor, Dr. Anggraini Barlian, in the School of Life Sciences and Technology, Institute of Technology Bandung (ITB), and all professors there for their continuous support and also initiating the first encounter for me with Prof. Masahiro Kino-oka and BPSE Laboratory. I also want to thank all of my friends outside the laboratory who made my life so colorful here in Japan.

Last but not least, I declare the most profound gratitude to my family – my parents and sisters, also my best friends, who always gave me unconditional love, motivation, and support during my study in Japan.

Fitria Dwi Ayuningtyas